UC-404
LBL-27850
October 1989

Materials and Chemical Sciences Division
Lawrence Berkeley Laboratory
University of California

TENTH ATOMIC PHYSICS PROGRAM WORKSHOP

PROGRAM AND ABSTRACTS

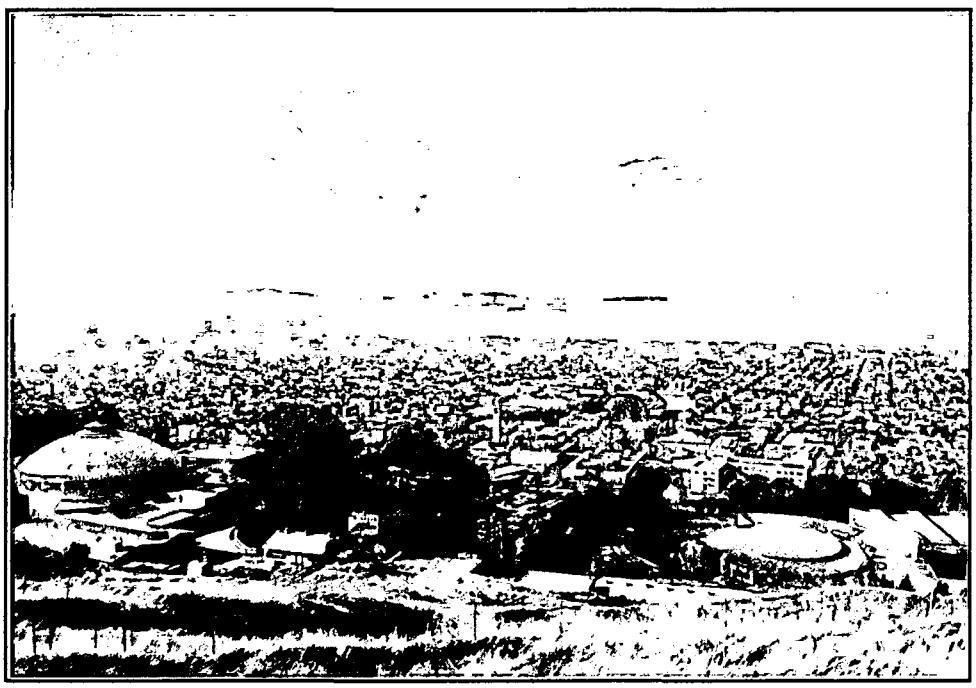

U.S. Department of Energy
Office of Energy Research
Office of Basic Energy Sciences
Division of Chemical Sciences

November 8–9, 1989

Berkeley, California

Prepared for the U.S. Department of Energy under Contract Number DE-AC03-76SF00098

DISCLAIMER

LBL-27850

TENTH ATOMIC PHYSICS PROGRAM WORKSHOP

PROGRAM AND ABSTRACTS

November 8–9, 1989

Berkeley, California

Materials and Chemical Sciences Division
Lawrence Berkeley Laboratory
1 Cyclotron Road
Berkeley, California 94720

October 1989

This work was supported by the Director, Office of Energy Research, Office of Basic Energy Sciences, Chemical Sciences Division, of the U.S. Department of Energy under Contract Number DE-AC03-76SF00098.

Program Schedule

Xth ATOMIC PHYSICS PROGRAM WORKSHOP
Basic Energy Sciences
Division of Chemical Sciences
U.S.Department of Energy

November 8-9, 1989
Lawrence Berkeley Laboratory
Berkeley, California

WEDNESDAY, NOVEMBER 8

0815 Registration

0900 Introduction

Welcome: Charles Shank, Director, Lawrence Berkeley Laboratory
Program overview: Joe Martinez, Program Manager, DOE Headquarters

SESSION I: ION-ATOM COLLISION THEORY
Chair: Alex Dalgarno, Harvard University

0920 Post Collision Effects
Joe Macek, Unversity of Tennessee and
Oak Ridge National Laboratory **1**
0945 Correlation
Jim McGuire, Kansas State University **5**
1010 Alignment and Orientation
Neal Lane, Rice University **9**

1035 BREAK

SESSION II: NEW EFFORTS
Chair: Val Kostroun, Cornell University

1100 Dielectronic Recombination in He-like Argon
Lew Cocke, Kansas State University **13**
1130 Charge Transfer Neutralization Collisions
Ed Thomas, Georgia Institute of Technology **17**
1200 Ion-Surface Collision Vacancy Production
Fred Meyer, Oak Ridge National Laboratory **21**

1230 LUNCH

SESSION III: LASER PHYSICS
Chair: Steve Smith, University of Colorado

1330 Laser Quantum Noise
Michael Raymer, University of Oregon **25**
1400 Statistical Fluctuations in Lasers
Raj Roy, Georgia Institute of Technology **29**

1430 Quantum Effects in an Intense Laser Field
F. T. Hioe, St. John Fisher College **33**
1500 Polarized Electron-Polarized Atom Collisions
Mike Kelley, National Institute for Standards and Technology **37**

1530 BREAK

1600 Tour of Bevalac, Advanced Light Source and Cyclotron ECR facilities
Guides: Harvey Gould, Fred Schlachter, and Mike Prior, LBL

1700 RECESS

1630 DINNER

THURSDAY, NOVEMBER 9

SESSION IV: SPECTROSCOPY OF ATOMS
Chair: Tom Gallagher, University of Virginia

0830 Energy Transfer in Excimer Lasers
John Keto, University of Texas **41**
0855 Atomic Oxygen
Arlee Smith, Sandia Laboratories-Albuquerque **45**
0920 Hydrogen Atom in Collision
John Kielkopf, University of Louisville **49**
0945 Relativistic Hydrogen Systems
Howard Bryant, University of New Mexico **53**

1010 BREAK

SESSION V: SPECTROSCOPY OF IONS
Chair: Mike Prior, Lawrence Berkeley Laboratory

1030 Photon Emission Lifetime Measurements
Bob Dunford, Argonne National Laboratory **57**
1100 Lifetimes of Highly Charged Ions
Larry Curtis, University of Toledo **61**
1130 Inner Shell Photoionization Cross Sections
Keith Jones, Brookhaven National Laboratory **65**
1200 Hyperfine Structure of Y II
Linda Young, Argonne National Laboratory **69**

1230 LUNCH

SESSION VI: HIGH VELOCITY COLLISIONS
Chair: Rand Watson, Texas A & M University

1330 Distinguishing Electron-Electron Interactions
Pat Richard, Kansas State University **73**
1400 Electron Correlation and Multiple Capture
John Tanis, Western Michigan University **77**

1430 Collisions with Dense Electron Targets
Sheldon Datz, Oak Ridge National Laboratory **81**

1500 Status of Lamb Shift Measurements
Harvey Gould, Lawrence Berkeley Laboratory **87**

1530 SUMMARY: J. V. Martinez

1600 ADJOURN

PAPERS

PRESENTED

Theoretical Atomic Physics
Oak Ridge National Laboratory

I. Non Relativistic Atomic Physics *(C. Bottcher, G. Bottrell and M. Pindzola)*

We have now completed studies on $p + H$ and $C^{6+} + Ne$ collisions using our three dimensional TDHF codes. In the case of $p + H$, calculations have been made at two ion velocities, $v = 1$ and 2 atomic units, and in the case of $C^{6+} + Ne$ at one velocity $v = 6$ of experimental interest. For each velocity and a range of impact parameters, we have extracted excitation and capture probabilities, and secondary electron spectra in the target and projectile frames. Typical energy distributions are shown in Fig. 1. The $p + H$ runs at $v = 2$ show evidence of "ridge" electrons, trailing behind the projectile at a relative velocity $v_e = v/2$. We expect that a definitive picture will emerge when the angular distributions are plotted.

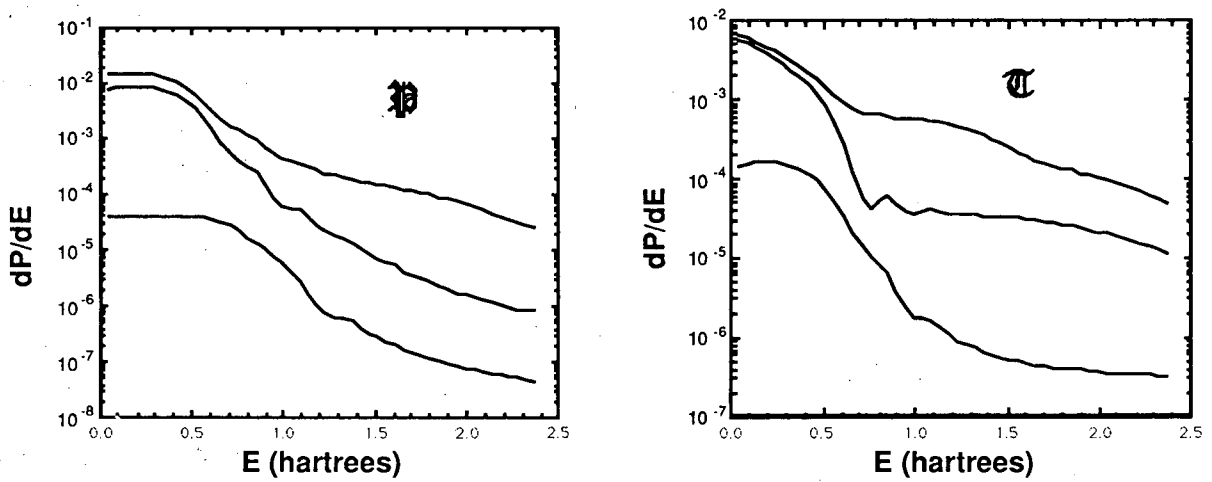

Figure 1: Secondary electron energy distributions in projectile (P) and target (T) frames for a $p + H$ collision at $v = 1$. The curves refer to three impact parameters: top, $b = 0.5$, middle, $b = 2.5$, lowest, $b = 5.5$.

We are also applying the TDHF codes to multiphoton ionization in laser-atom interactions. The first step was to reproduce the results of older 2D codes. We now have the unique capacity to model interactions with circularly polarized radiation.

The 3D lattice techniques have now been adapted to study correlation in the coulomb three body problem. We are now examining the double excitation and ionization of two electron atoms, and the decay of autoionizing states in external fields.

II. Relativistic Atomic Physics *(C. Bottcher, M.R. Strayer and J.S. Wu)*

We have completed a number of studies of lepton pair production using both lattice and perturbation methods. We have the unique capacity to do calculations of either type on parallel supercomputers. A potentially significant development is a novel nonperturbative

"semiclassical light cone" technique, which may resolve some outstanding questions regarding the validity of perturbation theory.

We have made some applications to accelerator design questions, in particular to the question of the effect of capture from the vacuum on beam lifetimes. We are currently extending these calculations to SSC energies.

III. Post-Collision Effects in Auger Electron Spectra *(J. H. Macek)*

When an Auger electron emitted from a stationary target overtakes the projectile ion which excited the autoionizing state, the wave function of the electron is focused by the potential of the projectile. This focusing effect is observed experimentally as an enhancement of the number of electrons emitted in the forward direction. Observations of this effect for the reaction

$$He^+ + He \longrightarrow He^{**} + He^+ \longrightarrow He^+ + e^- + He^+ \tag{1}$$

at $5keV$ He^+ lab energy and the $2s^2\ ^1S$, $2p^2\ ^1D$, $2s2p^1P$ autoionizing states have been reported. We have developed a theory of this effect [3] by writing the electron wave function in the final state as

$$\psi(\vec{r},\vec{R}) \ = \ \psi(\vec{r})F(\vec{r},\vec{R}) \tag{2}$$

where $\vec{r}$ is the electron coordinate relative to the target, $\vec{R}$ is the projectile- target distance, $\psi(\vec{r})$ is the electron wave function for the state of $He^+ + e^-$ in the absence of the projectile. We then show that the Auger line-shape is given by the modulus of

$$A(E) \ = \ -iA_0 \int_0^\infty F(0,\vec{v}t)^* t^{-iZ_P/v} \exp[i(E - E_0 + i\Gamma/2)t]dt \tag{3}$$

where $\vec{v}$ = projectile velocity, E = electron energy, E_0 = energy of the autoionizing state, Γ = line width of the state, Z_P = charge of the projectile ion, and $|A_0|^2$ gives the intensity of the line. We have evaluated Eq. (3) when $F(0,\vec{R})$ is a hypergeometric function characteristic of Coulomb interactions. We find a strong enhancement of the electron distribution in the forward direction for reaction (1) in agreement with observations.

IV. Theory of Radiative Electron Capture *(J. H. Macek)*

Intuitively, the radiative capture of an electron loosely bound to a target T by a projectile ion P of velocity $\vec{v}$ in the laboratory frame proceeds via a free-bound transition from a continuum electron state $\psi_{\vec{v}}^+$ of P to a bound state ϕ_f , also of P. This intuitive picture is just the impulse approximation (IA) which Briggs argued was appropriate for highly charged ions P. We have shown how this approximation emerges from a general theory based on a second-order distorted-wave approximation (DWBA).[4] Our derivation shows that it is necessary to take proper account of heavy particle scattering *and* the nonrelativistic limit of the infrared divergence present in all processes involving charged particles.

Future Plans

1. We will employ our new PCI theory, described in Section III, to fit available data on the excitation of Auger lines in helium excited by slow positive ions. Our object is to test the relative phases of amplitudes given by Eq. (3) using various approximations for $F(0,\vec{R})$. Both angular and energy distributions will be considered.

2. We will employ the IA to compute the capture of electrons to high Rydberg and continuum states of one-electron systems. We will also employ this approximation to compute capture cross sections and anisotropy parameters for doubly excited states of two-electron ions.

V. New Sum Rule for Total "Particle" Production in Coincidence with a Hole *(R. L. Becker)*

It is well known that the cross sections for inclusive-single (i.s.) excitation, direct ionization, and electron transfer can be expressed by terms which refer explicitly only to single electron transitions, and that their sum, the cross section for i.s. "particle" production, equals that for i.s. hole production. A similar equality is sometimes assumed for these processes in coincidence with a vacancy in a particular shell to infer, for example, the cross section for direct ionization accompanied by a specific hole, h, as equal to the h vacancy cross section minus the cross sections for transfer and for excitation in coincidence with h. The assumed equality is not correct. We have shown [5] that the sum of cross sections for i.s. "particle" production processes in coincidence with h equals that for the production of h plus that for the production of two holes, one of which is h. The latter corresponds to double electron transition terms in which the electron which goes into the "particle" state does not come from h. Current effort is being given to the derivation of additional sum rules for higher-order processes and to their interpretation given by breaking down inclusive sums into number-exclusive parts.

VI. Strong Enhancement Over the Single-Electron Value of Direct Ionization in Coincidence with a Specified Vacancy *(R. L. Becker)*

Coupled-channels calculations of ionization and of electron transfer in coincidence with a hole in the K or L shell were done for neon with He^{2+} and C^{6+} projectiles over the energy range $0.2 - 1.7 MeV/amu$ by making use of our new sum rule. The enhancement resulting from double electron transition terms is particularly large for ionization. It grows strikingly with the projectile charge and varies with the impact energy, reaching 21.6 for a K hole in Ne produced by C^{6+} at $0.83 MeV/amu$. Additional calculations for Ne and Ar will be done. An experiment to test the theory is proposed.

References.

1. *Electron Pair Production from Pulsed Electromagnetic Fields in Relativistic Heavy-ion Collisions*, C. Bottcher and M.R. Strayer, Phys. Rev. **D39**, 1330 (1989) .

2. *Feynman-Monte Carlo Calculations of Electron Capture at Relativistic Collider Energies*, M.J. Rhoades-Brown, C. Bottcher and M.R. Strayer, Phys. Rev. **A40**, September (1989) .

3. *Theory of Angle-Dependent Auger Transitions in Ion-Atom Collisions*, R. O. Barrachina and J. H. Macek, J. Phys. **B22**, 2151 (1989).

4. *Strong Potential Wave Functions with Elastic Channel Distortion*, J. Macek and K. Taulbjerg, Phys. Rev. **A38**, 6064 (1989).

5. *On the Cross Sections for Electron Transfer, Ejection, and Excitation in Coincidence with a Hole in a Specific Shell*, R. L. Becker, Acta Physica Hungarica **65**, Nos. 2-3 (1989) (special issue in honor of D. Berenyi), in press.

III. THEORY FOR MULTIPLY CHARGED IONS

J. R. Macdonald Laboratory
Kansas State University, Manhattan, KS 66506-2601

Correlation in Atomic Scattering

J. H. McGuire, J. C. Straton and Y. D. Wang

We have studied various aspects of dynamic correlation occurring in high velocity ion-atom collisions. One case considered is double excitation of helium by few Mev/u protons, anti-protons and other ions. We have expanded the full quantum mechanical probability amplitude in powers of the interaction of the projectile with the target electrons, keeping the first two terms in this perturbation expansion. The first order term is linear in Zp/v, where Zp and v are the charge and velocity of the projectile. The second order term, quadratic in Zp/v, extends the independent electron approximation (to lowest order in Zp/v) to include correlation in the two electron asymptotic states by using configuration interaction (CI) wavefunctions. Straton has evaluated the resulting amplitude for single and double excitation or de-excitation from arbitrary states in closed analytic form. The first order term, which contains all contributions first order in Zp/v including shakeup, two step one (TS1) and ground state correlation, is the dominant term at high collision velocities. Calculations are underway for double excitation into the n=2 manifold where data from both Pedersen and Hvelplund and Giese *et al.* are now available for ion impact and data for anti-proton impact are expected soon. We are able to identify where interference between the first order and second order terms arise, *i.e.* where differences between double excitation by protons and anti-protons originate.

A second example of an effect of electron correlation occurs in the transfer-ionization reaction $p + He \Rightarrow H + He^{++} + e$ when transfer occurs in a two-step process where one target electron scattering from the projectile is re-scattered in the direction of the projectile in a collision with the second target electron. This two-step Thomas process is characterized by two ridges in the distribution of the recoil electrons. The sharp ridge is a consequence of conservation of overall energy and momentum, while the broader ridge corresponds to conservation of energy in the intermediate state in a double scattering process. The shapes of these ridges reflect the effects of energy non-conservation in intermediate states of the collision. This process has been observed recently for the first time by Schuch *et al.* We have worked out simple formulas for the loci of both the sharp and broad ridges in the recoil distributions for systems of arbitrary mass.

Theoretical Atomic Parameters for Highly Excited Charged Ions

C. P. Bhalla

We have completed extensive calculations of atomic parameters for doubly excited Li-like ions in the intermediate coupling scheme with the inclusion of effects due to configuration interaction. The states corresponding to $1s2\ell n\ell'$ configurations were considered for $n \leq 8$. These calculations were used to obtain fluorescence yields, nonradiative branching ratios and line factors for dielectronic satellite lines. The results from the present calculations

are presented in Fig. 1 for the total dielectronic recombination rate coefficients (DR) versus electron temperature. Theoretical cross sections for resonant transfer and excitation followed by a stabilizing radiative transition were compared with experimental data for $F^{6+} + H_2$, $Ca^{17+} + H_2$ (see Fig. 2), and Ca^{17+} + He collisions. Extensive calculations for doubly excited Be-like argon and tinanium were also completed.

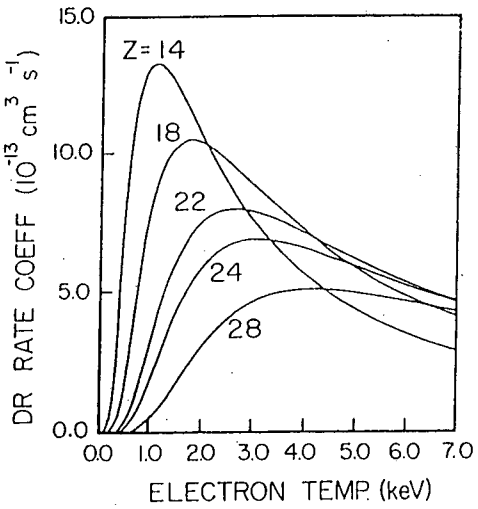

Fig. 1

Fig. 2 Comparison of theoretical and experimental cross sections (multiplied by 1.06) for capture and excitation followed by $K\alpha$ and $K\beta$ x-ray decays for $Ca^{17+} + H_2$ collisions vs projectile energy. The solid line represents the theoretical cross sections; Curves A, B, and C show, respectively, the contributions of $1s2s2p^2$ *LSJ*, $1s2s2p3p$ *LSJ*, and of states of electron configurations $1s2s2pnp$, $1s2s2pnd$, $1s2snp$, and $1s2s3pnp$ (n<9).

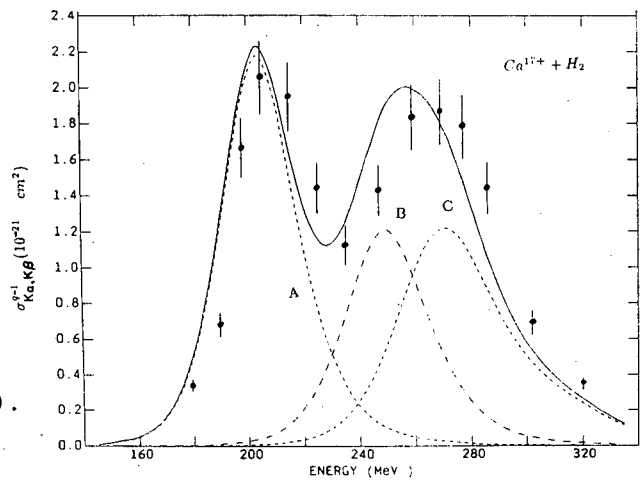

Charge Transfer in Ion-Molecule Collisions and Two-Electron Processes in Ion-Atom Collisions

C. D. Lin and R. Shingal

By treating the electronic molecular wave functions as a linear combination of atomic orbitals from the two atoms, the electron capture amplitude in ion-molecule collisions can be expressed as a coherent superposition of two single electron capture amplitudes in ion-atom collisions with the relative phase dependent on the collision velocity and the orientation of the molecule. This model was used to predict the dependence of electron capture cross sections in ion-molecule collisions. The total capture cross sections averaged over the orientation of the molecules for $H^+ + H_2$ and $He^{++} + H_2$ collisions have been calculated and compared with experiments. The total capture probabilities *vs* scattering energies at a fixed 3° scattering angle measured by Everhart and coworkers in the 60's for $H^+ + H_2$ are explained for the first time using the present model.

We also studied two-electron transitions, such as double capture, transfer excitation, and double excitation in ion-atom collisions to examine the role of electron correlation as well as the one-step *vs* two-step mechanisms for the two-electron processes. The calculations are carried out using a two-electron close-coupling code where electron correlations in the description of electronic wave functions are explicitly included. We found that the independent electron model in general is only capable of predicting qualitative features of two-electron processes. Specific calculations have been carried out for the double capture in He^{++} + He, in C^{6+} and O^{8+} on He, and for the transfer excitation in He^{+} + H. The independent electron model has been applied to examine all the two-electron processes in bare ions (Z=1-9) on He over an extended energy region to compare with existing calculations.

List of Selected Publications

1. "Ionization of Helium by Fast, Highly Charged Projectiles"
   I. Ben-Itzhak and J.H. McGuire
   Phys. Rev. A 38, 6422 (1988).
2. "Impact Parameter Treatment of High Velocity Electron Capture from Diatomic Molecules at Fixed Orientation"
   Y.D. Wang, J.H. McGuire and R.D. Rivarola
   Phys. Rev. A (in press).
3. "Recoil Distributions in Particle Transfer"
   J.H. McGuire, J.C. Straton, W.J. Axmann, T. Ishihara and E. Horsdal-Pedersen
   Phys. Rev. Letters 62, 2933 (1989).
4. "Density Matrices of the n=2 and 3 Manifolds of H Atoms Produced in p-H Collisions at 1-50 keV Impact Energies"
   A. Jain, C.D. Lin and W. Fritsch
   J. Phys. B 21, 1545 (1988).
5. "State-Selective Double-Electron Capture in He^{++} + He Collisions at Intermediate Energies"
   A. Jain, C.D. Lin and W. Fritsch
   Phys. Rev. A 39, 1741 (1989).
6. "An Orientation-Dependent Atomic Model for Ion-Molecule Collisions: Applications to H^{+} + H_2"
   R. Shingal and C.D. Lin
   Phys. Rev. A 40, 1302 (1989).
7. "Auger and Radiative Deexcitation Rates and Energies of $3\ell 3\ell'$ States of Helium-like Argon and Silicon"
   K.R. Karim and C.P. Bhalla
   Physica Scripta 38, 795 (1988)
8. "Dielectronic Recombination Rate Coefficients for Some Selected Ions in Helium Isoelectronic Sequence"
   K.R. Karim and C.P. Bhalla
   Phys. Rev. A 39, 3549 (1989)
9. "Resonant Transfer and Excitation in Collisions of Li-Like F^{6+} and Ca^{17+} with Light Targets"
   C.P. Bhalla and K.R. Karim
   Phys. Rev. A 39, 6060 (1989)

THEORETICAL ATOMIC AND MOLECULAR SCIENCES: EXCITATION, IONIZATION AND CHARGE TRANSFER IN LOW TO INTERMEDIATE ENERGY ATOMIC COLLISIONS

Neal Lane

Physics Department and Rice Quantum Institute
Rice University, Houston, TX 77251

The theoretical atomic and molecular physics program at Rice University focusses on the nature and interplay of physical mechanisms that control excitation, ionization and charge transfer in collisions involving atoms, ions and molecules. While the emphasis is on heavy-particle collisions involving few-body systems, selected studies are carried out on collision processes that are influenced by "external effects," such as those that arise in dense plasmas, near surfaces, or in the presence of external fields. The choices of systems and processes studied are influenced by experimental data in hand or anticipated and by the interests and needs of the national energy research program. Several projects involve ongoing collaborations with DOE national laboratories.

Research progress in the past few years has been primarily in the following areas: 1) alignment and orientation in ion-atom (Li^+/He, H^+/He, He^+/H) and atom-atom (H/He, Li/He, Na/He) collisions; 2) elastic scattering and charge-transfer in ion-atom (H^+/He,Ne,Ar; Li^{3+}/Li, He^{2+}/Na; and He^{2+}, C^{4+}, O^{6+}/He) and ion-molecule (H^+/H_2, He^+/H_2) collisions; 3) Penning ionization of alkali atoms (Li, Na, K) by metastable helium atoms and ion-pair formation in He^*/Li and alkali atom (Li/Na, Li/Cs) collisions; 4) quenching of intermediate-state Na (6s-9s) Rydberg-atoms in thermal-energy collisions with rare gas (He, Ne, Ar) atoms; 5) a theory of electron-impact ionization of highly stripped ions in dense, high-temperature plasmas.

In the following section, we will briefly describe three projects where significant recent progress has been made but where questions remain and research is continuing.

A) Differential and integral elastic and charge-transfer cross sections for collisions of low-energy protons by helium and other rare-gas atoms and H_2 molecules.

In order to assist with the interpretation of the recent high-resolution measurements of differential elastic and charge-transfer cross sections of Stebbings' group at Rice, we have performed several two-state MO-ETF calculations for H^+/He, Ar collisions and single-state calculations of elastic scattering in H^+/Ne collisions. Agreement with the measurements is found to be excellent for H^+/He, both for elastic scattering and charge transfer, except at the largest angles.[1] Agreement is also excellent for the single-state elastic cross sections for H^+/Ne scattering; this is not surprising since the measurements suggest that the charge-transfer cross section for this system is very small. Studies of other similar collision systems are underway.

As an aside, we mention other calculations carried out for

the HeH^+ system: cross sections for low-energy (meV to 50eV) radiative and non-radiative charge-transfer in He^+/H collisions, in collaboration with B. Zygelman and A. Dalgarno;[2] and a comparative study of the integral alignment of H(2p) arising from H^+/He and He^+/H collisions.[3]

Our study of proton-H_2 collisions, also stimulated by the recent high-resolution measurements of differential elastic and charge-transfer collisions in the energy range 0.5 to 5.0 keV by Stebbings' group at Rice, employs the diatoms-in-molecule (DIM) method to calculate the electronic wave functions and a two-state MO-ETF semiclassical approach to the collision dynamics. The theoretical results reproduce the structural features of the elastic and single (and double) charge-transfer differential cross sections and, in general, are in good qualitative agreement with the measurements.

B) Selective-state charge transfer in He^{++}/Na and Li^{3+}/Li collisions

An MO-ETF semiclassical (16-state) close coupling calculation of cross sections for charge transfer to excited states of He^+ resulting from He^{2+}/Na collisions has been carried out at low-keV energies,(i.e., 1-7 keV/amu). A pseudopotential has been used to represent the frozen Na^+ core. The dominant final states are found to be $He^+(n=3)$, populated by avoided curve crossings with the inital-channel curve in the region of R= 25-35 a.u. The calculated total charge-transfer cross sections are in fairly good agreement with existing measurements, lying about 20% above the experimental results.[5] An MO-ETF semiclassical (18-state) close coupling calculation of charge transfer to excited states of Li^{2+} in Li^{3+}/Li collisions has been carried out at low-keV energies. The dominant final states are found to be $Li^{2+}(n=4)$, populated by an avoided curve crossing with the initial-channel curve in the region of R=25 a.u. Such strongly selective excitation processes may be of interest in x-ray laser applications.

C) Quenching of intermediate-n Rydberg Na(ns) atoms in thermal collisions with rare gas atoms

In an effort to understand the mechanism for population of high-l states in Rydberg-atom collisions with atoms and molecules, we have applied a multi-state MO-ETF semiclassical close coupling method to Na(ns)/He collisions at thermal energies. The collision basis included 14 molecular states determined in a CI calculation in which the Na^+ core and the He atom were represented by pseudopotentials. We found, in agreement with the measurements of Gallagher and Cooke,[5] that depopulation of Na(6s) is dominated by downward transitions; whereas, for Na(9s) both upward and downward transitions are important. As to the question of high-l population, we found that for Na(9s), the strongest transition is a two-step process from 9s to 8p and on to 7f. Thus, there appears to be a propensity rule for s to f transitions; since higher-l Rydberg states of the n=7 manifold are nearly degenerate with 7f, we presume that very long-range coupling continues the ladder population of high-l states.[6] Studies of quenching by other rare-gas atoms and the implications for collisions with polar and non-polar molecules are underway.

Significant progress has been made on several other projects, and papers reporting these results have been presented at meetings and submitted (or in preparation) for publication.

Acknowledgement

The work reported here is supported in part by the U.S. Dept. of Energy, Office of Basic Energy Sciences, Division of Chemical Sciences and the Robert A. Welch Foundations and involves collaborations with experimental scientists at Rice and other institutions as well as a number of students and more senior theoretical scientists: Mineo Kimura (Argonne National Laboratory), who holds an adjunct faculty appointment at Rice University and plays a key role in many of this groups research projects; Jon Weisheit, Nely Padial, Bill Archer, Anil Kumar, Ronald Dixson, (Rice University); Paul Clark (Princeton University); James Cohen and Richard Martin (Los Alamos National Laboratory); Greg Hatton (Texaco Research, Houston); and visiting collaborators: T. Watanabe, H. Sato, N. Shimakura, K. Fujima, and W. Fritsch.

References:

1. L.K. Johnson, R.S. Gao, R.G. Dixson, K.A. Smith, N.F. Lane, Phys. Rev. A **40**, (1989).
2. B. Zygelman, A. Dalgarno, M. Kimura, and N.F. Lane, Phys. Rev. A **40**, 2340 (1989).
3. R. Hippler, H. Madeheim, H.O. Lutz, M. Kimura and N.F. Lane, Phys. Rev. A **40**, 3446 (1989).
4. R.D. Dubois and L.H. Toburen, Phys. Rev. A **31**, 3603 (1985).
5. T.F.Gallagher and W.E.Cooke, Phys. Rev. **A19**, 2161 (1979)
6. A. Kumar, N.F. Lane and M. Kimura, Phys. Rev. **A39**, 1020, (1989).

Five recent representative publications

M. Kimura and N.F. Lane, "Alignment and orientation of the excited H(2p) orbital following H + He collisions at intermediate energies," Phys. Rev. A **37**, 2900 (1988).

N.T. Padial, J.S. Cohen, R.L. Martin, and N.F. Lane, "Theoretical Penning electron-energy distributions for alkali-metal atoms: He($2^{1,3}S$) collisions with sodium and potassium," Phys. Rev. A **40**, 117-124; see also Phys. Rev. A **39**, 2715-17 (1989).

A. Kumar, N.F. Lane, and M. Kumura, "Quenching of low-lying Rydberg states of Na colliding with ground-state He," Phys. Rev. A. **39**, 1020 (1989).

B. Zygelman, A. Dalgarno, M. Kimura, and N.F. Lane, "Radiative and non-radiative charge transfer in He^+ + H collisions at low energy, Phys. Rev. A **40**, 2340-49 (1989).

L.K. Johnson, R.S. Gao, R.G. Dixson, K.A. Smith, N.F. Lane, R.F. Stebbings, and M. Kimura, "Absolute differential cross sections for small-angle H^+ -He direct and charge-transfer scattering at keV energies, Phys. Rev. A **40**, (to appear in 1989).

I. LOW ENERGY COLLISIONS INVOLVING MULTIPLY CHARGED IONS

J.R. Macdonald Laboratory
Kansas State University, Manhattan, KS 66506-2601

Capture Reaction Studies Using Molecular Ion Collisions

Tom J. Gray, I. Ben-Itzhak, J.C. Legg, Nabil Malhi, Kevin Carnes, Roger Key and Vince Needham

We report the current status of our work on second Born processes in capture reactions using low velocity ions in collisions with a thin CH_4 gas target. These experiments were designed to study both the standard forward angle Thomas peak and the large angle Thomas peak associated with double projectile scattering.[1] For the system $^{13}C^+ + CH_4 \rightarrow {}^{13}CH^+ + CH_3$ the large angle Thomas peak is predicted to occur at a scattering angle of 73° while the standard forward angle Thomas peak is predicted to be at a scattering angle of 4°. To date there have been no definitive measurements reported for the large angle Thomas peak. In studies involving electron capture[2] in ion-atom collisions, the results are inconclusive.

We have assembled a low energy (E≤10qkV) molecular ion accelerator using existing equipment in the laboratory. We have added optical elements and a Wien filter (for incident ion beam selection). The system has been tested with beam. Improvements in ion transport have been made through modifications in the ion source alignment components. The accel-decel feature of the gas target has been checked experimentally. Accel-decel allows for separation of mass-changed reaction products from mass-conserved final states in the post-collisions area following the target cell. Final system tests are in progress prior to initiation of benchmark tests based upon measuring angular distribution for $He^{++} + He \rightarrow He^+ + He^+$ and $He^{++} + He \rightarrow He^\circ + He^{++}$ collisions as reported previously by Gao *et al.*[3]

Formation of Doubly Charged Metastable Molecular Ion Ne_2^{2+} in Sub-MeV Stripping Collision $Ne_2^+ + Ar \rightarrow Ne_2^{2+}$†

I. Ben-Itzhak

We have performed an experiment in which the long-lived Ne_2^{2+} molecular ion was first observed.[4] The Ne_2^{2+} was produced by charge stripping a 900 keV Ne_2^+ beam in an Ar gas target. The mean lifetime of the Ne_2^{2+} was found to be larger than about 1 μsec. A calculation of the adiabatic potential curves of doubly charged molecular ions done by Penkina and Rebane[5] predicted that the Ne_2^{2+} is not bound in the electronic ground state since there is no minimum in the adiabatic potential curve. The experimental evidence for its existence suggests that either the detected Ne_2^{2+} was in an excited electronic state or that the theoretical approximation used for the Ne_2^{2+} gound state calculation is not accurate enough. A more detailed calculation of doubly charged rare-gas dimers, including electronically excited states and metastable states is needed. The Ne_2^{2+} molecular ion is the fifth observed doubly charged noble gas diatomic molecular ion. The ones reported before are: $NeXe^{2+}$, $ArXe^{2+}$, $NeKr^{2+}$, and He_2^{2+}.

† The research was done in collaboration with the atomic physics group at the Technion, Haifa, Israel; I. Gertner, D. Zajfman and D. Bortman.

KSU EBIS – Source Operation

M. P. Stöckli and C. L. Cocke

During the past year the KSU EBIS has been brought into operation. It has operated with electron currents up to 70 mA and electron beam energies between 2 and 6 keV. Beams of argon have been extracted and identified by charge state selection in charge states up to and including +18. The lower charge states, such as Ar^{+12}, are created in less than 10 ms, while containment times of about 2 sec are necessary to produce bare Ar.[6] Experiments have been carried out using the analyzed beam at the extraction energy of the source, with no post-acceleration of the ions. A post-acceleration beam line is being installed and is expected to be operational in the fall of 1990.[7,8]

KSU EBIS – Dielectronic Recombination in Heliumlike Ar

R. Ali, C. P. Bhalla, C. L. Cocke and M. Stöckli

We have observed dielectronic recombination of heliumlike ions in the KSU EBIS with the monoenergetic electrons in the source electron beam. The process has been detected in two ways:

1) X-Ray Yields: Ar K x rays from the source interior were detected with a Si [Li] detector aligned to view the confinement region of the source through the collector and gated to collect data only during the confinement time of the source. Ar K_α and K_β were resolved, with K_δ and higher x rays blended together by the detector resolution. The yields of these x rays as a function of electron energy reveal strong enhancements at the KLL, KLM and KLN dielectronic resonances. Work is in progress to compare the relative strengths of these yields in each x ray channel with theoretical predictions of the relevant resonant strengths and branching ratios.

2) Ion Yields: The dielectronic recombination resonances seen above in the x-ray yields alter in a major way the ionization equilibrium balance in the source plasma. On resonance, the inventory of Ar^{+16} ions in the source is depressed, and the inventory of Ar^{+15} ions enhanced, by the recombination of heliumlike ions with electrons in the beam. By extracting the ions periodically and measuring the relative intensities of the different charge states, we can sample the charge state distribution of the ions within the source plasma as a function of electron energy.

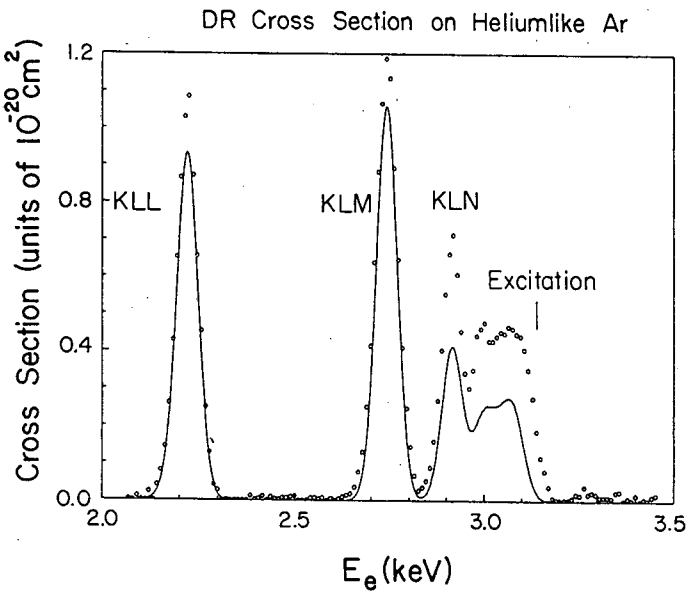

Fig. 1. Cross sections for dielectronic recombination on Ar^{+16}. Open circles: experimental from EBIS; solid line: theory (Ref. 10).

The effect of KLL, KLM, KLN and higher dielectronic resonances on the equilibrium balance is large. It can be shown that these data can yield absolute cross sections for dielectronic recombination provided the cross section for ionization of lithiumlike argon is known. We have normalized our data to calculated values of the latter cross section,[9] and obtain experimental DR cross sections in good agreement with theory for KLL and KLM resonances, but in poor agreement for higher resonances (see Fig. 1).[10]

References

1. K. Dettmann and G. Leibfried, Z. für Phys. 218, 1 (1969).
2. E. Horsdal-Pedersen, J. Phys. B 20, 785 (1987).
3. R.S. Gao, L.K. Johnson, D.A. Schafer, J.H. Newman, K.A. Smith and R.F. Stebbings, Phys. Rev. A 38, 2789 (1988).
4. I. Ben-Itzhak, I. Gertner, D. Zajfman and D. Bortman, submitted to Phys. Rev. A (1989).
5. N.N. Penkina and T.K. Rebane, Opt. Spectrosk. 62, 514 (1987). N.N. Penkina and T.K. Rebane, Opt. Spectrosk. 46, 454 (1979).
6. M.D. Stöckli, C.L. Cocke and P. Richard submitted to Rev. Sci. Instrum. (1989).
7. See Publication no. 1.
8. See Publication no. 5.
9. S. Younger, J. Quant, Spectrosc. Radiat. Transfer 2, 329 (1981).
10. R. Ali, C.P. Bhalla, C.L. Cocke and M. Stöckli, submitted for publication (1989).

List of Publications

1. "The KSU CRYEBIS"
   Martin P. Stöckli, J. Arianer, C.L. Cocke and P. Richard
   Nucl. Instrum. & Methods B40/41, 1020 (1989).
2. "Low Divergence Low Energy Recoil Ion Source"
   T.J. Gray, I. Ben-Itahak, N.B. Malhi, V. Needham, K. Carnes and J.C. Legg
   Nucl. Instrum. & Methods B40/41, 1049 (1989).
3. "Angular Differential Cross Sections in Low Energy Charge Exchange Collisions"
   C.L. Cocke
   Journal de Physique C1, 19 (1989).
4. "Magnetic Precision Alignment of a Long Horizontal Ultra-Straight Solenoid"
   Martin P. Stöckli, C.L. Cocke, J.A. Good and P. Wilkins
   Proceedings of "International Symposium on Electron Beam Ion Sources and Their Applications"
   ed. by Ady Hershcovitch, AIP, New York (1988) p. 281.
5. "The KSU CRYEBIS Program"
   Martin P. Stöckli, C.L. Cocke and P. Richard
   Proceedings of "International Symposium on Electron Beam Ion Sources and Their Applications"
   ed. by Ady Hershcovitch, AIP, New York (1988) p. 115.
6. "Non-Franck-Condon Transitions in Two-Electron Capture from D_2 by Low-Energy, Highly Charged Ar Projectiles"
   J.P. Giese, C.L. Cocke, W.T. Waggoner, J.O.P. Pedersen, E.Y Kamber and L.N. Tunnell
   Phys. Rev. A 38, 4494 (1988).

CHARGE TRANSFER NEUTRALIZATION OF C^+ AND O^+ AT LOW ENERGIES

by E. W. Thomas and T. F. Moran

School of Physics and Chemistry, Georgia Institute of Technology
Atlanta, Georgia 30332

We study charge transfer neutralization of C^+ and O^+ in a target gas differentiating between neutralization of the ground state

$$C^+ (^2P) + X \rightarrow C + X^+ \text{ and } O^+ (^4S) + X \rightarrow O + X^+ \quad (1)$$

and neutralization of the metastable states of the same ions

$$C^+ (^4P) + X \rightarrow C + X^+ \text{ and } O^+ (^2D, ^2P) + X \rightarrow O + X^+ \quad (2)$$

at energies from 10 to 500 eV. The motivation is to provide cross sections for use in the modelling of impurity transport at the edge of a thermonuclear plasma device. There is no existing data at these low energies applicable to the edge plasma potential. Existing data at higher energies (1,2,3,4,5) is often contradictory due, perhaps, to use of use of ion beams with mixed ground and metastable state composition. Ions of carbon and oxygen produced by electron impact dissociation of molecular species may be in both ground and metastable states so that a flux of ions from a source, or a plasma, is an unknown mixture of the two species. There is preliminary evidence that, at low energies, the metastable states have cross sections an order of magnitude higher than the ground state(1,2). Thus in the practical neutralization of an ion beam the behavior may be dominated by the metastables.

The ions are produced in a controlled energy electron impact source; in practice we normally use dissociative ionization of CO to provide both species of interest. Control of electron energy can alter the relative proportion of the species. For example it is possible to chose an energy sufficient to create ground state species but below the threshold for metastable formation. To diagnose the fraction of metastables in the beam we exploit the large differences between ground and metastable state attenuation. The flux of ions transmitted through a gas cell I, is related to the target density n (molecules/cc), cell length ℓ (cm), cross sections for neutralization of ground state species $\sigma(g)$ and cross sections for neutralization of metastable species (m) by

$$I = I_o (1-f) \exp - n\ell\sigma(g) + I_o f \exp - n\ell\sigma(m) \quad (5)$$

where I_o is the beam flux incident on the cell and f is the metastable fraction of the beam. Plotting Ln I/I_o as a function of n would give a curve that is the sum of two linear terms. If $\sigma(g)$ and $\sigma(m)$ differ greatly then the curve may be analyzed into the two separate components, the cross sections $\sigma(g)$ and $\sigma(m)$ determined from the slopes of the two terms and f determined from the ratio of the two components. The apparatus consists of an electron impact ion source, quadrupole mass analysis of the ions followed by transmission through a four cm long target cell and detection of transmitted ions by pulse counting. We assess the reliability of the cross section magnitudes to be ± 10% with a reproducibility of between 23% and 10% depending on energy.

For carbon ions there is only a single metastable state $C^+(^4P)$ and the ground state C^+ (^2P). Neutralization of C^+ (^4P) in H_2 has the surprisingly high cross section of 20 to 12 x 10^{-16} cm^2 at 10 to 500 eV; it joins smoothly to other data (1,3,4) at higher energies and changes by only a factor of three over the four order of magnitude energy range from 10 eV to 100 KeV. The ground state cross section is about 0.3 x 10^{-16} cm^2 at 10 to 100 eV and rising to higher energies. Again our data join smoothly to other data (1,3,4) with the cross section rising from 100 eV to reach 10 x 10^{-16} cm^2 at 100 KeV. Previous work by others (3) shows that both cross sections have the same value above 30 KeV.

The case of oxygen ions is potentially a little more complicated because there may be two metastable states, O^+ (^2D) and O^+ (^2P). Our attenuation studies reveal only a single contribution attributable to metastables. This probably means that both metastable cross sections are (almost) equal as has been suggested recently by Lavollee and Henri(6). An alternative, but unlikely, explanation is that only one species is present. The cross sections for neutralization in H_2 behave similarly to those for carbon. The metastable cross section is very high at about 10 x 10^{-16} cm^2 at 10eV and remains (with the benefit of previous work 2,3,4) almost invariant with energy to 100 KeV. The ground state cross section is much lower, 0.5 x 10^{-16} cm^2, at 10 eV rises with energy and equals the metastable cross section above 30 KeV.

Most previously published data sets (all at higher energies) are consistent with the present work (1,2,3,4) and also with each other. The major discrepancy is with the work of Nutt et al.,(5) which ranges in energy from 0.1 to 10 KeV; at low energies this agrees neither with the magnitudes of the other data (1,2) nor with its energy dependence. We have identified the source of the discrepancy and suggest that the data of Nutt et al.,(5) be treated with caution. One should also note that the very important cross sections for C^+ and O^+ on atomic H, published also by Nutt et al.,(5) were established directly by normalization, at each energy, to data for H_2; thus the data for H must also be regarded with caution.

The very high cross sections for C^+ and O^+ metastables in H_2 may be rationalized as due to an accidental resonance leaving H_2^+ in an excited vibrational state. Neutralization of the ground state involves a large energy defect and is therefore expected to have a small cross section.

We have shown that the metastable fraction of C^+ ions from dissociation of carbon containing molecules may range for 6 to 30% depending on source gas and source conditions; a significant factor is collisional de-excitation if source density is high. At any metastable fraction in this range the attenuation of an ion beam in the energy range 10 eV to 1000eV is dominated by the metastable component; the influence of the ground state is small or negligible.

The experiments are currently being extended to the same processes for an atomic H target using a cross beam configuration with H being obtained from a Slevin r-f discharge source. This is a far more complex experiment due to the presence of two species in the target (atomic as well molecular hydrogen) and two species in the ion beam (ground and metastable states). Here the ground state cases may be near resonant and the metastable states are far from resonance and may have smaller cross sections.

The attenuation technique will probably not work here and we shall instead detect the secondary ions of the target species for various metastable fractions in the projectile beam. These cases are potentially amenable to detailed theoretical analysis due to the well known energy level structures of the OH^+ and CH^+ systems.

REFERENCES

1. T. F. Moran and J. B. Wilcox, J. Chem. Phys. **68**, 2855 (1978).

2. T. F. Moran and J. B. Wilcox, J. Chem. Phys. **69**, 1397 (1978).

3. J. M. Hoffman, G. H. Miller, and G. J. Lockwood, Phys. Rev. A **25**, 1930 (1982).

4. R. A. Phaneuf, F. W. Meyer and R. H. McKnight, Phys. Rev. A **17**, 534 (1978).

5. W. L. Nutt, R. W. McCullough and H. B. Gilbody, J. Phys. B **12**, L 157 (1979).

6. M. Lavollee and G. Henri, J. Phys. B **22**, 2019 (1989).

PUBLICATIONS FROM THIS WORK

1. Yaodung Xu, T. F. Moran and E. W. Thomas, **"Charge Transfer Reactions of Ground $C^+(^2P)$ and Metastable $C^+(^4P)$ Ions with H_2 Molecules"**, Physical Review A (accepted).

2. **"Charge Transfer Reactions of Ground $O^+(^4S)$ and Metastable $O^+(^2D,^2P)$ Ions with H_2 Molecules"**, J. Phys. B. (submitted).

COLLISIONS OF LOW-ENERGY MULTICHARGED IONS

C. C. Havener, F. W. Meyer, and R. A. Phaneuf

Physics Division, Oak Ridge National Laboratory
Oak Ridge, Tennessee 37831-6372

Experimental investigations of low-energy interactions of multiply charged ions with neutral atoms and solid surfaces have continued. The experiments were performed at the ORNL-ECR Multicharged Ion Research Facility. The primary objective is to obtain a better quantitative understanding of such interactions at energies where the internuclear motion is slow compared to the orbital motion of the active bound electrons in the system, and a quasi-molecular description of the interacting system is appropriate. The ion-surface interaction studies have been carried out using apparatus on loan from the ORNL Solid State Division. Summaries follow of progress made during the past year in each area.

Merged-Beams Studies of Electron Capture by Multiply Charged Ions at Low Energies

At sufficiently low collision velocities, the attractive force due to the ion-induced dipole or polarization interaction between the reactants permits collisions to sample internuclear separations which are smaller than the impact parameter, and may lead to an enhancement of the cross section for ion-neutral reactions. Such an effect should be observable in electron capture collisions at eV energies if a favorable potential-energy curve-crossing exists for that system.[1] Recently-published[2] merged-beams experimental data from this laboratory for O^{5+} + H(D) collisions are suggestive of such an enhancement, although no such evidence was found in subsequent measurements[3] for N^{3+}, N^{4+}, and N^{5+}.

To extend these studies, and to provide benchmark data for theoretical calculations, cross sections have been measured for electron capture in O^{3+} + H(D) and O^{4+} + H(D) collisions at energies ranging from 1 eV/amu to 1 keV/amu. The merged-beams technique permits measurements to be made over a wide range of interaction energies, provides a large angular collection of reaction products, and produces independently absolute cross-section measurements. The data are presented along with other experimental and theoretical results in Figs. 1-3. For both O^{3+} + H and O^{4+} + H collisions, the merged-beams data join smoothly with other measurements[6] at the higher energies based on ion-beam - gas-target methods, and verify the normalization methods used for the latter. In the O^{3+} + H case, the measurements lie significantly below theoretical calculations[7,8] at energies below 100 eV/amu, where a significant contribution from capture to the 3p state is predicted. The measured cross section is in fact consistent with the calculation[8] for capture to the 3s state down to 10 eV/amu, and suggests that the calculation may overestimate the 3p contribution by roughly a factor of two. No calculations for O^{4+} + H are available in the energy range of the present measurements.

During the next period, the merged-beams technique will be extended to ions of higher initial charge, q. Since the polarization interaction scales as q^2, enhancement of the cross section at eV energies due to "trajectory effects" may be observable. Li-like Ne^{7+} is an interesting candidate for several reasons. Modifications to the ion optics of the ORNL-ECR source which are in progress are expected to provide the improvements in beam intensity and divergence which will be required

for such studies. Longer-range plans call for installation of a gas neutralizer and a field-ionizer to study electron-capture from excited hydrogen atoms.

Multicharged Ion-Surface Interactions

Exploratory investigations of grazing multicharged ion-surface interactions have also continued. A more detailed picture has begun to emerge of the role of inner-shell processes in the production of discrete Auger transition features in the emitted electron energy distributions. In a series of measurements[4,5] for 20-90 keV multicharged N, O, and F projectile ions interacting with Cu and Au single crystals, Auger emission from both the projectile and the target has been observed and identified. The projectile Auger electrons result from the decay of inner-shell vacancies either carried into the collision, or produced by vacancy transfer from empty outer projectile levels via pseudocrossings or rotational coupling of molecular orbitals. The latter mechanism may also lead to the creation of inner-shell vacancies in the target, which give rise to Auger emission characteristic of the metal. Detailed analysis of these features gives information about the time scales for neutralization of multicharged ions during their interaction with the metal surface.

While a number of improvements have been made to the present experimental arrangement for the study of multicharged ion-surface interactions, this apparatus does not permit more detailed follow-up investigations. Based on the promise shown by these exploratory studies, a separate proposal has been prepared and submitted to develop specific new apparatus and a vigorous comprehensive program to study ion-surface interactions under well-defined physical conditions. Goals of future studies include investigation of above-surface neutralization of very slow multicharged ions (which will require a deceleration stage), analysis of details of the observed Auger features which might give insight into the neutralization process, as well as the use of a combination of energy- and angle-resolved measurements to exploit the Doppler effect to obtain information about the origin of low-energy electrons (i.e., target or projectile). In all these studies, the target and projectile species, as well as the projectile charge will be systematically varied to ascertain the role of atomic structure and target bulk properties (e.g., valence-band electron density) in multicharged ion-surface interactions.

RECENT PUBLICATIONS

1. C. C. Havener, M. S. Huq, F. W. Meyer, and R. A. Phaneuf, "Electron Capture by Multicharged Ions at eV Energies," J. Phys. (Paris) **50**, Coll. C1, 7 (1989).

2. C. C. Havener, M. S. Huq, H. F. Krause, P. A. Schulz, and R. A. Phaneuf, "Merged-Beams Measurements of Electron-Capture Cross Sections for O^{5+} + H at Electron-Volt Energies," Phys. Rev. A **39**, 1725 (1989).

3. M. S. Huq, C. C. Havener, and R. A. Phaneuf, "Low-Energy Electron Capture by N^{3+}, N^{4+}, and N^{5+} from Hydrogen Atoms Using Merged Beams," Phys. Rev. A **40**, 1811 (1989).

4. C. C. Havener, K. J. Reed, K. J. Snowdon, N. Stolterfoht, D. M. Zehner, and F. W. Meyer, "Evidence for Production of Inner-Shell Vacancies in Slow Multicharged F Ions Interacting with a Cu Surface," Surf. Sci. **216**, L357 (1989).

5. F. W. Meyer, C. C. Havener, S. H. Overbury, K. J. Reed, K. J. Snowdon, and D. M. Zehner, "Inner-Shell Processes as Probes of Multicharged Ion Neutralization at Surfaces," J. Phys. (Paris) **50**, Coll. C1, 263 (1989).

OTHER REFERENCES

6. R. A. Phaneuf, I. Alvarez, F. W. Meyer, and D. H. Crandall, Phys. Rev. A **26**, 1892 (1982).

7. S. Bienstock, T. G. Heil, and A. Dalgarno, Phys. Rev. A **27**, 2741 (1983); T. G. Heil, S. E. Butler, and A. Dalgarno, Phys. Rev. A **27**, 2365 (1983).

8. M. Gargaud, R. McCarroll, and L. Opradolce, Astron. Astrophys. (in press).

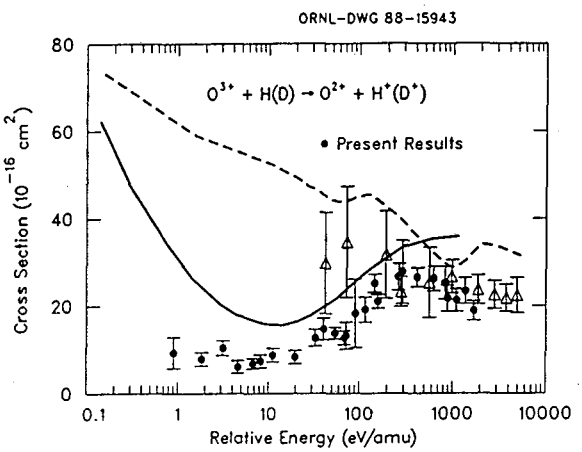

Fig. 1. Comparison of merged-beams data for O^{3+} + H(D) with other measurements (Ref. 6) and theoretical calculations (Refs. 7,8). The dashed curve is from Ref. 7, the solid curve from Ref. 8.

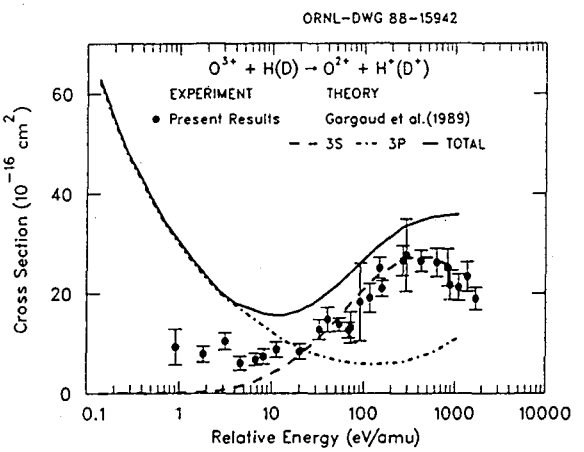

Fig. 2. Comparison of merged-beams data for O^{3+} + H(D) with theoretical calculations (Ref. 8) for capture into the 3s and 3p states.

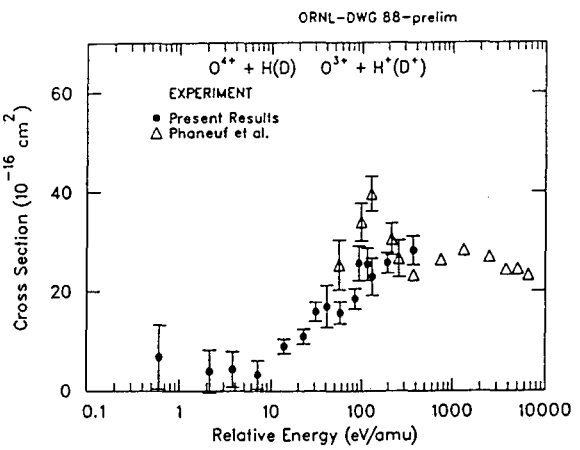

Fig. 3. Comparison of merged-beams data for O^{4+} + H(D) with other measurements (Ref. 6).

Nonlinear Dynamics of Multimode Lasers

M. G. Raymer
Department of Physics
University of Oregon

We are continuing our studies of multimode lasers, with an emphasis on understanding the relative roles of quantum noise and deterministic chaos in controlling the full-scale fluctuations of mode amplitudes.

I. Theoretical Modelling of Multimode Laser Dynamics

In a recent paper [1] we have carried out numerical simulations of the equations of motion presented in our earlier study of multimode lasers. [2] The equations describe mode coupling by gain saturation and four-wave mixing in a standing-wave cavity, and include the effects of quantum noise. In our earlier study we found experimentally and theoretically that quantum noise plays virtually no role in the dynamics when the laser is operated in excess of a few percent above threshold.[2] Our recent calculation, on the other hand, predicts that at pumping powers corresponding to 0.1% above threshold, or lower, the effects of quantum noise should become dominant. This result is important because it shows that a transition can occur between deterministically chaotic dynamics, well above threshold, to noise-driven dynamics, just above threshold.

This transition is evident in Fig. 1, which shows the correlation time τ_c of the mode intensities in a multimode dye laser, as a function of excess above threshold. The triangles show the prediction without quantum noise added, while the circles include quantum noise. The dashed line is a simple estimate based on rate equations.

This result is important, because the technique of intracavity laser spectroscopy (ILS) relies on having large values of τ_c to achieve its ultrahigh sensitivity. We have predicted a maximum value for τ_c, and thus a maximum sensitivity for ILS.

II. Experimental Studies

A. Ti:Sapphire Laser

We have constructed a Ti:Sapphire, and plan to study its dynamical behavior. Ti:Sapphire is an interesting new laser material which is receiving a lot of attention for its wide tunability in the near IR. We plan to study its dynamics near threshold in an attempt to observe the type of behavior shown in Fig. 1.

B. Micro-cavity Dye Lasers

One way to enhance the quantum noise in an effort to see the effects shown in Fig. 1 is to use a micro-cavity, ie. a cavity with very small mode volume. This effectively increases the field strength of the noise photons in the gain medium. We have designed and have had constructed a dye laser with cavity length equal to $50\,\mu$m. It consists of two high-reflectivity mirrors, spaced by $50\,\mu$m, with dye solution flowing between them.

A difference between this laser and the laser modelled in Fig. 1 is that in this case the lasing level's lifetime is shorter than the cavity lifetime, while in Fig. 1 the opposite is true. This will have quite a large effect on the dynamics, because of the phenomenon of relaxations ocillations. We plan to address this question theoretically.

References

1. Transition from quantum-noise-driven to deterministic dynamics in a multimode laser, M. Beck, I. McMackin, and M. G. Raymer, to appear in Phys. Rev. A (1989).
2. Instabilities and chaos in a multimode, standing-wave, cw dye laser, I. McMackin, C. Radzewicz, M. Beck, and M. G. Raymer, Phys. Rev. A 38, 820 (1988).

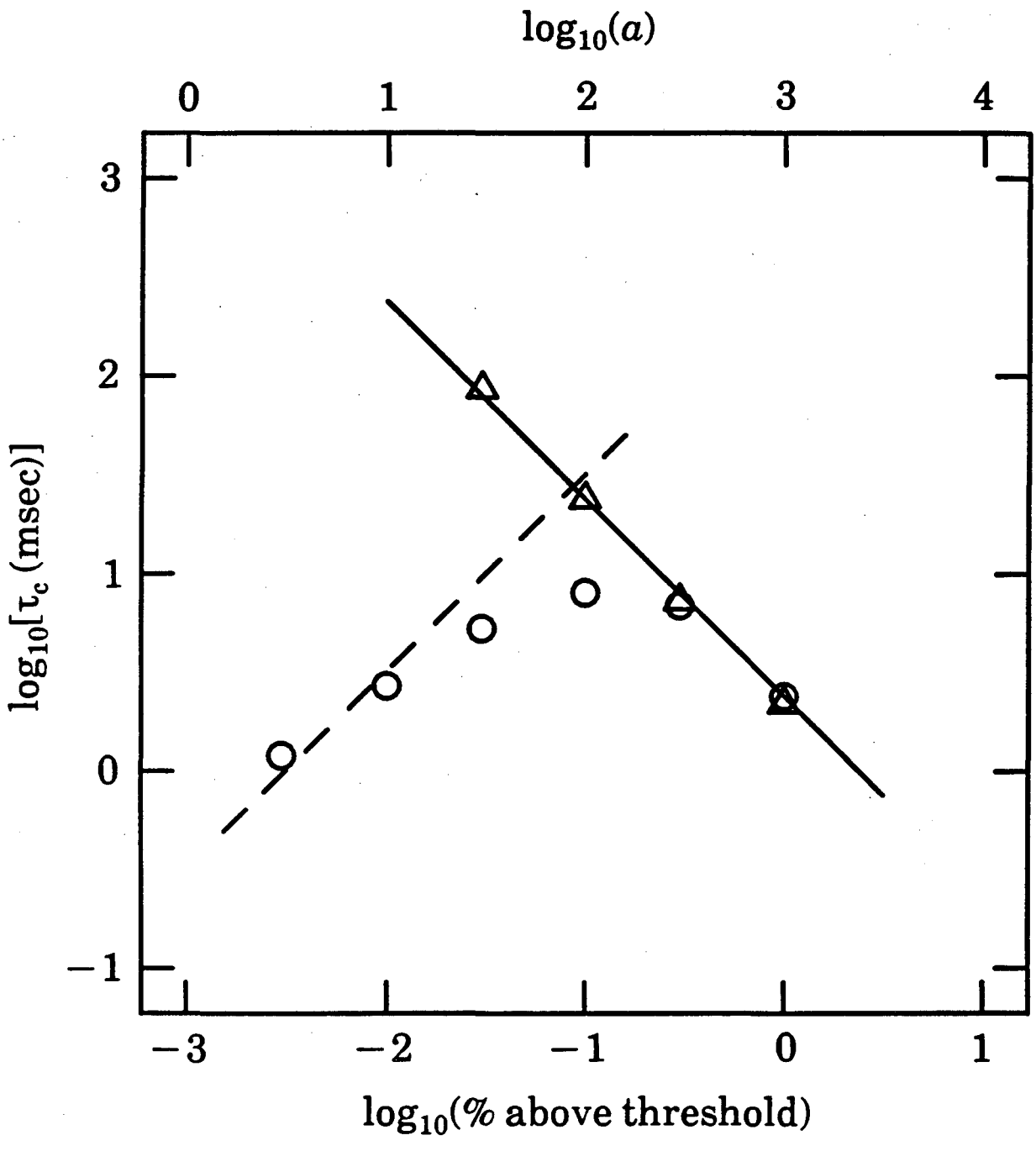

Fig. 1. Mode-intensity correlation time versus percent above lasing threshold. Triangles (circles) are without (with) quantum noise.

Statistical Fluctuations in Lasers

Rajarshi Roy
School of Physics
Georgia Institute of Technology
Atlanta GA 30332

Introduction:

The object of our research program is to investigate the interaction of signals and noise in laser systems and to develop accurate models of statistical fluctuations in lasers. The results of this investigation will not only extend our basic understanding of noise in nonlinear optical systems, but will aid the technologically important quest for stable light sources and ultra-sensitive detection techniques in optical communications and atom-field interactions.

Tunable lasers are essential for optical spectroscopy; they are also extremely important sources for optical communications, radar and information processing applications. Dye lasers, which are extensively used, and the very recent Titanium doped sapphire laser, both possess a wide tuning range and are excellent examples of tunable lasers. Ti: sapphire lasers (tuning range 700 nm to 1000 nm) will replace many infrared dyes (many of which are carcinogens and extremely toxic in nature) in the near future and promise to be one of the most important new lasers for scientific and technological applications. The laser operates at room temperature, and can be pumped by an Argon ion laser. We have recently built a continuous wave Ti: sapphire ring laser in our laboratory.

Novel applications of tunable lasers have great potential in research and industry. Two such novel applications, stochastic resonance and super-regenerative detection, have been demonstrated very recently in our laboratory. We present a brief account of progress over the past year on measurements of laser noise and studies of laser dynamics in our laboratory. Proposed research on these topics is also outlined.

Laser Noise Measurements:

New techniques for the measurement of laser noise source parameters (strength and time scale) have been developed in our laboratory and demonstrated on dye lasers.[1,2] The concept of first passage times was employed to separate the contributions of quantum and pump noise in single mode dye lasers and determine quantitatively the noise source parameters. The propagation of pump (primary) laser noise to the dye (secondary) laser has been studied and an accurate model developed for the power spectrum of secondary lasers. The intensity fluctuations and, very recently, the linewidth of single mode dye laser systems have been measured and their dependence on pump noise has been investigated. The linewidth measurements were performed with a supercavity Fabry-Perot interferometer and a digital oscilloscope, which allowed us to examine single scans and averaged spectra of the laser.

The results of these experiments allow us to accurately model the fluctuations (of the complex electric field) in dye lasers used for spectroscopic measurements and predict the results of spectral measurements performed with dye lasers on atoms and molecules. We have developed new computer algorithms to simulate accurately the fluctuations of laser fields. We have recently (in collaboration with G.S. Agarwal) calculated the spectrum of scattered light from an atom interacting simultaneously with a coherent field and a chaotic field of arbitrary bandwidth.

Stochastic Resonance:

A very counterintuitive phenomenon, stochastic resonance, was demonstrated for the first time on an optical bistable system (a bidirectional dye ring laser) in our laboratory.[3,4] In stochastic resonance, an enhancement of the response of a bistable system to a periodic modulation (by as much as 12 dB) is obtained on **addition** of noise with prescribed characteristics at the system input. This phenomenon occurs only in nonlinear systems, and could be used to enhance signal to noise ratios in optical systems that employ bistable devices for signal processing. We have analysed the occurrence of stochastic resonance in dye lasers; it will be very interesting to examine the situation for the Ti:sapphire laser, where the time scales and dynamics are very different.

The spontaneous emission level in these lasers is much lower than in dye lasers; however, the relative magnitudes of the upper level decay rate (4.5×10^5 sec^{-1}) and typical cavity decay rate (10^7 sec^{-1}) require that the dynamics of the population be fully incorporated in calculations. We will develop models for the Ti:sapphire laser that will include the effects of noise and nonlinear dynamics for both single mode and multimode lasers. We expect qualitatively different features of laser behavior to appear than in dye lasers.

Super-regenerative Detection:

We have shown that a Q-switched tunable dye laser can be used as an ultrasensitive detector (external signal fluxes corresponding to 0.2 photons on the average within the laser cavity) with a high degree of frequency selectivity (≈10 MHz).[5] A dynamic range of detection of over 70 dB has been demonstrated with an injected signal from a helium neon laser. The light from the He-Ne laser was injected into the cavity of a dye ring laser after attenuation by neutral density filters. The dye laser was tuned to resonance with the He-Ne laser and Q-switched with an acousto-optic modulator.

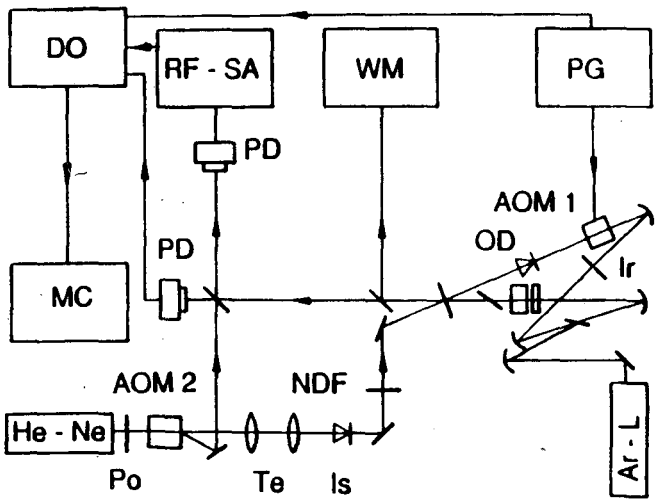

Fig.1 Experimental arrangement for the detection of weak signals via the decay of unstable states. Ar-L: Argon laser; Ir: iris diaphragm; OD: optical diode; AOM1, AOM2: acousto-optic modulators; PG: pulse generator; WM: wavemeter; NDF: neutral density filter; Te: telescope; Is: optical isolator; RF-SA: radio frequency spectrum analyser; PD: photodiode; Po: polarizer; He-Ne: helium neon laser; MC: microcomputer; DO: digital oscilloscope.

Injected signals were detected down to picowatt levels by measurement of the initiation times of the dye laser. The initiation time was defined as the time taken for the Q-switched laser intensity to build up to 2% of the steady state value. The dependence of the initiation time on the strength of the injected signal is logarithmic as shown below, resulting in the large dynamic range of the detection technique. The effect of detuning of the dye laser from the He-Ne laser wavelength was also investigated, and a bandwidth of ≈10 MHz was determined for the detector. Thus the technique is unaffected by any light present outside this range.

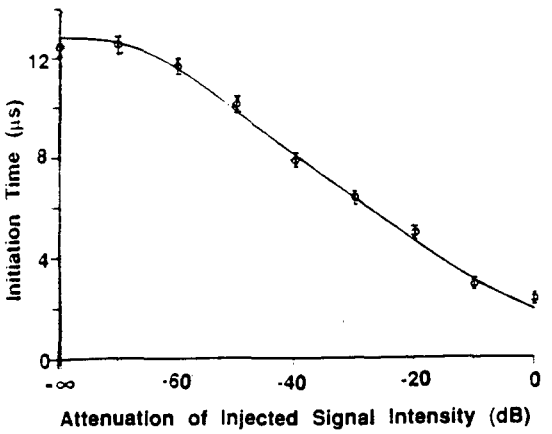

Fig. 2: Initiation time of the dye laser intensity vs. the attenuation of the injected (He-Ne) laser intensity. The solid line is obtained from stochastic simulations of a laser model developed by us with no fit parameters. The two lasers are tuned to resonance with each other.

We propose to demonstrate that it will be possible to increase the sensitivity of the detection technique and the dynamic range by four orders of magnitude with a Ti: sapphire laser. Design of detection systems with wide acceptance angles and the potential for wavelength multiplexing with an array of detectors make the technique worth investigating for certain types of optical communication applications, where it will have distinct advantages over conventional techniques.

Our research will benefit from the fact that F.T. Hioe, M.G. Raymer and S.J. Smith participate in this DOE program. There are several common points of interest and it is anticipated that there will be a strong synergism in our research with theirs, and that aspects of our work will complement their studies.

References:

1. "Colored Noise in Dye Laser Fluctuations", R. Roy, A.W. Yu and S. Zhu, in **Noise in Nonlinear Dynamical Systems**, edited by F. Moss and P.V.E. McClintock, Cambridge University Press, 1989.
2. "Power Spectra and Spatial Pattern Dynamics of a Ring Laser", A.W. Yu, G.P. Agrawal and R. Roy, J. Stat. Phys. **54**, 1223 (1989).
3. "Observation of Stochastic Resonance in a Ring Laser", B. McNamara, K. Wiesenfeld and R. Roy, Phys. Rev. Lett. **60**, 2626 (1988).
4. "Stochastic Resonance in a Bistable Ring Laser", G. Vemuri and R. Roy, Phys. Rev. **A39**, 4668 (1989).
5. "Detection of Weak Signals Via the Decay of Unstable States", I. Littler, S. Balle, K. Bergmann, G. Vemuri and R. Roy, submitted to Phys. Rev. Lett. (1989).

Population Transfer and Multiple Solitary Pulse Propagation in Many Level Atomic Systems

F. T. Hioe
Department of Physics
St. John Fisher College
Rochester, New York 14618

This report summarizes the new results obtained in the last twelve months from July 1, 1988 and the research work in progress. We have obtained a number of interesting results concerning various aspects of a multilevel quantum system interacting with an intense laser field. Among them, we have found a simple analytic solution that suggests a novel method for population transfer in a three-level system driven by delayed pulses, which is found to fit very well with the result of a recent experiment. Also we have found various specific conditions and pulse shapes, depending on the atomic level structures, that would permit simultaneous optical pulses to propagate through an N-level atomic medium without attenuation.

(1) Population Transfer in Three-State Systems

The problem of efficient transfer of population to thermally unpopulated atomic or molecular levels, such as high lying Rydberg states or molecular vibrational levels, that are not accessible by one photon transitions, is of crucial importance in many atomic physics projects. Even though a three-state system involving a two-photon transition of population can be readily solved numerically for any given condition, questions such finding the optimum conditions for complete population transfer from state 1 to state 3, or for complete return of population from state 1 to state 1, are best analyzed and answered from solving the problem analytically. We have derived a number of analytic solutions for the three-state systems which are applicable to an infinite variety of incident pulse shapes and detunings, and we have obtained the conditions, in each case, for complete population transfer from one state to another, and for complete population return which is important for the problem of multiple soliton propagation.

A remarkable and unexpected result emerges from these analytic results. To achieve an efficient transfer of population from state 1 to state 3 that would not be sensitively dependent on the input

parameters such as the laser pulse shapes, intensities and frequency modulation, the atoms or mulecules should interact first with the laser pulse for the 2-3 transition and then with the laser pulse for the 1-2 transition, the pulses being overlapped in time. That is, a counter-intuitive procedure is suggested. We also showed that as the pulse strengths are increased, (i) this procedure approaches that of adiabatic rapid passage, and (ii) it minimizes the occupation probability of the intermediate state (state 2) and thus makes the efficiency of population transfer from state 1 to 3 relatively unaffected by radiative or collisional damping of the intermediate level 2. This analytic prediction has been found to fit very well with the result of recent experiments performed by Prof. K. Bergmann and his collaborators at the University of Kaiserslautern in West Germany in which they carefully analyzed the excitation of sodium molecules by two spatially displaced laser beams.

A related theoretical prediction, involving also a counter-intuitive way of varying the one-photon detuning but in which concurrent instead of delayed pulses were used, was proposed by us as long ago as in 1983. An experimental test of the efficiency of this procedure can be done in experiments involving the production of hydrogen atoms in the high angular momentum states. We predict that an efficient population transfer can be accomplished by either tuning the frequency of the incident laser pulse or by appropriate Stark shifting the levels by a varying external electric field in such a way that the interaction is first between the uppermost pair of levels and last with the lowermost one. This is again a counter-intuitive interaction sequence.

(2) Simultaneous Optical Soliton Propagation

Considerations of various types of dynamic symmetries have led us to the discovery of various specific conditions which would permit the lossless propagation of multiple simultaneous optical solitons through an atomic medium consisting of N transition levels. The lossless soliton propagation generally requires several conditions: For the N dipole-connected energy levels of each atom of the atomic medium whose energies are ordered in a certain way, the dipole moments have to satisfy certain relations; the atomic medium must be partially excited out of its ground state initially; and the pulse amplitudes have to satisfy appropriate relations. In addition to the well known hyperbolic-secant pulse shapes which are

found to be appropriate for some specific conditions, we have found analytically a whole new set of "higher order" soliton pulse shapes appropriate for other conditions. For example, one of these higher order solitons has a pulse shape in terms of $\zeta = t - z/v$, where z is the direction of propagation and v its velocity, proportional to

$$\frac{\sqrt{8}}{\tau} \frac{\cosh(-\zeta/\tau)}{8 + \sinh^2(-\zeta/\tau)}$$

where τ is the pulse length. This pulse has two maxima at $\zeta/\tau = \pm \ln(\sqrt{6} + \sqrt{7}) = \pm 1.628307$.

Proposed research for the coming year

We are continuing our analytic work on determining the optimum conditions for population transfer in terms of the pulse separation and pulse strengths of the two delayed pulses for the excitation of three-level systems. We are also going to study the adiabatic rapid passage involving multiple delayed pulses in the counter-intuitive sequence for a general N-level system.

We have begun to study the above-threshold ionization (ATI) of a model atom interacting with an intense laser field. We are interested in distinguishing features of ATI which are dependent of from those which are independent of the potential. The problem of population trapping will also be studied.

The group theoretical approach to the problem of dynamic symmetries which we initiated and which have produced abundant new, unexpected results and provided much insight to many problems will be continued. We will explore other dynamic symmetries in the multiphoton excitation process.

Publications

1. C.E. Carroll and F.T. Hioe, Two-photon resonance in three-state model driven by two laser beams, J. Phys. B22, 2633 (1989)
2. F.T. Hioe, Lossless propagation of optical pulses through N-level systems with Gell-Mann symmetry, J. Opt. Soc. Am. B6, 1245 (1989)
3. F.T. Hioe, Lossless propagation of optical pulses through N-level systems with SU(2) symmetry, J. Opt. Soc. Am. B6, 335 (1989)
4. F.T.Hioe, Certain stability type and integrable two-dimensional Hamiltonian systems, Phys. Rev. A39, 2628 (1989)
5. F.T. Hioe and C.E. Carroll, Coherent population trapping in N-level quantum systems, Phys. Rev. A37, 3000 (1988).

Spin Dependence in Electron — Atom Collisions

M. H. Kelley, J. J. McClelland, and R. J. Celotta

Radiation Physics Division
National Institute of Standards and Technology
Gaithersburg, MD 20899

This experimental project centers on the study of low energy electron–atom collisions in which the colliding particles are prepared in well defined states via laser optical pumping. This type of state resolved experiment provides substantially more information about the scattering process than measurements of the scattering cross section alone. Our primary interest is the direct observation of the role played by electron spin, through exchange and the spin-orbit interaction, in elastic and inelastic collisions. Additionally, we study the collisional transfer of angular momentum in inelastic scattering.

The experimental apparatus consists of crossed beams of electrons and sodium atoms, each of whose initial state is prepared through the use of optical pumping techniques. Both electrons and atoms are spin polarized either parallel or antiparallel to a quantization axis perpendicular to the horizontal scattering plane. The target atoms are pumped with circularly polarized laser light tuned to a particular hyperfine resonance line. The electrons are generated by photoemission in a GaAs polarized electron source with circularly polarized incident photons. The intensity of electrons scattered through some angle is measured with a channel electron multiplier as a function of the incident electron energy and initial state of the incident electrons and atoms. At each scattering angle, the scattering intensity is recorded for each of the four possible relative spin orientations of the incident beams. These intensities are combined into asymmetries, which are directly related to the normalized differences between the scattering cross sections for the various relative spin orientations.

Our measurements to date have included studies of both elastic scattering from ground state atoms, and studies of the 3S–3P transition. Our elastic studies are performed with the optical pumping region "upstream" in the atom beam, so the sodium atoms in the target region are spin-polarized in the ground state. The inelastic studies are done "superelastically," by placing the optical pumping region directly in the scattering center, and detecting only those electrons which de-excite the laser-excited atoms, thereby gaining the 2.1 eV excitation energy of the 3P state. Superelastic measurements are equivalent to the time inverse of coincidence measurements of the inelastic process, and hence yield the same sort of state-to-state scattering information.

The aim of this work is to provide as complete a set of data as possible on electron–sodium scattering at a few specifically chosen incident energies. Thus we are concentrating on generating sets of spin- and angular momentum-resolved elastic and superelastic results at the same energies (in fact, the superelastic data are obtained at an incident energies 2.1 eV lower than the elastic results, since they are "time-inverse" studies). Eventually, we hope to probe, in a state-selective manner, as many inelastic and superelastic transitions in the sodium atom as are feasible, so a complete comparison with *ab initio* calculations can be made.

In previous years, we have measured elastic scattering at 54.4 eV, and superelastic scattering at 52.3, 17.9 and 2 eV. This year has been spent for the most part on elastic scattering. To accompany the earlier 17.9 eV superelastic results, we have measured the elastic spin asymmetry at 20 eV incident energy, shown in Fig. 1. The spin asymmetry is defined as "antiparallel" minus "parallel" intensities divided by the total intensity, and represents the normalized difference between singlet and triplet scattering cross sections. The curve shows that the asymmetry

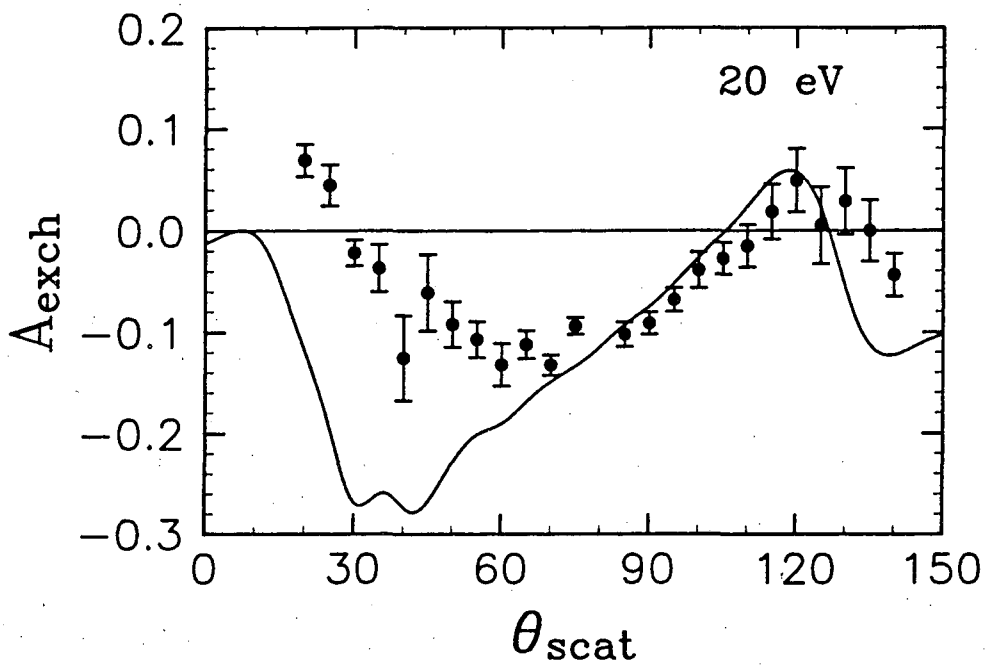

Figure 1: Elastic spin asymmetry vs. scattering angle. (•) experiment; (——) theory (D.H. Oza, Phys. Rev. A **37**, 2721(1988).

is quite large in magnitude and negative in sign over most of the angular range. A value of $-1/3$ corresponds to pure triplet scattering, so it appears that the triplet cross section is quite dominant over the singlet at most angles. The solid line in the plot is a 2-state close-coupling calculation by Oza, which, though qualitatively in agreement with experiment, shows some significant differences.

In previous elastic measurements at 54.4 eV, we obtained the surprising result that spin-orbit and exchange effects can be of the same magnitude in as light a scattering target as sodium. This raises the possibility that a "joint" asymmetry may exist, consisting of the difference between scattering from spin "up" and "down" atoms with unpolarized electrons. This asymmetry, predicted but never observed, is zero if either the spin-orbit effect or exchange alone is present, but can be non-zero if both are significant. We have conducted a systematic search for this joint asymmetry at incident energies of 20, 54.4, and 70 eV, and the results are shown in Fig. 2. 70 eV was chosen as an energy where the cross section has the deepest minimum, so any small effect would be more visible. We have shown that the "joint" asymmetry is smaller than 1% at all the energies and angles that were measured, and hence it is unlikely that this is a significant effect in sodium.

Current efforts are concentrated on measuring elastic scattering at 10 eV incident energy, combined with superelastic measurements at 7.9 eV. The next step is to measure elastic scattering below the ionization threshold, specifically at 4.1 eV to go with the earlier superelastic results at 2.0 eV. Other energies below the ionization threshold will then be probed, since dramatic effects can be expected in this energy region. In the coming year, we also expect to replace our retarding field energy analyzer on the electron detector with a hemispherical analyzer, which will enable us to probe other inelastic transitions in sodium.

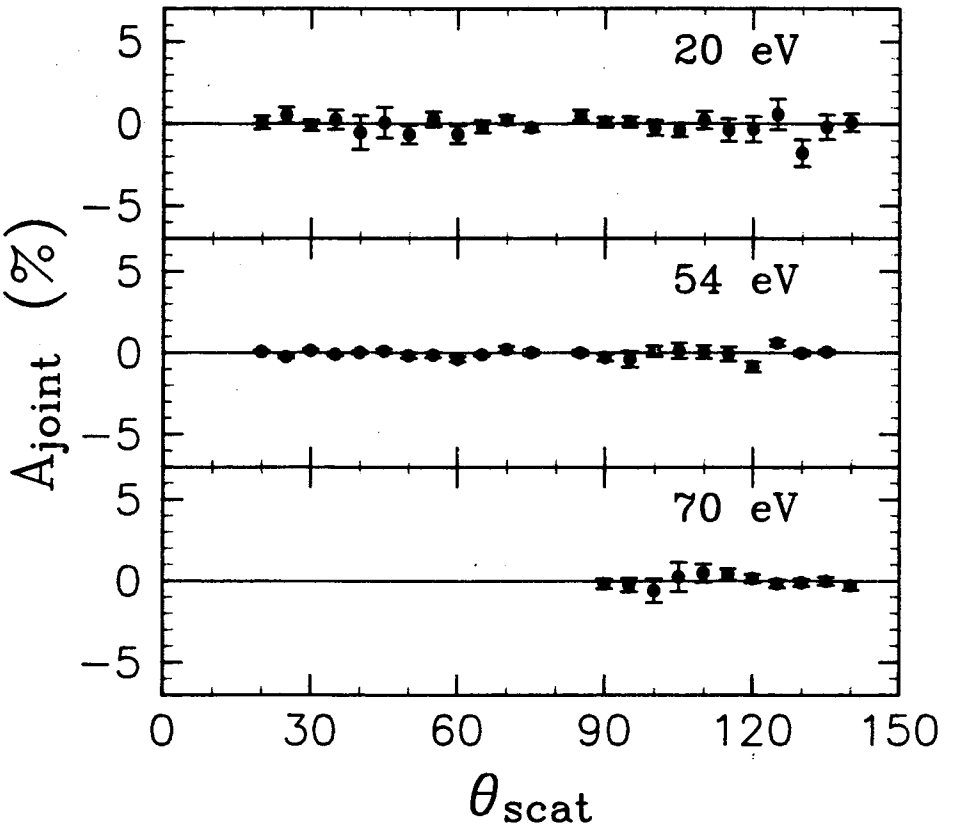

Figure 2: Joint asymmetry vs. scattering angle.

Recent Publications Relevant to this Project

1. J.J. McClelland, S.J. Buckman, M.H. Kelley and R.J. Celotta, "Search for a Joint Spin-orbit and Exchange Asymmetry in Elastic Electron Scattering from Spin-polarized Sodium," (submitted to J. Phys B).

2. J.J. McClelland, M.H. Kelley and R.J. Celotta, "Superelastic Scattering of Spin-polarized Electrons From Sodium," Phys. Rev. A **40**, 2321–2329 (1989).

3. J. J. McClelland, M. H. Kelley, and R. J. Celotta, "Spin-Orbit and Exchange Effects in Low Energy Elastic Spin-Polarized Electron Scattering from Spin-Polarized Na," Phys. Rev. Lett. **58**, 2198–2200 (1987).

4. J. J. McClelland, M. H. Kelley, and R. J. Celotta, "Large Angle Superelastic Electron Scattering," J. Phys **B20**, L385–L388 (1987).

5. I. V. Hertel, M. H. Kelley, and J. J. McClelland, "Analysis of Collisional Alignment and Orientation Studied by Scattering of Spin- Polarized Electrons from Laser Excited Atoms," Z. Phys. **D6**, 163–183 (1987).

KINETIC STUDIES FOLLOWING STATE-SELECTIVE LASER EXCITATION

John W. Keto
Physics Department
University of Texas at Austin, TX 78712
September 1989

Introduction

We have now completed studies of state-to-state electronic energy transfer from excited atoms of xenon to chlorine. These reactions are relevant to the modeling the kinetics of the XeCl excimer laser. Energy transfer from excited rare gases to chlorides are expected to occur by a harpoon reaction,

$$Xe^* + Cl_2 \rightarrow Xe^+ + Cl_2^- \rightarrow XeCl^* + Cl, \qquad (1)$$

where transfer from the reactant channel to the ionic intermediate occurs by charge transfer. Since the crossing radius is expected to increase with increasing excited state energy, one might expect in a simple model that the reaction rate would be larger for higher lying excited states. In contrast as the radius of the crossing R_c increases, the probability for charge transfer decreases as $\exp(-\alpha R_c)$. In order to examine this effect in detail, we have extended our previous measurements to excited atoms over a broad energy range and made direct comparison between the experiments and quantum calculations of the reaction rates.

We have also made measurements of deactivation cross sections and radiative lifetimes for excited Xe atoms with 5d, 6p, 6p', 7p, and 7p' valence electrons in argon buffers. These results are relevant to kinetic models of the infrared xenon laser; and they are a significant improvement in the precision of the known radiative lifetimes.

II. Experiment

Xe* is excited in a two photon transition[1] using a frequency doubled dye laser. Product channels are observed by their fluorescence, or by laser induced fluorescence using a second laser of different color. The time dependence of the fluorescent light intensity is determined by the distribution of arrival times for the first photon following excitation. By measuring the exponential decays as a function of pressure, we obtain a Sturm-Volmer plot to determine the reaction rates,k, $\nu = \nu_{rad} + k[n]$. We find the decay rates for excited Xe* to be described by

$$\nu_q = \nu_0 + k^{(2)}_{Xe}[Xe] + k^{(3)}_{Xe}[Xe]^2 + k^{(2)}_{Cl}[Cl_2] + k^{(3)}_{Cl,Xe}[Xe][Cl_2] \qquad (2)$$

where ν_0 is the radiative rate and $k^{(2)}_i$, $k^{(3)}_i$ represent bimolecular or termolecular reaction rates. In Table I, we summarize the rates measured for energy transfer to Chlorine[i] in the form of thermally averaged cross sections Shown for comparison are reaction rates calculated from cross sections equal to πR_c^2, where R_c is the crossing radius of the $Xe^* + Cl_2$ potential curve and the $Xe + Cl_2^-$ curve which is determined using the electron affinity at the Cl_2 equilibrium distance. The data agree nicely with this simple harpoon model for higher ionization energies; for states with smaller ionization potentials this simple model grossly overestimates the cross sections when compared with the experiment. This shows the effect of the reduced charge transfer probabilites expected at larger crossing radii.

III. Reaction Model

A harpoon reaction model employing multiple crossings based on the formalism of Bauer et al [2] and Gislason and Sachs[3] was developed to explain the experimental cross sections.[ii] The model calculates the Landau-Zener transition probability for each intermediate ionic crossing with the reactant surface. The transition matrix elements H_{12} are represented as a product of the electronic interaction (modeled by the empirical result of Olson et al [4] and a Frank-Condon factor for the $Cl_2 \rightarrow Cl_2^-$ transition. The model predicts near unit probability for a transition to the ionic surface for impact parameters less than 20Bohr, and once transfer occurs, the pair is captured by dissociation of Cl_2^- to form XeCl*. A summary of the cross sections for the Olson model is also presented in Table I.

Table I. Reaction Cross-Sections for Xe* with Cl_2

State	IP(eV)	σ(Å²) v = 0 Olson	v = 1 Olson	(300°K) Olson	H12 fitted	(πR_c^2)	(Experimental)
$6p[5/2]_2$	2.44	384	422	386	397	321	329 ± 8
$6p[3/2]_2$	2.30	457	442	456	468	393	406 ± 5
$6p[1/2]_0$	2.19	551	461	545	566	472	474 ± 5
$6p'[1/2]_0$	2.29	475	449	474	488	403	593 ± 27
$6p'[3/2]_2$	2.37	418	432	419	430	366	504 ± 13
$7p[5/2]_2$	1.17	108	574	136	840	27,838	831 ± 52
$7p[3/2]_2$	1.13	80	491	105	744	52,433	978 ± 32
$7p[1/2]_0$	1.11	69	453	92	697	76,748	799 ± 22
$5d[1/2]_1$	2.21	534	457	529	546	472	282 ± 10

Detailed examination of plots of the cross section as a function of impact parameter[ii] shows that the exponential decrease in H_{12} begins to decrease the cross section relative to πR_c^2 obtained in the calculation for the higher lying states. The Olson empirical model produces cross sections which decrease too rapidly with decreasing ionization probability, suggesting that the model uses an exponential coefficient which is too large for xenon $5p^5np$. In developing his model, Olson did not expect accuracy greater than observed in Table II. We have fitted an exponential coefficient using a form for the matrix elements suggested by Smirnoff.[ii] This model gives a better agreement with experiment over the whole energy range. A model including dependence of angular momentum could use quantum defect calculations to determine the charge transfer probabilities.

IV. Termolecular Reactions

The termolecular rate, $k^3_{Cl\ Xe}$, can be determined by plotting the difference rate, $\Delta\nu$,

$$\Delta\nu = \nu_q - \nu_0 - k^2_{Xe}[Xe] - k^3_{Xe}[Xe]^2 - k^2_{Cl}[Cl_2] - k^3_{Cl}[Cl_2]^2 ,$$

as a function of xenon pressure at fixed chlorine pressure. The quench rate due to the xenon component of the mixture was measured previously in our laboratory, and recently improved.[iii] We used a large Cl_2 pressure of 10 Torr in order to emphasize the effects of $k^3_{Cl\text{-}Xe}[Xe][Cl_2]$ over the quenching caused by xenon. The termolecular rates are reported

Table II. Termolecular rates ($k^3_{Cl\text{-}Xe}$) for Xe* $5p^56p$ with Cl_2

State	Termolecular rates (10^{-28} cm^6/sec) (This work, Xenon)	(This work, Argon)
$6p[1/2]_0$	3.5 ± 0.5	<0.5
$6p[3/2]_2$	1.4 ± 0.5	<0.1
$6p[5/2]_2$	1.8 ± 0.5	<0.1

in Table II. The errors include all the uncertainties in measuring the other quench rates. For pure xenon buffer gases, while for argon buffers we observe no termolecular reactions. We have developed a model agree with these results.[ii] The model assumes that the reaction cross section is enhanced by reducing the ionization potential of the excited atom during collisions with the third body. We plan further tests of the model by measuring the termolecular rates in krypton buffers.

VI. Quenching of Xe* $5p^56p$ Atoms in an Argon Buffer gas

We extended the measurements reported in last years abstract to states of lower ionization potential.The results are summarized in Table III. The measured radiative lifetimes for the states are reported in Ref. iii.

Table III. Total collisional quench rates for Xe* $5p^5np,np'$ (n=6,7) in xenon.

	Bimolecular rates ($10^{-12}cm^3/sec$)			
state	This work	Setser	This Work	Setser
	Xenon	Xenon	Argon	Argon
$6p[5/2]_2$	116 ± 3	96 ± 3[c]	82 ± 4.0	82 ± 5.0[c]
$6p[3/2]_2$	101 ± 3	82 ± 5[c]	40 ± 2.0	47 ± 5.0[c]
$6p[1/2]_0$	5.9 ± 0.5	5.8 ± 0.5[c]	200 ± 4.0[a]	140 ± 10[c]
$5d[1/2]_1$	197 ± 26[a]	···	5.9 ± 0.4[b]	30 ± 5.0[c]
$7p[5/2]_2$	462 ± 9···	278 ± 62[d]	259 ± 20	240 ± 20[f],340 ± 70[g]
$7p[3/2]_2$	522 ± 8···	282 ± 70[e]	348 ± 32	230 ± 20[f],300 ± 30[g]
$7p[1/2]_0$	493 ± 8	417 ± 108[d]	256 ± 34	190 ± 30[f]
$6p'[3/2]_2$	426 ± 10	262 ± 170[d]	179 ± 14	160 ± 2[f],140 ± 10[g]
$6p'[1/2]_0$	423 ± 8	262 ± 170[d]	247 ± 14	280 ± 30[f]

a) extracted from zero argon pressure intercepts by combining the argon quenching data of the Xe*$6p[1/2]_0$ at 828.2nm and $5d[1/2]_1$ at 125nm. A different intercept for the argon quenching curves was obtained for each different xenon pressure.

b) extracted from the slow component in the Xe* $6p[1/2]_0$ decay curves. See Ref.iii

c)J.K. Ku and D.W. Setser, J. Chem. Phys. **84**, 4304(1986).

d) L. Allen, D.G. Jones, and D.G. Schofield, J. Opt. Soc. Am. **59**, 842(1969).

e) Weighted mean value of two measurements of Allen et al.

f)H. Horiguchi, R.S.F. Chang, and D.W. Setser, J. Chem. Phys. **75**, 1207(1981).

g) G. Inoue, J.K. Ku, and D.W. Setser, J. Chem. Phys. **81**, 5760 (1984).

VI. Future Work

We are repeating the termolecular studies for harpoon reactions of Xe and Cl_2 in krypton buffers. We are investigating laser assisted reactions of Xe and Cl_2 pairs both as collision complexes and as bound dimers in a supersonic beam. We are measuring high resolution spectra of rare gas dimers and clusters formed in a supersonic jet using both photoionization and laser induced fluorescence.

VII. References

1. T. D. Raymond, N. Bowering, C.Y. Kuo and J. W. Keto, Phys. Rev. **A29**, 721 (1984).
2 E. Bauer, E. R. Fisher, and F. R. Gilmore, J. Chem. Phys. **51** ,4173(1969).
3. E. A. Gislason and R. Sachs, J. Chem. Phys. **62**, 2678(1975).
4. R. E. Olson, F. T. Smith, and E. Bauer, Appl. Opt. **10**, 1848(1971).

VII. Publications

i. M. R. Bruce, W. B. Layne, Enno Meyer, and J. W. Keto,"Reactive Quenching of Two-Photon Excited Xenon Atoms by Cl_2", J. Chem Phys. **92**, in press.

ii. M. R. Bruce, W. B. Layne, and J. W. Keto,"A Multichannel Harpoon Model for Reactive Quenching of Xe by Cl_2", J. Chem Phys. **92**, in press.

iii. M. R. Bruce, W. B. Layne, A. Whitehead, and J. W. Keto, "Radiative Lifetime and Collisional Deactivation of Two-Photon Excited Xenon in Argon and Xenon", J. Chem Phys. **92**, in press.

iv. Roger H. Taylor, Jacek Borysow, and J. W. Keto, "*Raman-Induced Kerr Effect Spectroscopy of Rare Gas Dimers and Molecular Ions* ", Proceedings of the 4th Int'l Laser Science Conf.,Atlanta, Ga., AIP Physics Conf. Proceedings No. **146**, Advances in Laser Science-4, Eds: W.C. Stwalley and Marschall Lapp, New York, 1989.

v.Thomas L. Gaussiran II, Roger H. Taylor, James L. Higdon, and John W. Keto, "*A Multi-pass Prism Monochromator for Coherent Raman Spectroscopy*", Appl. Optics **28**, 1657-1660(1989).

Oxygen spectroscopy, autoionizing lineshapes, and oscillator strengths*

Arlee Smith
Division 1164
Sandia National Laboratories
Albuquerque, NM 87185

I. Oxygen measurements

Our knowledge of the autoionizing levels of atomic oxygen has grown considerably in recent years. Spectroscopy of O discharges has identified a large number of levels and laser excitation spectroscopy has characterized the linewidths and ionization branching ratios for a few of them. Consequently, the odd parity autoionizing levels are relatively well known. The even parity levels are not. Only a few of these levels are tabulated and their widths have not been measured. We are using laser ionization methods to locate and characterize a few key even parity levels. We are also measuring the oscillator strengths for a core changing transition and for transitions from excited states to autoionizing levels. Our primary motive is to identify and precisely characterize efficient laser ionization pathways for atomic oxygen.

Singly ionized O has three low energy levels, ^4S, ^2D, and ^2P. The S state has the lowest energy while the D and P states form the excited ion core for the autoionizing levels of interest to us. These are formed by the addition of an np electron. Twelve series are expected. They are designated $(^2D)np'\ ^{3,1}P,D,F$ and $(^2P)np''\ ^{3,1}S,P,D$. We have demonstrated in preliminary experiments that we can excite the lower lying levels in these series.

We generate an effusive beam of atomic oxygen by passing a mixture of He and O_2 through a microwave discharge. Pulse-amplified single-mode lasers are used to two-photon excite the ^3P ground state to $3p\,^3P$ transition then to pump the $3p\,^3P$ - $3s'\,^3D$ core changing transition and finally to excite the autoionizing levels. The ions are measured using a time-of-flight mass spectrometer. In experiments to date, we have shown that the $3p'$ F and D levels are both narrow (<0.1 cm^{-1}) and both ionize efficiently. Our estimate of the absorption cross sections for $3s'\,^3S$ - $3p'\,^3F$ is $5x10^{-13}$ cm^2 with an autoionizing lifetime of about 200 ps. Our measured the $3p\,^3P$ - $3s'\,^3D$ oscillator strength is 1.7 x 10^{-4} with an uncertainty of a factor of two. We

*This work was performed at Sandia National Laboratories and supported by the U.S. Department of Energy under contract no. DE-AC04-76DP00789 for the Office of Basic Energy Sciences, Division of Chemical Sciences.

have also located the $4p'\,^3F$ state for the first time.

These measurements were made using an actively stabilized Littman laser (see below) to pump the two-photon step. Because this Doppler free transition very narrow, the small pulse-to-pulse frequency jitter in this laser introduces noise on our ion signals that make precise measurements impossible. We have replaced the Littman laser with a cw ring dye laser and the noise is greatly reduced. We expect this will allow much more precise measurements of linewidths and cross sections. We intend to repeat the measurements cited above and to extend them other even parity autoionizing levels.

II. 130nm coherent source development

In past years we have detailed our progress in developing a more efficient coherent vacuum ultraviolet source based on sum-frequency mixing in Hg vapor. Our goal is a 130 nm source (the resonant wavelength for O) with near diffraction limited beam quality and high mixing efficiency. We developed a recipe for achieving these goals based on our measurements of Hg dipole matrix elements and a computer model of the mixing process. Over the past two years, our predictions have been validated by a demonstration experiment at Spectra Technology Inc. with mixing efficiency exceeding 7% in a high quality beam with a pulse energy of 1.5 mJ in a 2 ns pulse. In the past year the primary development has been the indentification of the ultimate efficiency limiting process. As expected it is stimulated Raman scattering of the 130 nm light by the Hg vapor. Above a threshold intensity, the 130 nm light is absorbed and converted to infrared light while pumping the Hg 6S - 8S Raman transition.

In support of this work we have also continued the development of a Maxwell-Bloch computer model of resonant mixing. This is an extension of our earlier steady state model for mixing and has a much broader range of validity. We plan to use this code to better understand the role of ASE and interference effects in resonant frequency mixing.

III. Development of single mode tunable pulsed lasers.

Last year we reported that we had developed a method for actively stabilizing Littman type single mode dye lasers so that single mode scans extending over several hundred wavenumbers is possible. We have since demonstrated that the laser can be frequency locked to an external reference cavity. We have also demonstrated continuous scanability from 550 to 850 nm using a variety of dyes and solvents. One

of the short commings of this laser for some applications is the pulse to pulse frequency jitter of 100 - 200 MHz. This proved to be a problem in our O measurements where the jitter in magnified 4x by the nonlinearity of the O pumping process. The resulting jitter is significantly larger than the O transition linewidth or the laser's transform-limited linewidth and hence was a source of noise in our measurements. This jitter may be due to fluctuations in our flowing dye gain medium. A potential solution is to substitute a solid state medium to provide greater optical stability. Recently developed solid state laser materials - especially Ti:Sapphire - have other advantages as well such as broader tuning ranges, higher efficiency, and higher energy storage capacity than dyes. Thus they are attractive alternatives to dyes in these lasers. We have demonstrated the use of Ti:Sapphire as the gain medium in single mode operation. The pulse energy in much higher than the dyes at >1 mJ in a 2 ns pulse. The demonstrated tuning range is 750 to 850 nm. We have not yet measured frequency jitter. We plan to try other solid state media in the future.

IV. Recent publications

1. "Optimization of two-photon-resonant four-wave mixing: application to 130.2 nm generation in mercury vapor", A. V. Smith, W. J. Alford, and G. R. Hadley, J. Opt. Soc. Am., 5, 1503, (1988).

2. "High-efficiency, energy-scalable, coherent 130-nm source by four-wave mixing in Hg vapor", C. H. Muller III, D. D. Lowenthal, M. A. DeFaccio, A. V. Smith, Opt. Lett., 13, 651, (1988).

3. "Widely-tunable single-longitudinal-mode pulsed dye laser", T. D. Raymond, P. Esherick, A. V. Smith, to be published in Opt. Lett.

Spectroscopic Studies of Hydrogen Atom and Molecule Collisions

John Kielkopf
University of Louisville, Louisville, KY 40292

The purpose of this program is to study atomic and molecular collisions with neutral hydrogen. Atomic line profiles, molecular line intensities, continua from radiative dissociation, and radiation during close collisions, are phenomena that depend on atomic and molecular interactions and dynamics. Although the atom and diatomic molecule are simple systems for theoretical modeling, experimental work of this sort offers two major challenges: the dissociation of the molecule at densities sufficiently high for the observation of neutral collision broadening of the atom, and the application of tunable laser spectroscopy in the vacuum ultraviolet to this task.

One way to make atomic hydrogen at densities of 10^{19} cm^{-3} or greater is to start with H_2 and dissociate it in an electrical discharge. Most previous experiments with atomic hydrogen have been done at low density, where atoms are flowed from a glow discharge. At high gas pressure, in arcs for example, the electron density is so high that charged-particle collisions overwhelm the neutral effects. Most of the breadth of the atomic lines derives from Stark broadening under those circumstances. Our solution is to use a repetitively pulsed discharge in which current flows for about one microsecond between two hemispherical electrodes separated by a few millimeters. The electron density has been measured through Stark broadening of the Balmer series, and it shows an exponential decay with a 1/e time of a few microseconds. These discharges can be initiated by gating a thyratron to connect a capacitor charged to a voltage greater than required to break down the gap. In this case, the discharge channel, which is only about 2 mm in diameter, will wander more than its own diameter from shot-to-shot. Experiments to correct this problem, and to permit operation at very high pressures, led to the use of an excimer laser as a trigger. XeCl (308 nm) or ArF (193 nm) radiation focussed on the cathode of the source, produces ionization that will start the discharge. The resulting plasma is not a laser-produced plasma as such because it is maintained by the charge stored on an external capacitor, but it reproduces with precision from shot-to-shot. Furthermore, the lowered supply voltage in the laser-triggered discharges reduces the electron density and makes it possible to extend the operating pressure range at least to atmospheric pressure, where total dissociation would produce 5×10^{19} atoms/cm^3.

After the discharge is no longer self-luminous, the dissociated gas returns to equilibrium with the surrounding cool molecular gas rather slowly. Even the near wing of Lyman α is optically thick for hundreds of microseconds, while the electron density falls to a level that permits observation of neutral effects within tens of microseconds after the discharge initiates. Thus there is a wide window in the time domain where laser spectroscopy of the atom is possible. For single-photon excitation of the 1s-2p transition in atomic hydrogen, tunable laser light at 1215 Å was generated by frequency tripling a tunable 3645 Å dye laser with Kr gas. The near wing resonance profile of Lyman α was measured in this way with the thyratron-triggered hydrogen source and the excimer laser pumping the dye laser train. These experiments exposed the sensitivity of the tripled 1215 Å light to the mode structure and intensity of the dye laser, and the difficulty of maintaining spatial overlap between the tripled dye laser

beam and the hydrogen source. Profiles of Lyman α within 15 cm^{-1} of line center were obtained and the atomic hydrogen density was measured as a function of time. In the meantime, we have added a YAG laser to pump the dye lasers, which frees the excimer for use on the hydrogen source. Work with this new combination is just starting, but since it will permit more than two orders of magnitude increase in atomic density, we expect to be able to probe a region beyond 100 cm^{-1} from the line center. It is this region where asymmetry and satellites characterizing close atomic encounters should first appear.

Farther from Lyman α, most prominently around 1600 Å, transitions from bound $B\ ^1\Sigma$ states to the continuum of the $X\ ^1\Sigma$ state dissociate the molecule and produce continuum radiation. The continuum is interspersed with, and often masked by, the corresponding Lyman band bound-bound transitions. This continuum is structured, typically with several oscillations, and can be observed in absorption from a low temperature atomic gas, or in emission from the electronically excited molecule. It offers a simple opportunity to study a well-defined half-collision, as the molecule dissociates from its initial internuclear separation. We developed a technique for recording the continuum by observing the molecular spectrum with a scanning high resolution (10^6 resolving power) spectrometer. The digitized spectra are filtered to remove the line radiation and give the continuum, while the line spectra are fitted with calculations from the known molecular structure. In this way, both the continuum and the distribution of excited states are acquired.

When the same process is applied to the emission spectrum of the pulsed atomic hydrogen source, especially with initial molecular gas densities of the order of one atmosphere, very high rotational states of H_2 appear. Although the vibrational energy distribution is comparable to that in a positive column low density discharge, the dissociative continuum seems to be suppressed with a modified structure. This suggests that radiative dissociation of H_2 is dependent on the rotational excitation.

In the case of completed, free atom, collisions, the enhancement in the continuum at 1600 Å becomes a satellite band due to binary H-H interactions via the B state. Satellites of this type are evident whenever the difference potential for the initial and final states exhibits an extremum. One should occur, for example, on the C state, but only a 100 or so cm^{-1} to the blue of the line center. Spectral line profiles through these regions are very dependent on density and temperature. For the atomic gas, a change in temperature alters the initial velocity distribution, and thereby the duration of the collisions. An increase in density means an increased probability of multiple-perturber collisions. There is even a significant probability that, at densities of the order of 10^{20} cm^{-3}, three hydrogen atoms will approach close enough to produce observable features in the line wing.

The free-free atomic spectra calculations are complicated by numerical difficulties, and by such physical factors as the ensemble statistics, the complexity of the potentials, and non-adiabatic processes. In collaboration with N. Allard, we have been developing methods for dealing with these problems. Calculations of the temperature dependence of the free-free hydrogen spectra, with some simplifying assumptions, predict very strong features at 1600 Å. For temperatures of the order of 1000 K, such satellites are considerably sharpened from the predictions of high temperature models. By using an expansion of the spectrum in powers of the density,

we see evidence that three-body collisions will produce observable effects. Of course, one question is the nature of the H_3 potential surface itself, but if the two-body interactions are even approximately additive, the new continua should appear in the ultraviolet near 2200 Å.

In work on the molecule, experiments on two-photon excitation of the EF double-well state of H_2 were completed this year. We measured photo-ionization rates from the excited states, fluorescence intensities, and fluorescence spectra for molecular densities from 10^{15} to 10^{19} cm^{-3}. The excitation and ionization rates were modelled theoretically, and the spectra were compared with computed simulations. These analyses suggested that, although the two-photon excitation was to a state of the inner well, the fluorescence occurred from the $B^1\Sigma$ state following a cascade, or excitation transfer, through intermediate states of the outer well. The results support a model in which collisions of neutral excited H_2 and ground state H_2 are responsible for this fluorescence. The experiments demonstrate that optical emission following state selective excitation provides information about the neutral final states to which ion product detection is insensitive.

During the coming year our efforts will be directed to taking advantage of the combination of the excimer laser and the tunable YAG-pumped dye laser to produce and probe neutral collision phenomena in transient species. The core of the self-broadened Lyman α resonance line will be measured for a range of densities, up to 10^{20} cm^{-3}, by direct absorption at 1215 Å in the 1s-2p transition, and by two-photon depolarization spectroscopy at 2430 Å in the 1s-2s transition. Measurements for broadening by noble gases will be made in the same way. The spectrum of the far wing will be studied to determine the shape of the satellite region and search for effects from more than one perturber. In part, this can be done by measuring the emission spectrum of the high pressure pulsed source, but four-wave mixing of two dye lasers in Kr provides an alternative for laser absorption spectroscopy. Theoretical calculations of the Lyman alpha profile will be made with improved potentials, and with allowance for non-adiabatic effects.

We are also interested in looking at four-wave mixing in atomic hydrogen, which should produce tunable radiation near Lyman γ around 972 Å. Previous attempts to observe the effect have been thwarted by the background from the incident lasers and limited incident laser power. The use of an indium foil filter to suppress the background, and the improved dye laser together with a BBO crystal to boost power at 2430 Å, should make it possible to detect the four-wave mixing signal.

Recent Publications

Excited state populations of H_2 in the positive column of a glow discharge, K. Myneni and J. Kielkopf, J. Phys. B **21** (1988) 2871-2878.

Unusual fluorescence from H_2 excited by multiphoton processes, J. Kielkopf, K. Myneni, and F. Tomkins, J. Phys. B **22** (1989) in press.

Multi-perturber effects on Lyman α, N. Allard and J. Kielkopf, Astr. Astrophys. submitted.

RELATIVISTIC ATOMIC BEAM SPECTROSCOPY

H. C. Bryant
Department of Physics and Astronomy
The University of New Mexico
Albuquerque, NM 87131

During the late spring and summer of 1989, extensive data were taken for three experiments in the HIRAB facility at LAMPF. These data are currently being analyzed. In the following we* present a preview of these measurements and observations.

I. Interaction of relativistic H^- ions with matter (LAMPF Expt. 1076)

We have measured the yields of various excited states of H° resulting from directing beams of H^- ions at energies up to 800 MeV through thin carbon foils. For the foil thicknesses we have studied, ranging from 20 to 200 $\mu g/cm^2$, an appreciable fraction of the H^- beam survives intact, some H^- ions are stripped down to protons, and the remainder is distributed over the states of H° . We have complete data on the yields of n = 1, 2, 3, 4, 5 and 10, 11, at 800 MeV and less complete data at lower energies. Fig. 1 illustrates the nature of these data with the yield curves for n = 1 and n = 11. The curves are not normalized to each other. The n = 1 yield was determined by laser-exciting the n = 1 state to n = 13 which was then ionized in the motional field of an electron spectrometer. The n = 11 yield was determined by selective ionization directly. The solid lines are a best fit of the simplistic formula,

$$\text{yield} = A[\exp(-cx) - \exp(-bx)],$$

where x is the foil thickness. Note that the maximum H° (1) yield occurs at a thickness of about 2000 Å whereas the maximum H° (11) yield is at 4000 Å.

Our data seem to favor a production mechanism for excited H° atoms by a relativistic H^- beam passing through carbon foils which is, at least in part, diffusive. That is, the progressive increase in foil thickness at the maximum yield with principal quantum numbers tentatively bespeaks a stepwise excitation.

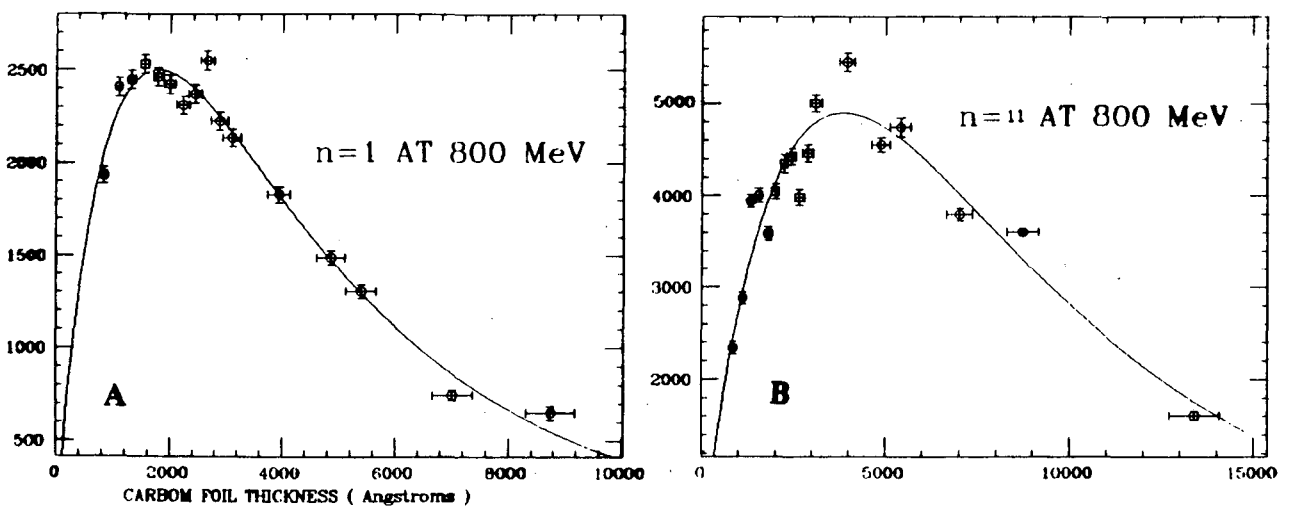

Figure 1

II. High Excitation and double escape in the negative hydrogen ion (LAMPF Expt. 1121)

An extensive survey of doubly-excited $^1P^\circ$ resonances in H^- lying above the n=4 threshold ($H^- + \gamma \rightarrow H^\circ (4) + e$) has been completed up to the n=8 threshold. Fig. 2 exhibits "typical" data in which the yield of hydrogen atoms with n≥4 is plotted. Three resonances are cleanly seen. The energy scale has been fixed by the photoionization of foil-produced hydrogen atoms; the energy resolution is of the order of 5 meV. We have taken similar data, using the fourth YAG harmonic and 800 MeV, showing structures for n ≥ 5, 6, and 7.

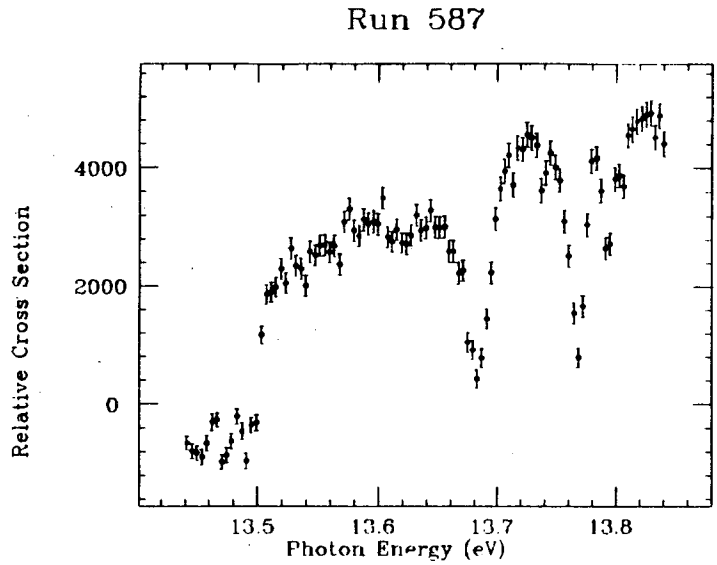

Figure 2

Analysis of these data is underway to extract widths and energies of the structures observed in a systematic way.

Observations of states above n=8 and into the two electron continuum were hampered by a severe background of protons produced upstream of our apparatus. Based on our experience gained the past summer, we are modifying our experimental arrangement to suppress the background in our next experimental run.

An experiment to improve the energy resolution was quite successful. By varying the phase of the last two sectors of the accelerator, the momentum spread of the beam at 716 MeV was reduced by a factor of 5. With this improvement the apparent FWHM of the n=2 , $^1P^\circ$ Feshbach resonance was 1.8 meV.

III Multiphoton detachment of electrons the H^- ion (LAMPF Expt. 1127)

Our very preliminary observation of multiphoton ionization of H^- using a CO_2 (10.6μ) laser and H^- beam at 581 MeV in the fall of 1988 was followed by an extensive series of measurements at 800 MeV during the late spring and summer of 1989 using an improved apparatus.

The H^- ion, one of the simplest 3 body systems, has no intermediate resonances between the ground state and the one-electron photodetachment threshold at 0.754 eV. Moreover, the detached electron feels only a short range potential as it leaves, so that modeling of the fundamental processes involved should be clean, and measurements therefore likely to

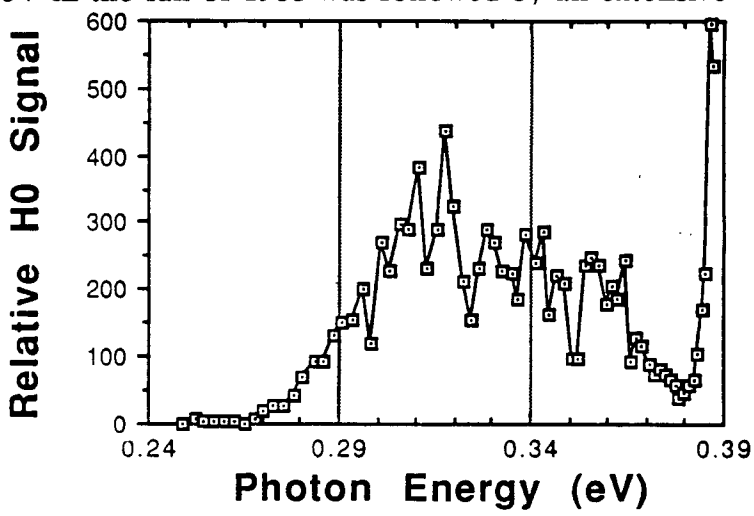

Figure 3

lead to fundamental understanding. The fact that the photon energy can be Doppler-tuned over almost a decade in photon energies (0.05-0.4 eV, for the 10.6μ line) adds to the uniqueness of this measurement.

Figure 3 displays some preliminary data showing the relative yield of neutral H° atoms from 800 MeV H^- multiphoton detachment as a function of the center of mass photon energy. The laboratory frame laser pulse energy was kept constant at 0.65-0.75 Joules/pulse while the angle of intersection α between the H^- and laser beams was varied to change the photon energy. The signal has been normalized to a constant interaction volume by multiplying the count rate by $|\sin\alpha|$. Distinct thresholds for 2 and 3 photons can be seen, but the fluctuations in the "three photon peak" may be noise. A large amount of data has been taken and a much clearer picture should emerge after our analysis is complete.

Future Plans

Progress we have made in all three efforts described above begs to be followed up with more careful and precise measurements. In the case of foils, the distribution of ℓ values would be very illuminating. With the doubly excited and two-electron continuum studies, we plan to make measurements with the ArF (193 nm) line as well as the YAG, making use of our new-found ability to narrow the momentum spread of the beam. Finally, the possibility of doing multiphoton studies on H^- opens up many new vistas including ATI and possibly optical harmonic generation.

Recent Publications

"Stability of the $^1P^\circ$ Shape resonance in H^- in moderate electric fields," G. Comtet, C.J. Harvey, J.E. Stewart, H.C. Bryant, K.B. Butterfield, D.A. Clark, J.B. Donahue, P.A.M. Gram, D.W. MacArthur, V. Yuan, W.W. Smith, Stanley Cohen, Phys. Rev. A30, 1547 (1987).

"Observation of Motional-Field-Induced Ripples in the Photodetachment Cross Section of H^-," H.C. Bryant, A. Mohagheghi, J.E. Stewart, J.B. Donahue, C.R. Quick, R.A. Reeder, V. Yuan, C.R. Hummer, W.P. Reinhardt, L. Overman, Phys. Rev. Letters, 58, 2412 (1987).

"Response of the $^1P^\circ$ resonance near $n=3$ in the H^- Continuum to External Electric Fields," Stanley Cohen, H.C. Bryant, C.J. Harvey, J.E. Stewart, K.B. Butterfield, D.A. Clark, J.B. Donahue, D.W. MacArthur, G. Comtet, W.W. Smith, Phy. Rev. A 36, 4728-4736 (1987).

"Effects of Electric Fields on the Photodetachment Cross Section of the H^- Ion Near Threshold," J.E. Stewart, H.C. Bryant, P.G. Harris, A.H. Mohagheghi, J.B. Donahue, C.R. Quick, R.A. Reeder, V. Yuan, C.R. Hummer, W.W. Smith, S. Cohen, Phys. Rev. A 38, 5628 (1988).

"Observation of Multiphoton Detachment of the H^- Ion," C.Y. Tang, P.G. Harris, A.H. Mohagheghi, H.C. Bryant, C.R. Quick, J.B. Donahue, R.A. Reeder, Stanley Cohen, W.W. Smith, J.E. Stewart, Phys. Rev. A 39, 6068 (1989) (Rapid Communications).

*Workers participating in these measurements include:
W.W. Smith, C.Y. Tang, C.R. Quick, P.G. Harris, A. Mohagheghi, J.B. Donahue, R.A. Reeder, H. Sharifian, J.E. Stewart, H. Toutounchi, S. Cohen, T.C. Altman, D.C. Rislove and H.C. Bryant.

Atomic Physics at ATLAS*

R. W. Dunford, H. G. Berry, M. L. A. Raphaelian,†
D. A. Church, C. J. Liu and B. J. Zabransky
Argonne National Laboratory, Argonne, Il 60439

Recent atomic physics experiments at the ATLAS heavy-ion accelerator have included ultraviolet spectroscopy of two- and three-electron nickel and bromine, and measurements of forbidden lifetimes in one- and two-electron nickel and bromine. Plans are underway for precision X-ray spectroscopy of one- and two-electron calcium, improved UV spectroscopy of two-electron bromine, and further forbidden lifetime measurements. We also have a program in atomic physics using the ECR ion source which was built for the Uranium Upgrade of ATLAS. This program includes measurements of state-selective electron capture cross sections in ion-atom collisions, studies of polarization transfer in ion-atom collisions using an optically pumped polarized Na target, and studies of ion-atom collisions using electron spectroscopy. Another project to be done at ATLAS is the study of the positron peaks which have been seen in heavy-ion collisions at GSI. In collaboration with the nuclear physicists, we are building an apparatus to study these peaks. It is planned to have the apparatus completed by the time the first Uranium beams become available at ATLAS in 1991.

In the following we describe some of the highlights of the experimental program at ATLAS.

Measurements of Forbidden Lifetimes

We recently completed precision measurements of the lifetimes of both the $2^2S_{1/2}$ state of hydrogen-like Ni^{27+} and the 2^1S_0 state of helium-like Ni^{26+}. These states decay to their groundstates primarily by the emission of two photons. Our experiment utilizes the standard beam-foil time-of-flight technique except that we require a coincidence between the two photons emitted in the decays.

The singles spectra from the two-photon decays form a continuous distribution with a broad maximum at half the transition energy which drops to zero at either endpoint. The sum of the energies of the two photons is equal to the transition energy (about 8 keV). Former measurements of the lifetimes of these states in other hydrogen-like and helium-like ions were based on singles rates. In this case, it is difficult to obtain a high precision result because of uncertainty in the shape of the background under the two-photon continuum and uncertainty in the dependence of this shape on foil-detector separation.

Our measurements were obtained in two separate runs at ATLAS using nickel beams at energies of 376 MeV and 674 MeV. After acceleration, the ions were stripped in a thick carbon foil and either the 26+ or the 28+ charge state was magnetically selected and directed to the atomic physics beamline. In the experimental area, a thin carbon target (12 $\mu g/cm^2$) was moved relative to three fixed Si(Li) detectors using a precision translation device. The coincidence rate was measured as a function of foil-detector separation to determine the lifetime. There was also a small ion-implanted, passivated X-ray detector attached to the target holder which was used for normalization.

Our result for the lifetime of the helium-like state is 156.1(1.6) ps which is slightly higher than the theoretical value of 154.3(0.5) ps calculated by G. W. F. Drake. This result provides a test of the relativistic corrections which increase the calculated lifetime by 4.3 ps. For the decay of the $2^2S_{1/2}$ state in hydrogen-like Ni^{27+} we find a lifetime of 217.1(1.8) ps which agrees with the theoretical value of 215.65 ps calculated by F. A. Parpia and W. R. Johnson. This result is the first measurement of the $2^2S_{1/2}$ lifetime to be sensitive to the relativistic correction to the two-photon decay rate and it is also the most sensitive test of the M1 contribution to this decay rate. We have also completed measurements of the lifetime of the 2^3S_1 level of helium-like bromine and we have observed the hyperfine quenching effect in the decay of the 2^3P_0 state of helium-like Ni. The latter experiment involved making precise measurements of the lifetime of this state in two different nickel isotopes (nickel-58 and nickel-61).

Polarized Sodium Target

We have developed a polarized sodium beam target which has been used at the Argonne PII ECR Ion Source to produce, by electron capture, beams of highly-charged ions with atomic and nuclear polarization. The system has also been used to study the dependence of the state-selective electron capture cross sections on the state-prepared Na atoms [Na(3s) or Na(3p)]. The sodium beam is optically pumped by a CR699-21 ring dye laser. We pump both groundstate hyperfine levels (F=2 and F=1) and cover the complete Doppler profile by imposing both side-bands and noise modulations on the laser spectral density distribution using electro-optic modulators. The polarization of the target was determined by measuring the circular polarization of the fluorescence induced by a weak linearly-polarized probe beam.

A circular polarization of 5.7 ± 0.7% of the N V 2s-2p (124 nm) emission line was observed after electron capture by a 5 keV/u N^{5+} beam incident on the polarized sodium target. The Stokes parameters of the VUV photons emitted after electron pick-up from the target were analyzed by a polarimeter consisting of a MgF_2 retardation plate, a 3-mirror linear polarizer and a channeltron. The MgF_2 retardation plate cuts off at wavelengths shorter than 115 nm and the quantum efficiency of the channeltron drops off rapidly at wavelengths longer than 150 nm, so the overall system conveniently isolates the N V 2s-2p emission line.

*This research was supported by the Department of Energy, Office of Basic Energy Sciences, under Contract W-31-109-ENG-38.
†Graduate student at the University of Illinois, Chicago.

Recent Publications

1. Lifetime of the 2^1S_0 State of Helium-Like Ni^{26+}, R. W. Dunford, H. G. Berry, K. O. Groeneveld, M. Hass, E. Bakke, M. L. A. Raphaelian, A. E. Livingston, L. J. Curtis, Phys. Rev. A38, 5423 (1988).

2. State-Selective Electron Capture, R. W. Dunford, C. J. Liu, H. G. Berry, R. C. Pardo, M. L. A. Raphaelian, Journal de Physique, Colloque C1, supplement au n01, Tome 50, C1-337 (1989).

3. Subshell Selective Electron Capture (2-105 keV/amu) Studied by VUV Spectroscopy in O^{6+} + He Collisions, C. J. Liu, R. W. Dunford, H. G. Berry, R. C. Pardo, K. O. Groeneveld, M. Hass, M. L. A. Raphaelian, J. Phys. B22 1217 (1989).

4. Lifetimes of Two-Photon-Emitting States in Helium-Like and Hydrogen-Like Nickel, R. W. Dunford, M. Hass, E. Bakke, H. G. Berry, C. J. Liu, M. L. A. Raphaelian, and L. J. Curtis, Phys. Rev. Lett. 62 2809 (1989).

5. Atomic Physics Measurements Using an ECR Ion Source Located on a 350 kV High-Voltage Platform, R. W. Dunford, H. G. Berry, C. J. Liu, M. Hass, R. C. Pardo, M. L. A. Raphaelian and B. J. Zabrnaksy, Nucl. Intrum. & Meth. B40/41, 9 (1989).

SEMIEMPIRICAL STUDIES OF ATOMIC STRUCTURE

L. J. Curtis, Department of Physics and Astronomy
University of Toledo, Toledo Ohio 43606

The structure and properties of highly ionized and highly excited atoms are studied in a program that combines experimental measurements, *ab initio* computations, and semiempirical systematization and parametrization. During the past year, emphasis has been placed on the determination of atomic lifetimes and transition probabilities in a number of different types of systems. Brief descriptions of a few of these projects are given below.

Lifetime Measurements of Quintet Levels in Carbon I

Although the singlet and triplet spectra of C I have been comprehensively studied, only the $2s2p^3\ ^5S$ and $2s2p^2 3s\ ^5P$ terms have been established for the quintet system. The ^5P levels lie above the first (doublet) ionization limit, but well below its parent (quartet) ionization limit. Thus autoionization to the triplet continuum is energetically possible, but forbidden to Coulomb interactions in LS coupling by the $\Delta S=0$ selection rule. Intermediate coupling opens autoionization channels through triplet-quintet mixing and leads to lifetimes that are strongly J-dependent. In order to investigate these radiative and autoionization effects, we performed a combined theoretical and experimental study of the lifetimes of the individual fine structure levels of the $2s2p^2 3s\ ^5P$ term. The experimental portion was carried out by beam foil excitation methods, and the theoretical calculations were made using the multiconfiguration Hartree-Fock program of Cowan, which includes both radiation and autoionization. The wavelength separations of the lines are about 0.5 Å, which creates special problems. While the beam foil source copiously populates these states, its inherent Doppler broadening precludes them from being completely resolved spectroscopically. However, since these lines were found to be relatively free of cascades, blends, and backgrounds, it was possible to determine the lifetimes of the individual fine structure levels by performing a three dimensional array of intensity vs wavelength vs time measurements. Fig.1 shows a sample decay curve, indicating the sharp variation in lifetime content over the unresolved multiplet profile. The experimental lifetimes show a strong J-dependence with $\tau(J=3)=2.5(5)$ns and $\tau(J=1,2)=0.3(1)$ns, in good agreement with the theoretical calculations.

Fig.1

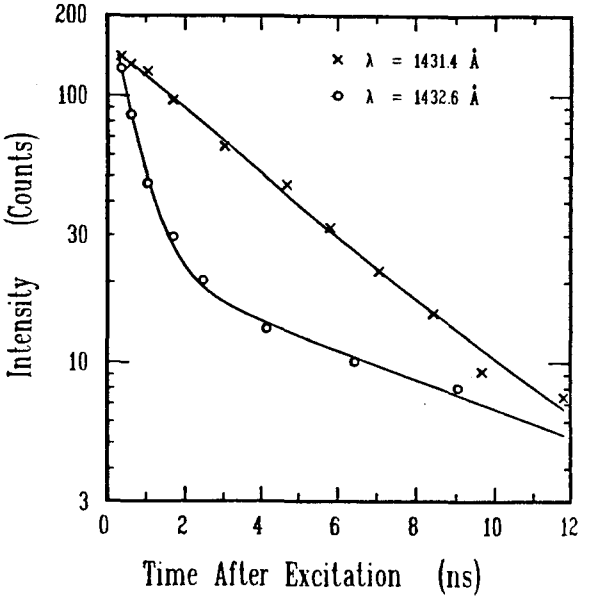

Comprehensive calculations for ns and np lifetimes in the Na and Cu sequences

Although ns-np resonance transitions in alkalilike isoelectronic sequences involve a single electron outside a closed shell, the specification of their lifetimes has both experimental and theoretical subtleties. Theoretically, core polarization and other types of electron correlation, spin-orbit coupling and other relativistic interactions, and the relative advantages of Breit-

Pauli and fully relativistic treatments have a strong isoelectronic variation. Experimentally these intrashell decay channels are repopulated by faster extrashell transitions and by the yrast chain, so the decay curves exhibit both growing-in and growing-out cascades, making curve fitted lifetime extraction unreliable. Thus, a tendency for experimentally determined lifetimes to exceed theoretical estimates has long been attributed to cascade distortions in experimental data. However, recent new experimental determinations using the ANDC method, which exploits dynamical correlations among cascade-related decay curves, now provide reliable lifetime determinations for both the Na and Cu isoelectronic sequences. While these results remove a large portion of the previous discrepancies, it appears that the experimental lifetimes still tend to be slightly longer than many theoretical estimates after cascade effects have been eliminated. We have developed a means for accurately predicting these lifetimes by incorporating measured or semiempirically determined atomic structure data into the prediction of the lifetime. We have used the Hartree-Slater approach, which involves the integration of the Schrödinger equation with a realistic potential, constrained to yield the experimental binding energy. The model potential includes the single electron central field, the spin-orbit interaction, and the core polarization potential (as determined from spectroscopic data by the empirical dipole polarizability). Fig.2 compares our results with a number of other published calculations and with the experimental ANDC results for the Cu sequence.

Fig.2

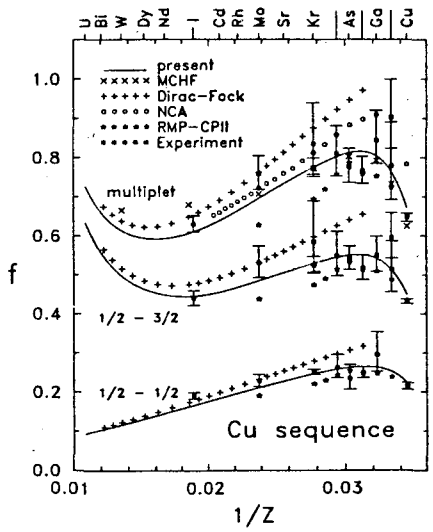

Fig.3

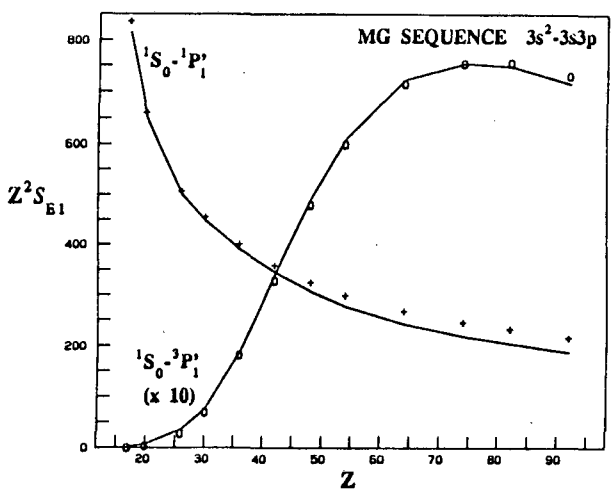

Use of semiempirical singlet-triplet mixing angles to specify E1 *and* M1 *transitions in two valence electron systems*

As described above, transition probabilities for single valence electron systems are often accurately predicted by methods that incorporate measured energy level data into the calculation. We have sought to develop methods by which results obtained for single valence electron systems can be applied to two valence electron systems through semiempirical specification of the effects of intermediate coupling. For systems with two out-of-shell electrons, singlet-triplet and L-state mixing within a given configuration manifests itself in the energy splittings, oscillator strengths, and g-factors of the constituent levels. In intermediate coupling, the wave functions of levels with common J become a mixture of LS basis states that are not subject to the ΔL and ΔS selection rules that restrict their constituent amplitudes. The degree of intermediate coupling usually increases with

increasing ionicity along an isoelectronic sequence (although counter examples exist). In fully *ab initio* calculations, intermediate coupling is implicitly included in the construction of the wave function, but we have developed a formalism (based on the specification of electrostatic Slater energies and spin-orbit energies) to empirically determine the mixing amplitudes explicitly from energy level data, to combine these with methods normally applied to single electron systems, and thereby to semiempirically specify oscillator strengths and g-factors for two-electron systems in intermediate coupling. An example treating the resonance and intercombination lines in the Mg sequence is shown in Fig.3. Here the singlet-triplet mixing angles have been determined from the energy splittings among the four $^{1,3}P$ levels in this configuration. The transition moment used is that corresponding to the neighboring Na sequence, multiplied by a constant (Z independent) empirical factor. Similiar results have been obtained for other nsn'p and nsn'p^5 configurations in the Be and Ne isoelectronic sequences, as well as for np^2 and np^4 configurations in the Si and S isoelectronic sequences. The use of empirical mixing angles has also been applied to the specification of magnetic g-factors in intermediate coupled systems.

Forbidden transitions in highly ionized one and two electron systems

In a collaboration with Argonne National Laboratory, we have performed lifetime measurements for two-photon 2E1 decays of the $2\ ^1S$ state in heliumlike Ni^{26+}, the $2\ ^2S$ state of hydrogenlike Ni^{27+}, and of the M1 decay of the $2\ ^3S$ state in heliumlike Br^{33+}. In the hydrogenlike system, the decay of this $2\ ^2S$ is branched between the 2E1 and M1 processes, whereas in the heliumlike system the $2\ ^1S$ decays entirely by 2E1 and the $2\ ^3S$ decays entirely by M1. The data were obtained using the Argonne Tandem Linac Accelerator System (ATLAS) at beam energies of 376 and 674 MeV, using beam foil excitation and Si(Li) detection. Our lifetime studies for the two-photon decays are the first such measurements based on the coincidence technique. In addition to demanding a coincidence, it was also required that the two detected photons have the proper summed energy, virtually eliminating problems of background subtraction. For the heliumlike and hydrogenlike two photon decays we obtain results of 156.1(1.6)ps and 217.1(1.8), which can be compared theoretical values of 154.3(0.5)psand 215.45ps.

Partial list of publications within the latest two years:

[1] C.E. Theodosiou and L. J. Curtis, *"Accurate Calculations of* 3p *and* 3d *Lifetimes in the Na Sequence,"* Phys. Rev. A **38**, 4435-45 (1988).

[2] R.W. Dunford, H.G. Berry, K.O. Groeneveld, M. Hass, E. Bakke, M.L.A. Raphaelian A.E. Livingston and L. J. Curtis, *"Lifetime of the* $2\ ^1S_0$ *State of Heliumlike* Ni^{26+}, Phys. Rev. A **38**, 5423-25 (1988).

[3] L.J. Curtis, *"Computation of* M1 *Decay Rates in Intermediate Coupling using Empirical Spectroscopic Data,"* J. Phys. B: At. Mol. Opt. Phys. **22**, L267-71 (1989).

[4] L.J. Curtis and C.E. Theodosiou, *"Comprehensive Calculations of* 4p *and* 4d *Lifetimes for the* Cu *Sequence,"* Phys. Rev. A **39**, 605-615 (1989).

[5] R.W. Dunford, M.Hass, E. Bakke, H.G. Berry, C.J. Liu, M.L.A. Raphaelian and L.J. Curtis, *Lifetimes of Two-Photon-Emitting States of Heliumlike and Hydrogenlike Nickel,"* Phys. Rev. Letters **24**, 2809-12.

ATOMIC PHYSICS RESEARCH*

K. W. Jones and B. M. Johnson
Brookhaven National Laboratory
Upton, New York 11973

Atomic physics experiments using bending magnet radiation at the X-26 port of the National Synchrotron Light source are in progress. The work is centered on the study of multiply-charged ions produced following the photoionization of the K shell.

The beam line was improved during the past year by the addition of a 1:1 focussing mirror. The mirror was designed to collect 4 mr of radiation in the horizontal plane and essentially all the radiation emitted in the vertical plane. The material used for the mirror was Zerodur. A 50-nm coating of platinum was vacuum evaporated on the mirror in order to improve the reflectivity. The mirror is supported in a vacuum chamber such that height, pitch, yaw, and rotation can be adjusted using computer controlled stepping motors. When operated at a grazing angle of 4.4 mr total reflection of the incident white beam was obtained up to a photon energy of 17 keV.

The focal properties of the mirror were determined by measuring the image size and shape as a function of pitch, angle, and distance from the mirror. At optimum positions a size of about 1 mm in the horizontal and about .5 mm in the vertical was achieved. This is comparable to the dimensions of the emitting electron beam. The beam flux was estimated from the spectrum of photons scattered from the beam by the air in the hutch and from the intensity of the argon k-x ray peak produced by ionization of the small amount of argon in the air and by the K-x rays produced by irradiation of a standard chromium sample (1). A value of 2×10^{16} photons/s/cm^2 was found. This represents an enhancement of over two orders of magnitude compared to the flux in the unfocussed beam, in agreement with the acceptance of the mirror. The energy range covered is from 3.2 to 17 keV. The low energy cut-off occurs because a beryllium window is used to isolate the beam line from the ring vacuum.

The focussed beam was used in several experiments with a Penning ion trap in collaboration with atomic physics groups at Texas A and M University, the University of Tennessee, Argonne National Laboratory, and Oak Ridge National Laboratory. The aim of the work was twofold: the higher flux makes it feasible to search for multiple ionization of the K shell in a gas target, such as argon and ionization dependence of rate coefficients obtained by observing the decay of the stored ions can be found at extremely low kinetic energies for the ions, 600 K with the trap electrodes at 1.5 Volts. A typical spectrum obtained for the relative populations of stored Xe ions is shown in Figure 1.

The incident photon beam was chopped with a tantalum shutter so that the time of production of the trapped ions was well defined. The rate constants for charge-exchange of Ar^{q+} ions colliding with neutral argon atoms in the trap were then determined by measuring the number

*Research supported by the Fundamental Interactions Branch, Chemical Sciences Division, Office of Basic Energy Sciences, US Department of Energy, under Contract No. DE-AC02-76CH00016.

of stored ions as a function of the storage time of the ion in the trap in order to find e^{-1} decay constants τ. A plot of $1/\tau$ as a function of the argon density, n, yields a straight line with a slope equal to the rate coefficient, k, since $k = 1/\tau$ where n is the number of argon atoms/cm^3.

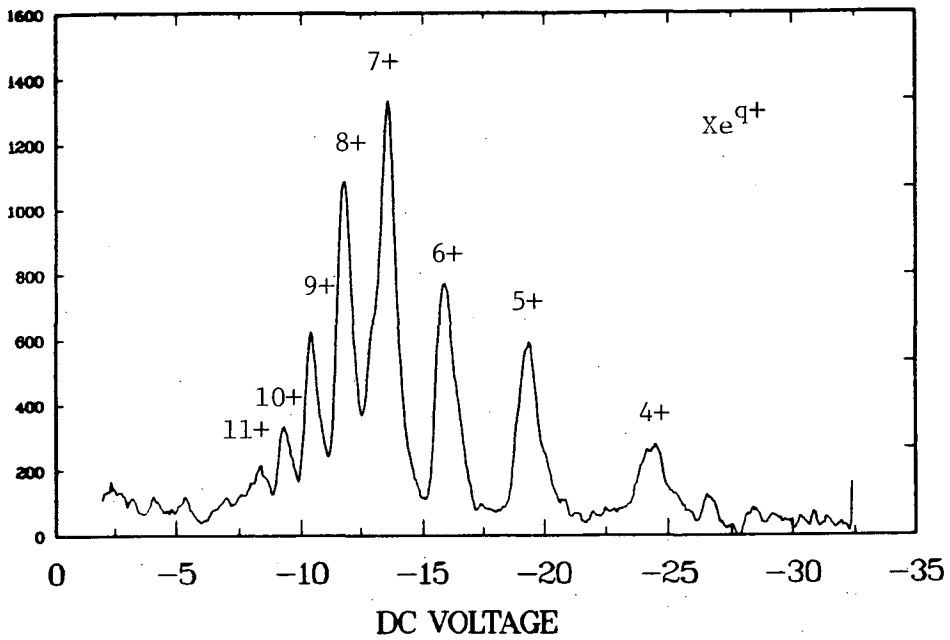

Figure 1. Charge-state distribution observed following photoionization of Xe in a Penning ion trap.

The improved experimental conditions have made it possible to obtain rate coefficients with a relative accuracy of about 10-15% although there is an overall uncertainty of about 50 % which comes from the calibration of the ion gauge used to measure the gas pressure in the trap. Further experiments will be performed to investigate the properties of additional collision systems. For example, the previous work (2) was recently extended to studies of rate coefficients for Ar^{q+} ions interacting with H_2.

We have previously pointed out (3) that synchrotron radiation could be a useful way of creating low energy ions in very high charge states by sequential ionization in a trap. The photon fluxes from a bending magnet are low for this use. Calculations did indicate that observation of the effect might be possible under the present beam line conditions. Careful observations were made to look for multiple production effects. There were some positive indications that such an effect was observed, but a more refined data analysis will be necessary to make it possible to conclude that the photoionization of ions was indeed observed.

We have previously suggested that present generation synchrotrons can produce photon beams of sufficient intensity for use in crossed photon-ion beam experiments. This has been demonstrated by the group at Daresbury in practice in several experiments with a low-energy ion source. We have gone through a design exercise to see if the idea could be implemented with highly-charged ion beams. In our work we assumed that ions would be produced by use of a combination of a tandem Van de Graaff accelerator and synchrotron booster accelerator.

Production of ions up to fully stripped is feasible with this combination. Our results show that it is possible to construct a heavy ion storage ring in close proximity to the NSLS which could store the ions for experiments with the NSLS photon beams. Our results and similar studies for use of an electron-cyclotron resonance ion source (ECRIS) by Wuilleumier (4) show that studies of multiply-charged ions with synchrotron radiation are feasible.

1. K. Themner, P. Spanne, and K. W. Jones. Nuclear Instrum. Methods, to be published.
2. Church, D. A., Kravis, S. D., Sellin, I. A., O, C. S., Levin, J. C., Short, R. T., Meron, M., Johnson, B. M., and Jones, K. W. Confined thermal multicharged ions produced by synchrotron radiation. Phys. Rev. A 36, 2487-90 (1987).
3. Jones, K. W., Johnson, B. M., and Meron, M. PHOBIS, A PHOton Beam Ion Source for production of multiply-charged atoms. Phys. Lett. 97A, 377-80 (1983).
4. Wuilleumier, F. J. Photoionization of atomic ions. A proposal for a European facility in Orsay. Presented at IVth European Physical Society Seminar on International Research Facilities, Zagreb, March 1989, to be published.

Recent Publications

Church, D. A., Kravis, S. D., Meron, M., Johnson, B. M., Jones, K. W., Sellin, I. A., O, C. S., Levin, J. C., and Short, R. T. Research with stored ions produced using synchrotron radiation. Nucl. Instrum. Methods B31, 262-4 (1988).

Meron, M. and Johnson, B. M. Electron-loss calculations using the free-collision model. Phys. Rev. A, submitted.

Meron, M., Johnson, B. M., Jones, K. W., and Church, D. A. Charge state evolution in an ion trap irradiated by VUV synchrotron radiation. Nucl. Instrum. Methods B31, 256-61 (1988).

Schuch, R., Meron, M., Johnson, B. M., Jones, K. W., Hoffmann, R., Schmidt-Böcking, H., and Tserruya, I. Quasimolecular x-ray spectroscopy for slow Cl^{16+} - Ar collisions. Phys. Rev. A 37, 3313-25 (1988).

Fast Beam/Laser Spectroscopy

T. P. Dinneen, N. B. Mansour, C. Kurtz, L. Young
Argonne National Laboratory, Argonne, Illinois 60439

This experimental program concentrates on the study of the structure of atomic and simple molecular ions in order to provide tests of ab initio theoretical calculations. The perturbation-free environment of an ion beam is used to make precision measurements of fine and hyperfine structure of both few- and many-electron systems using laser and radiofrequency techniques. The principal goal in the study of the few-electron ions is a rigorous understanding of relativistic and Lamb-shift effects in strong nuclear Coulomb fields. In the many-electron systems, the goal is to achieve, from first principles, an understanding of the observed hyperfine structure (hfs).

Experimental efforts are centered primarily at the BLASE (beam-laser) facility, where we have extended our study of psuedo two-electron systems from Sc II to the homologous Y II. The earlier studies in Sc II (see publications 1 and 3) showed major discrepancies between experimental hfs and standard MCDF calculations, presumably due to polarization of the [Ar] core. Systematic effects should be apparent by studying the [Kr] core in Y II. Measurements in Y II required use of the two-photon resonant Raman technique developed last year (see publ. 2). The precision of the two-photon measurements was greatly enhanced (5x) by the incorporation of a long, magnetically-shielded photon interaction region. The addition of this new detection region at BLASE allowed us to simultaneously install a laser interaction region at the ECR source to take advantage of the relatively high metastable content of the beams, where initial studies will probe the 1s2s ^3S - 1s2p $^3P_{0,1,2}$ transitions of the two-electron system, B IV.

Hyperfine Structure in Y II by Coherent Population Trapping

Measurement of hfs in Y II is complicated by the small spin (1/2) and magnetic moment of the nucleus, which conspire to give hfs splittings of $<$ 200 MHz in both the metastable $4d^2$ and excited 4d5p levels. In this situation, where the optical structure is unresolved, a determination of lower state intervals by laser-rf double resonance is essentially impossible since: (1) selective optical pumping is difficult, and, (2) at frequencies $<$50 MHz the rf wave perturbs the ion beam trajectories.

We have overcome these difficulties by stimulating resonant Raman transitions between the two lower hyperfine levels via a common upper state. The laser is passed through an electro-optic crystal to produce sidebands separated from the main laser frequency (carrier) by a chosen radio frequency. The carrier is tuned to one of the hyperfine components and the sideband scanned through another component, both transitions sharing a common upper level. At the radio frequency resonance a dip is seen in the fluorescence out of this three level system corresponding to population trapping in the two lower hyperfine states, Fig.1. Three of the four metastable states measured in yttrium used this technique giving splitings of 29 MHz, 66 MHz and 167 MHz in the $^3P_2$, $^1D_2$ and $^1G_4$ levels of the $4d^2$ configuration in Y II. The linewidth measured in the fluorescence dip is about 1 to 2 MHz compared to 600 kHz in the double resonance measurement. The ultimate resolution of this technique should only be limited by the transit time of the ions in the detection region ($\simeq 1\mu S$).

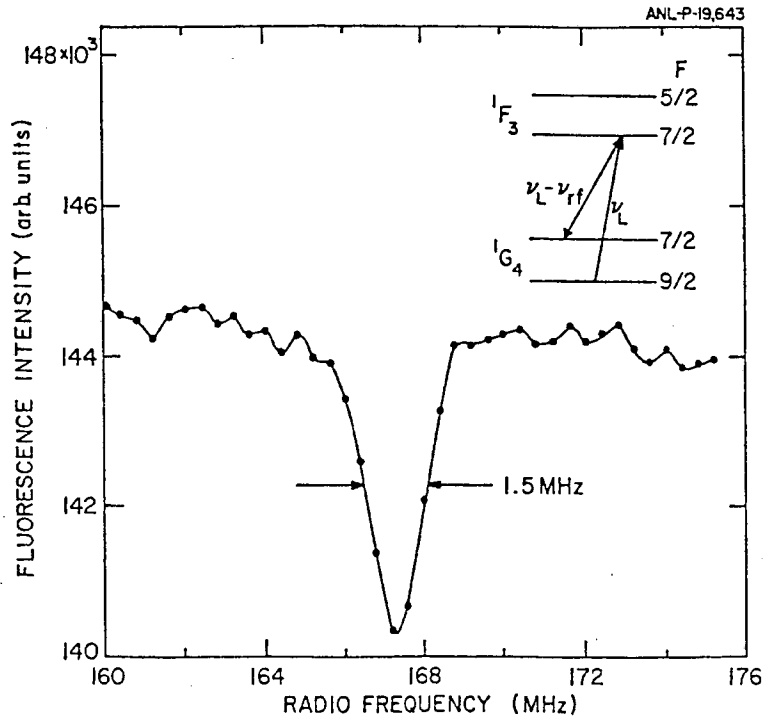

Fig.1. Population trapping in the two lower hyperfine levels in Y II by stimulating resonant Raman transitions.

Light shifts are a larger problem in the resonant Raman scheme than in laser-rf double resonance where the laser can be detuned by several GHz in the rf section by simply doppler shifting the ions. In the Raman method, however, the two photon resonance takes place in a single region so that the only detuning is on the order of the line splitting. Thus levels not involved directly in the two photon transition can perturb the measurement. The electro-optic also contributes to light shifts by producing two sidebands at $+- \omega_{rf}$ only one of which is used in the measurement. The light shift estimates vary from about 200 kHz in the case of $4d^2\ ^1G_4$ at 167 MHz to almost 2 MHz in $4d^2\ ^3P_2$ at 29 MHz.

A comparison with a MCDF calculation shows a result similar to that of scandium, where hfs of the singlet states $^1D_2$ and $^1G_4$ are in good agreement with theory and that of the triplet states are not.

Hyperfine Structure in N_2^+

We have undertaken a very high-resolution study of the first negative system of N_2^+ using Doppler-tuned laser fluorescence spectroscopy. As a result, we have fully resolved the hyperfine structure of the light diatomic molecule N_2^+ in the (1,2) vibrational band of the $B\ ^2\Sigma_u^+$-$X\ ^2\Sigma_g^+$ system for the first time.

In the (1,2) band, we found that the fine structure ordering was shifted, and that the hyperfine structure was strongly distorted in some rotational states. This complication in the structure, made the identification of the rotational levels difficult. We also measured the fine and hyperfine structure in the (0,1) band where we did not encounter these strong irregularities. Our observations imply that the rotational levels in both bands are perturbed. The weak perturbation observed in the (0,1) band arises from rotational levels in the vibrational levels v_A=9,10,11 of the $A\ ^2\Pi_u(\Omega=1/2)$ and $A\ ^2\Pi_u(\Omega=3/2)$ states. The strong perturbation observed in the (1,2) band arises from higher

vibrational levels in the A states. These perturbations have been predicted and modeled by R. W. Field et al.

A preliminary analysis of the (0,1) band gave spin rotation constants in agreement with previous measurements. The deperturbation analysis of the two vibrational bands is underway. Our results will be a sensitive test of deperturbation methods as well as of molecular wavefunction calculations.

Future Plans

We expect to extend our measurements to the two-electron B IV system at the ECR source as discussed earlier. Experimental challenges include: (1) production of sufficient metastable 1s2s ^{3}S population to be detectable by laser resonance methods, and, (2) minimization of velocity spread from the ECR source. The feasibility of extension to other members of the He-like sequence will be evaluated on the basis of this experiment. Active participation in the measurements of polarization transfer from an optically-pumped polarized Na target will continue. We also plan to construct a polarized hydrogen source to measure spin-dependent electron capture cross-sections in ion-atom collisions of interest for fusion research. The source is expected to be a replica of that originally developed in collaboration with the ANL Medium Energy Physics group for high energy electron scattering experiments.

This research was supported by the Department of Energy, Office of Basic Energy Sciences, under Contract W-31-109-ENG-38.

Publications 1988-1989

1. Hyperfine structure of Sc II: Experiment and Theory
   L. Young, W. J. Childs, T. Dinneen, C. Kurtz, H. G. Berry and L. Engstrom
   Phys. Rev. A **37**, 4213 (1988).

2. Stimulated resonance Raman spectroscopy: An alternative to laser-rf double resonance for ion spectroscopy
   L. Young, T. Dinneen, N. B. Mansour
   Phys. Rev. A **38**, 3812 (1988).

3. Laser-rf double-resonance measurements of the hyperfine structure in Sc II
   N. B. Mansour, T. Dinneen, L. Young, K. T. Cheng
   Phys. Rev. A **39**, 5762 (1989).

4. Laser/rf spectroscopic techniques in fast ion beams
   L. Young, N. B. Mansour, T. P. Dinneen
   Nucl. Inst. and Meth. **B40/41**, 860 (1989).

5. High-precision measurements of hyperfine structure in Tm II, N_2^+ and Sc II
   N. B. Mansour, T. P. Dinneen, L. Young
   Nucl. Inst. and Meth. **B40/41**, 252 (1989).

II. HIGH ENERGY COLLISIONS INVOLVING MULTIPLY CHARGED IONS

J. R. Macdonald Laboratory
Kansas State University, Manhattan, KS 66506-2601

Inner Shell Projectile Excitation and Ionization Due to Electron-Electron Interaction in Collisions of Fast Ions with H_2 and He Targets

P. Richard, T.J.M. Zouros, D. H. Lee, J. M. Sanders, J. L. Shinpaugh, T. N. Tipping, S. L. Varghese, K. R. Karim, C. P. Bhalla, R. Shingal, Y. D. Wang and J. H. McGuire

Evidence is presented of an excitation process in ion-atom collisions analogous to electron-impact excitation (eIE) in free-electron-ion collisions. The production of $(1s2s2p)^4P$ projectile states excited in collisions of $(1s^22s)$ O^{5+} and F^{6+} with He and H_2 targets, was found to increase with projectile energy above ~0.75 MeV/u, in agreement with an impulse approximation treatment of $1s \rightarrow 2p$ eIE of ions in collisions with "quasi-free" target electrons.[1]

The F^{5+} and O^{4+} $(1s2s2p^2)^3D$ and ^1D states formed by transfer-excitation (TE) in 0.25 - 2 MeV/u collisions of Li-like F^{6+} and O^{5+} $(1s^22s)$ with He and H_2 targets were studied using 0^0 Auger electron spectroscopy. Resonance-Excitation cross sections were extracted and found to be about 0.5–0.6 smaller than theory.

Binary Encounter Electrons Observed at Zero Degrees in Collisions of 1-2 MeV/amu Bare F, O, N, and C Ions with H_2 and He Targets

P. Richard, T.J.M. Zouros, D. H. Lee, J. M. Sanders, J. L. Shinpaugh and T. N. Tipping

The energy distribution of binary encounter electrons (BEe) produced in collisions of 1–2 MeV/amu, F, O, N, and C ions with H_2 and He gas targets was measured at 0° with respect to the beam direction. The measured BEe double differential production cross sections for bare ions are found to scale with Z_p^2 and approximately $E_p^{-2.6}$. An energy shift of the binary encounter peak below $4t$, where t is the cusp electron energy, is observed. BEe production was found to increase with decreasing projectile charge state.

High Velocity Ion-Molecule Collisions Studies

I. Ben-Itzhak, Tom J. Gray, J.C. Legg, Nabil Malhi, S. Ginther, Kevin Carnes and Vince Needham

Studies of a fast multiple time-sequenced coincidence system based upon a multiple-hit time-to-digital converter have been completed. A gas jet target has been installed and is currently under test.

Charge Transfer and Target Ionization in Collisions of Bare Projectile Ions Incident on Helium

P. Richard, J.L. Shinpaugh, J.M. Sanders, D.H. Lee, T.J.M. Zouros, T.N. Tipping, J. Hall and H. Schmidt-Böcking

Projectile ion final charge states were measured in coincidence with recoil ion final charge states for collisions of bare projectile ions incident on He. Absolute, partial cross sections were determined for the processes of single and double target ionization, single electron capture, and transfer ionization. For F^{9+} + He, the ratio of transfer ionization to single capture was observed to increase with decreasing projectile velocity in the range of 0.37 to 2.0 MeV/amu.[3] At 0.25 MeV/amu a sharp decrease in this ratio is observed.

Charge Exchange Processes in Fast Collisions of Highly Charged Ions and Ar Atoms†

I. Ben-Itzhak, P. Richard, J. L. Shinpaugh and J. M. Sanders

Cross sections for the production of Ar recoil ions in collisions with 1 MeV/amu O^{q+} and F^{q+} (q=2 to bare nuclei) were measured by the time-of-flight technique. The cross sections for the production, by pure ionization, of recoil ions reach a maximum in the vicinity of q=5-7. Calculated cross sections however, rise continuously and are lower than the experimental cross sections by as much as 4 orders of magnitude for high recoil-ion charge and low q. The large discrepancies between experiment and calculation, are accounted for by vacancy multiplication resulting from L-shell ionization followed by Auger decay.

† Work done in collaboration with Prof. R. Watson's group at Texas A & M Univ.

Coincident Delta Electron Spectra in Multielectron Ionization Events of High Multiplicity

B. Krässig, A. González, S. Hagmann and T. Quinteros

We have determined the spectral shape of delta-electron spectra in coincidence with the charge state of the emitting recoil ion in 0.53 MeV/u F^{8+} → Ne and $Cu^{15\text{-}18+}$ → Ne collisions. For low recoil charge states the coincident delta electron spectra resemble the non-coincident spectra for both types and all charge states of the projectile. However, for high recoil charge states we find the low energy part of the electron spectra strongly attenuated when the KK charge transfer channel is open (*e.g.* F^{8+}) but not when simply the projectile is highly charged (Cu^{18+}), the attenuation being more pronounced for higher recoil charge states.

Observation of Strong Directional Out of Plane Scattering in Two Center Multiple Ionizing Ion Atom Collisions

A. González, S. Hagmann, R. Koch, B. Krässig, T. Quinteros, A. Skutlartz and H. Schmidt-Böcking

We have measured the azimuthal and scattering angle distribution of projectiles in coincidence with recoil ions in charge states 3+ to 8+ for 0.53 MeV/u F^{8+} + Ne → F^{6+} + Ne^{q+}. For ionized electron multiplicities between one and six complete scattered particle distributions as functions of the azimuth were obtained. We derive transverse projectile and recoil momenta and find for high multiplicities strong deviations from two body kinematics. It is found that in these cases the ejected electrons play a significant role in the transverse momentum balance. The ionized electrons are emitted anisotropically and highly directional with respect to the scattering plane such that the electron emission pattern is best imagined as having a jet like feature.

Differential Cross Sections for Multiple Ionization of Ne and Ar by Fast Protons

E. Y. Kamber, C. L. Cocke, S. Cheng and S. L. Varghese

We have measured differential cross sections for single and multiple ionization of Ne and Ar by 3 and 6 MeV protons for scattering angles between 0.1 and 0.9 mrad. The data show that the relative probability for multiple ionization grows substantially with scattering angle in this range, in contrast to the single shell target results. A model which takes into account ionization with large angle scattering by both proton-nucleus and proton-electron collisions concludes that electron-proton collisions dominate the ionization process.

One and Two Electron Processes in Collisions of O^{+8} with D_2

E. Y. Kamber, C. L. Cocke, S. Cheng, V. Frohne and S. L. Varghese

This project is directed at understanding one and two electron ionization and capture processes which occur in the collision of bare oxygen nuclei with molecular deuterium targets. We have measured cross sections for oxygen energies between 8 and 20 MeV. The results show that ionization and excitation processes are of comparable importance and that transfer ionization is larger than capture over this projectile velocity range. Our experiments also measure the dependence of the capture/ionization-excitation probability on the orientation angle. Preliminary results show evidence for a strong dependence on the orientation angle of capture ionization/excitation.

High Resolution, State Selective Study of Transfer with Excitation in the $F^{8+} + H_2$ System

B. D. DePaola, R. Parameswaran and W. J. Axmann

We have completed an experiment using the $F^{8+} + H_2$ collision system, in which we studied in high resolution the projectile Auger electrons resulting from transfer excitation (TE). In this study no evidence of the 2eTE process was observed.

Binary Encounter Electrons Observed at Zero Degrees in Collisions of Fluorine with Lithium Vapor

B. D. DePaola, R. Parameswaran and W. J. Axmann

Using F^{4+} ions and our new metal vapor target cell, the binary encounter peak for lithium was observed for the first time. The peak showed contributions from both the K and L shell (with their correspondingly very different Compton profiles) of the lithium target.

List of Publications

1. "Projectile 1s → 2p Excitation due to Electron-Electron Interaction in Collisions of F^{6+} and O^{5+} Ions with He and H_2 Targets"
   T.J.M. Zouros, D.H. Lee and P. Richard
   Phys. Rev. Letts. 62, 2261 (1989).
2. "Projectile Charge-State Dependence of Zero-Degree Binary Encounter Electrons in Energetic Ion-Atom Collisions"
   P. Richard, D.H. Lee, T.J.M. Zouros, J.M. Sanders, and J.L. Shinpaugh
   To be submitted to Phys. Rev. A. 1989.
3. "Simultaneous Electron-Capture and Target Ionization in Bare-Fluorine – Helium Collisions"
   J.L. Shinpaugh, J.M. Sanders, T.N. Tipping, D.H. Lee, T.J.M. Zouros, P. Richard, J.M. Hall and H. Schmidt-Böcking
   Nucl. Instr. & Meth. in Phys. Res. B40/41, 36 (1989)
4. "Single Electron Capture by 0.5 – 1.5 MeV/u F^{9+} and F^{8+} on Hydrocarbon Gases"
   T.R. Dillingham, B.M. Doughty, J.M. Hall, T.N. Tipping, J.M. Sanders and J.L. Shinpaugh
   Nucl. Instr. & Meth. in Phys. Res. B40/41, 40 (1989).
5. "Dynamics of Inclusive Multi-Electron Emission in Charge Transfer Dominated Highly Charged Ion Atom Collisions"
   B. Krässig, A. González, R. Koch, T. Quinteros, A. Skutlartz, S. Hagmann
   Journal de Physique Vol. 50, (1989) C1-159.

CORRELATED CHARGE-CHANGING ION-ATOM COLLISIONS*

J. A. Tanis and E. M. Bernstein
Western Michigan University, Kalamazoo, MI 49008-5151

This work involves the experimental investigation of fundamental atomic interactions in collisions of highly-charged projectiles with neutral targets. Processes involving excitation, ionization, and charge transfer are investigated, for the most part, using coincidence techniques. A major emphasis of this work is to determine the role of the electron-electron interaction in these various collision processes. New measurements were conducted using accelerators at the Lawrence Berkeley Laboratory (LBL), Argonne National Laboratory (ANL), and Western Michigan University (WMU).

Resonant Transfer and Excitation

In an ion-atom collision, electron capture and projectile inner-shell excitation can take place simultaneously due to the electron-electron interaction, a process referred to as resonant transfer and excitation (RTE). The doubly-excited intermediate state can decay by x-ray emission or by electron (Auger) emission. RTE proceeds via the inverse of an Auger transition and is closely related to the free-electron-ion interaction of dielectronic recombination (DR). Four new investigations of RTE have been conducted:

(1) Projectile charge-state dependence of RTE in $Nb^{q+} + H_2$ collisions - The predicted charge-state dependence of DR cross sections involving $\Delta n \geq 1$ L-shell excitation was tested using measurements of RTE for $_{41}Nb^{q+} + H_2$ (q=28-32) collisions at 3.7 and 4.0 Mev/u. In this work, done at the LBL SuperHILAC, L x-ray emission was measured in coincidence with projectiles capturing an electron. The measured RTE cross sections show a strong charge-state dependence in substantial disagreement with theoretical calculations which predict nearly equal DR cross section values for Nb^{29+}, Nb^{30+}, and Nb^{31+}.

(2) Search for RTE in 130-160 MeV/u U^{89+} + C collisions - Calculations by us for uranium ions incident on H_2 and C indicated that RTE should account for a large fraction (>75%) of the total single capture events. As a test of this prediction we have measured the total single-electron capture cross sections for high energy collisions of U^{89+} in carbon using the LBL BEVALAC. Preliminary analysis of the data indicates that the contributions from RTE at the expected resonance energies of 134.5 and 153 MeV/u are significantly less than predicted. Additional measurements, which should provide a better test of the theory, are planned for $U^{89+} + H_2$ collisions.

(3) RTE with channeled ions - When ions are channeled between the ordered rows of a crystal, the ions interact mainly with the valence electrons. For very well-channeled ions RTE should occur with a high probability compared to direct capture and should have very narrow resonance widths. RTE was investigated for 267-320 MeV $Ti^{19,20+}$ ions channeled along the <110> axis in Au crystals of thickness 1200 A using the ATLAS facility at Argonne. Emerging charge states ranging from 17+ to 21+ were analyzed with a high resolution magnetic spectrograph. The results indicate a sharp maximum in the well-channeled single-capture fractions at the energies expected for RTE with the resonant widths being nearly 5 times narrower than those obtained in measurements with gas targets. New measurements, which can be compared to existing RTE data and calculations, are planned for $Ca^{17,18+}$ ions in Au crystals.

(4) RTE and 2eTE in $F^{6+} + H_2$ collisions - Recent measurements at Oak Ridge for 15-33 MeV $F^{6+} + H_2$ collisions indicated that the RTE cross sections are nearly a factor of two smaller than theory, and, furthermore, suggested a substantial

contribution on the high-energy side of the resonant maximum which could not be accounted for by RTE. The discrepancy was attributed to a process called two-electron transfer excitation (2eTE) in which the projectile is excited by one of the target electrons while the second electron is captured. In similar measurements for 17-36 MeV F^{6+} + H_2 collisions at WMU, we find cross sections substantially larger (by about 60%) than those obtained at Oak Ridge. Additionally, while our data show an extra contribution on the high energy side of the resonant maximum as in the Oak Ridge data, the energy dependence appears to be somewhat different. The origin of this high-energy contribution is not clear and further studies are needed.

Multiple-Electron Capture in Close Collisions

Previously, in measurements of electron capture coincident with projectile or target K x-ray emission, we found for 47 MeV Ca^{17+} + Ar that the cross sections for capturing multiple electrons exceeded significantly that for capturing a single electron. The K-vacancy-production for these collisions was found to be independent of the L-L electron transfer. New measurements (at the LBL SuperHILAC) of electron capture coincident with K x-ray emission were conducted for 47 MeV Ca^{q+} + Ar (q = 10-17). Electron-capture probabilities obtained from the data are a linear function of the number of initial projectile L-shell vacancies. The interactions responsible for the observed multiple capture are still under investigation.

Double Ionization of Helium by Fast Ions

Double ionization of He at high velocities is attributed to two simple mechanisms: (1) a two-step process in which both target electrons are removed in separate direct interactions with the projectile, and (2) a "shake-off" process in which the first electron is removed in a direct interaction with the projectile while the second electron is ejected when the resulting He ion relaxes to a continuum state. The latter process involves electron correlation as in the case of double ionization of helium by photons and is expected to dominate in the asymptotic limit of high projectile velocities. In measurements at WMU, double ionization of helium in relatively small impact parameter collisions with 0.5 - 2.5 MeV/u $O^{6,7+}$ ions was studied by associating target ionization with single-electron loss from the projectile. Double ionization was found to be considerably enhanced (4-6 times) and to deviate substantially from the energy and charge-state behavior observed for double ionization without accompanying electron loss from the projectile, i.e., pure ionization. The reason for this large discrepancy in double ionization between small and large impact parameters is not clear. Further experimental and theoretical studies of ionization in close collisions by highly-charged ions at high velocities are needed to understand these fundamental mechanism(s) of double ionization and to determine the connection to double photoionization.

Continuum Capture Accompanied by Bound-State Capture in Slow Collisions

Two-electron transfer leading to simultaneous bound- and continuum-state capture has been investigated for 60 keV O^{6+} + He using the ECR source at the LBL 88" Cyclotron Facility. In this work, yields for emerging O^{5+} and O^{6+} ions were measured in coincidence with continuum electrons. Essentially no continuum electron capture occurs coincident with emerging O^{6+} ions, suggesting that continuum capture is a correlated two-electron process at these low velocities. These results indicate that electron correlation is even more important than previously believed based on the results of earlier experiments. Additional studies for fully-stripped ions and heavier targets are in progress.

Single-Electron Capture and Loss vs. Target Z for O^{q+} Ions in Gas Targets

Total cross sections for electron capture and loss were obtained for 1 MeV/u O^{5-8+} ions colliding with D_2, He, Ne, Ar, and Kr targets in work done at WMU. The electron-capture measurements are in reasonable agreement with existing theoretical and empirical scaling rules although the results suggest a need to re-evaluate certain of these rules. The electron-loss cross sections differ appreciably from predictions of the plane-wave Born approximation, especially for the heaviest targets studied.

Charge-State Dependence of the Exit Energy of F ions Traversing Carbon Foils

A charge-state dependence has been observed for the exit energies of 0.87 MeV/u fluorine ions traversing carbon foils (13 to 25 $\mu g/cm^2$). The energy differences are largest for ions emerging with K-shell vacancies and small or zero for ions with a full K-shell and differing numbers of L-shell electrons. The results suggest that ions emerging with K-shell vacancies are produced in a relatively thin layer near the exit side of the foil and that the stopping power for these ions is charge-state dependent.

Future Plans

In addition to the planned studies mentioned above, it is anticipated that a collaboration will be initiated with Kansas State University using their new accelerator facility, and we also have an experiment (to measure dielectronic recombination) approved at the Indiana Cyclotron Facility utilizing the electron cooler and storage ring facility.

*Work supported in part by U.S. DOE, Office of Basic Energy Sciences, Division of Chemical Sciences.

PUBLICATIONS

"Multiple-Electron Capture in Close Nearly Symmetric Ion-Atom Collisions," A. S. Schlachter, E. M. Bernstein, M. W. Clark, R. D. DuBois, W. G. Graham, R. H. McFarland, T. J. Morgan, D. W. Mueller, K. R. Stalder, J. W. Stearns, M. P. Stockli, and J. A. Tanis, J. Phys. B21, L291 (1988).

"Enhancement of Radiative Auger Emission in Lithium-Like $_{23}V^{20+}$ Ions," E. M. Bernstein, M. W. Clark, K. H. Berkner, W. G. Graham, R. H. McFarland, T. J. Morgan, A. S. Schlachter, J. W. Stearns, M. P Stockli, and J. A. Tanis, J. Phys. B21, L509 (1988).

"Evidence for Electron Correlation During Double Capture in Fast (v~10a.u.) Collisions," J. A. Tanis, G. Schiwietz, D. Schneider, N. Stolterfoht, W. G. Graham, H. Altevogt, R. Kowallik, A. Mattis, B. Skogvall, T. Schneider, and E. Szmola, Phys. Rev. A39, 1571 (1989).

"Single-Electron Capture and Loss Cross Sections vs. Target Z for 1 MeV/u Oxygen Ions Incident on Gases," S. A. Boman, E. M. Bernstein, and J. A. Tanis, Phys. Rev. A39, 4423 (1989).

"Transfer Ionization in Ion Collisions with Helium," J. A Tanis, E. M. Bernstein, M. W. Clark, S. M. Ferguson, R. N. Price, and W. Woodland, Nucl. Instrum. Methods Phys. Res. B42, 523 (1989).

ACCELERATOR BASED ATOMIC PHYSICS AND EN TANDEM OPERATIONS AT OAK RIDGE NATIONAL LABORATORY

Physics Division, Oak Ridge National Laboratory, Oak Ridge, TN 37831

A. Dielectronic Excitation of Ions in Crystal Channels

(S. Datz, C. R. Vane, P. F. Dittner, J. Giese, J. Gomez del Campo, N. L. Jones, H. F. Krause, T. M. Rosseel, M. Schulz, and H. Schöne)

It has been shown that ions moving through a crystal channel with velocity $v_i >> v_f$ (where v_f equals the Fermi velocity of the electrons in the channel) may be viewed as being bombarded by a flux of electrons at $v \sim v_i$. Dielectronic excitation can occur when an ion travels through such a medium at appropriate velocities. In vacuum, the doubly excited state would decay either by an Auger process or by radiative stabilization. However, in a dense medium, collisional processes leading to further excitation and ionization can come into play and may even dominate. We channeled beams of H-like S^{15+}, Ca^{19+}, and Ti^{20+} and He-like Ti^{20+} and measured the emerging charge states and X rays. In the case of He-like Ti^{20+}, coincidences between X ray and charge capture were measured. In a comparison with theory, source terms arising from dielectronic excitation to KLL, KLM, KLN, and direct excitation of 1s → 2p, etc. are folded with the 10 eV Fermi distribution expected for the outer electrons in Si. The magnitude of the source terms are obtained from tabulated radiative and Auger rates and ionization and excitation cross sections estimated from Lötz and Seaton formulae, respectively. Close agreement between experiment and theory indicates possibilities for the study of collisions in dense media, e.g., short-lived singly and doubly excited states using this technique.

B. Radiative Electron Capture by Bare- and One-Electron Ions

(C. R. Vane, S. Datz, P. F. Dittner, H. F. Krause, and H. Schöne)

Radiative recombination is a fundamental process of positive ion neutralization in which a free electron is transferred to the ion with simultaneous emission of an energy- and momentum-stabilizing photon. When the active electron is initially weakly bound, the process is referred to as Radiative Electron Capture (REC). Sulfur ions channeled in a thin silicon crystal, we have made precise measurements of X rays emitted by fast, bare- and one-electron oxygen, and titanium ions passing through gas or solid targets. Measurements of REC for (100-225 MeV) O^{8+} in H_2 and He gases give centroid energies which match precisely with theory. For (300 MeV) Ti^{21+} and Ti^{22+} ions channeled in silicon and nickel crystals, X rays were detected in coincidence with unscattered Ti^{20+} and Ti^{21+}, respectively. These coincidence spectra permit the most precise measurements made to date for REC energies and profiles. We find that for 300 MeV Ti^{21+} and Ti^{22+} axially channeled in Si <100> and Si <110>, the REC centroid energy lies ~65 eV lower than predicted with peak profiles corresponding very well to those calculated for a Fermi target electron momentum distribution with a Fermi energy of 10.6 eV. Initial measurements in Ni <110> give an even lower peak energy (~120 eV lower than calculated).

C. Measurements of Pair Production and Electron Capture from the Continuum in Heavy Particle Collisions (S. Datz, C. R. Vane, and P. F. Dittner)

Using the facilities at CERN, we plan to measure the production cross section the energy and angular distribution of $e^{\pm}$ pairs produced in collision of 200-GeV/c per nucleon ^{32}S ions with Au. We also plan to measure in the same experiment the cross section for projectile capture of the electron produced in the pair. In addition to the intrinsic atomic physics interest in these phenomena, the results will have an important bearing on future experiments in particle physics using heavy-ion collisions. There have been several highly detailed perturbative calculations on pair production recently. However, a nonperturbative treatment indicates a possible error of a factor of ten at $\gamma_{cm} = 10$ (CERN-fixed target) and one hundred at RHIC energies ($\gamma = 100$). Only perturbative calculations have, thus far, been made for electron capture. No experimental measurements of these important properties have yet been made.

The experiment will utilize a thin Au target placed in the 200-GeV ^{32}S beam at the CERN SPS. Because of non-equality of the projectile and target masses, the pairs will be created with a most probable $\gamma \sim 4$ and extending up to $\gamma \sim 20$. Positron-electron pairs created in the forward direction with γ from 1 to 20 will be split and bent 180° into the detector plane on either side of the target. There they will strike an array of surface barrier solid state detectors. Sulphur ions which capture an electron from the pair would almost immediately lose it again because of secondary collisions in the target. However, this electron would have been accelerated to $\gamma = 200$, i.e., an ELC cusp electron and would be detected at ~20° to the beam direction.

D. Double Excitation of He by Fast Bare Ions (J. P. Giese, M. Schulz, J. K. Swenson, H. Schöne, S. L. Varghese C. R. Vane, M. Benhenni, P. F. Dittner, S. M. Shafroth, and S. Datz)

The double excitation of He by fast, bare projectiles has been measured as a function of the charge, Z, of the projectile. The cross sections for producing the doubly excited states have been found to vary between Z^2 and Z^3 depending on the particular final state. This suggests that the various doubly excited states may be populated by different excitation mechanisms. We have observed autoionization of He atoms following double excitation by electrons, protons, C^{q+} ($q = 4 - 6$), and F^{q+} ($q = 7 - 9$) projectiles at 1.5 MeV/amu. The auto-ionized electrons were detected using a high-resolution electron spectrometer at laboratory observation angles between 9.6° and 60° relative to the beam axis. A strong Fano profile is seen for all states indicating interference between the double excitation and direct ionization processes. The results for all projectiles indicate that excitation to the $2p^2(^1D)$ and $2s^2(^1S)$ states increases as $\sim Z^3$ while excitation to

the $2s2p(^1P)$ varies as $\sim Z^2$, where Z is the charge of the projectile. This result can be qualitatively understood by examining the Z dependencies of the proposed double excitation mechanisms. One mechanism involves a close collision between the projectile and one of the He electrons. This electron in turn interacts with the second electron and both are excited. This mechanism can be pictured as a 'shake-up' transition[4] and should vary as Z^2. The population of the 2s2p state is most probably due to this mechanism. A second mechanism involves a close collision of the projectile with each target electron, and should vary as Z^4. Interference of these two mechanisms is possible and can lead to a Z^3 dependence. This interference term is thought to be responsible for the Z^3 dependence of the $2p^2$ and $2s^2$ states.

E. Projectile Energy Loss Measurements as an N-body Problem in Fast Ion-Atom Collisions

(H. Schöne, S. Datz, P. F. Dittner, M. Schulz, J. P. Giese, H. F. Krause, and C. R. Vane)

Multiple target ionization by MeV/nucleon projectile ions which may, in addition, capture or lose an electron appears to be describable within a classical model. For example, the recoil-ion charge state produced have a distribution which is close to binomial, which is in agreement with the expectations of an independent particle model. The experiments performed probe the validity and limitations of classical approximations in multi-electron processes in fast ion-atom collisions. We have measured the projectile energy loss of 10 MeV C^{q+} ions colliding with He, Ne, Ar, and Kr. Simultaneously, we recorded the projectile and the recoil charge state as well as the energy of the ionized electrons. The projectile energy loss exceeded by a factor of $2 - 5$ the sum of the ionization potentials for a given degree of target ionization. The projectile transfers its energy mainly to the ejected target electrons. We observed a decrease of the mean electron energy with increasing target Z. While the energy loss and the projectile scattering angle increased with increasing recoil charge state, the inelasticity for producing a given charge state did not depend on the impact parameter. Despite a binominal recoil charge state distribution, we found for direct target ionization that the electron energy distribution depends on the degree of ionization. For multiple ionization accompanied by projectile capture no dependence of electron energy on the recoil charge state was observed.

F. Observation of Continuum Projectile Auger Transitions in Collisions of H-like Ions with H_2

(M. Schulz, J. P. Giese, S. Datz, P. F. Dittner, H. F. Krause, H. Schöne, and C. R. Vane)

We have continued our studies on projectile Auger spectroscopy of H-like ions colliding with H_2. Last year, we reported on the n- distribution and the projectile energy dependence of the emission of projectile Auger electrons of the KLn series for $n \leq 5$. In the present work, we focussed the interest on very high n states near the series limit. We measured electron spectra emanating from collisions of 29 to 37 MeV F^{8+} and 8 to 12 MeV C^{5+} with H_2. At the lowest energies, only low n-state lines could be observed. At higher projectile energies, a strong line was observed just above the KLn series limit in both collision systems. These lines cannot originate either from the KLn series or from a higher series since the lowest lying line of the next series (KMM line) occurs at considerably higher electron energies. The position of these lines above the KLn series limit then leads to the conclusion that they result from the decay of a state where one electron is in the L shell of the projectile and a second electron lies just above the continuum edge of the projectile. If this interpretation is correct, this would be, to the best of our knowledge, the first observation of a bound-continuum Auger transition.

G. High Resolution X-Ray Studies of the Chemical Environment of Sulfur Implanted in Silicon and Quartz

(C. R. Vane)

High-resolution sulfur K X-ray satellite spectra have been obtained for 24-MeV Si and 30-MeV Cl ions colliding with silicon and quartz targets containing ion-implanted sulfur at doses of 2.5 to 8.6 x 10^{16} atoms/cm^2. The normalized emission spectra exhibit variations in the intensity distributions of the satellite structures as a function of implant dose. The variations appear to be due to changes in the local valence electron density caused by changes in the local sulfur density. Sulfur X rays were detected from depths ranging from 500 to 200 anstroms below the target surface. This translates into an ability to detect changes in local chemistry of sulfur at concentrations of less than 0.2 atomic percent.

H. Observation of Landau Resonances Well Above Threshold in a High-Resolution (Δf = 70 MHz) Laser Photodetachment Study of O^-

(H. F. Krause)

Magnetic field effects accompanying O^- photodetachment have been investigated using a novel high-resolution crossed-beams apparatus that eliminates the effects of stark splitting due to v x B and minimizes Doppler

broadening. The apparatus has a spectral bandwidth below 70 MHz that corresponds to 30 nano-eV width for the photodetached electron. This resolution is 20 — 100 times higher than has been achieved heretofore in related studies. Periodic structures in the photodetachment cross section have been observed at laser frequencies well above the reaction threshold (0.037 — 0.124 eV). The gross periodicity observed matches the electron cyclotron frequency and is due to Landau resonances having very large quantum numbers (n = 1000 — 60,000). Landau resonances in photodetachment have not been previously predicted or observed well above threshold, at very low magnetic field strengths or at quantum numbers above n = 3. Periodicity at submultiples of the gross repetition frequency is due to Zeeman splitting in the $O^-(^2P_{3/2,\ 1/2}) \rightarrow O(^3P_{j\ =\ 2,1,0}) + e$ fine-structure transitions.

I. EN Tandem Operations
(P. F. Dittner and N. L. Jones)

During the past year, EN-12 was operated for 3,000 hours in support of the accelerator-based atomic physics program. A program of accelerator and facility upgrades continues. The high energy vacuum system was replaced in December, resulting in presures in the 10^{-9} Torr region on the high energy end of the accelerator. The terminal gas control valve was replaced and the foil changer reinstalled, resulting in better control and more flexibility of the beam charge state. These improvements coupled with improved optics and alignment, are allowing more useful beam on target for experiments. The charging belt developed a 6 x 8 inch damaged area that was discovered in December. This damaged area was repaired in place using a procedure developed by the EN-12 staff, allowing continued limited operation until a new belt could be purchased and installed. The new Radiation Monitoring and Protection System was completed and commissioned this year.

J. Prototype Construction for HISTRAP
(D. K. Olsen)

Three hardware prototype construction projects for HISTRAP, funded from the Laboratory Director's R&D Program, have been completed: a dipole magnet and field measuring system, a RF acceleration/deceleration cavity, and a vacuum test stand. A curved laminated prototype dipole magnet was 3-D designed at ORNL, engineered and constructed at the FNAL magnet factory, and field mapped and tested at ORNL. The dipole field quality at both high and low excitation meets HISTRAP requirements and the magnet could be used unattached in the ring. The prototype RF cavity was completed and tested at low power with 16 of the required 32 ferrite rings. These tests indicated that the required frequency swing of 15 to 1 can be achieved. The vacuum test stand, which models 1/16 of the ring circumference, achieved pressures of 4×10^{-12} Torr (a new record in large vacuum systems for this side of the Atlantic).

HIGH ENERGY ATOMIC PHYSICS

Harvey Gould, Laure Blumenfeld*, Ben Feinberg†, Vaclav Kostroun, Richard Mowat, Michael Prior, John Schweppe, and Karen Street§

Materials and Chemical Sciences Research Division, 71 - 259, Lawrence Berkeley Laboratory, University of California, Berkeley, CA 94720.

INTRODUCTION

The goal of this program is to understand the atomic collisions of relativistic ions and to test quantum electrodynamics in very high atomic number (Z) atoms. These are new areas of research involving physics not accessible at lower energies or with lower-Z ions. Our research is conducted at the Lawrence Berkeley Laboratory's Bevalac, the world's only relativistic heavy-ion accelerator. Recent results include the first measurement of electron-impact ionization of highly ionized very heavy ions (U^{88+}, U^{89+}, U^{90+}, and U^{91+}). This measurement was done by channeling relativistic uranium ions through Si single crystals (see publication 1). These and earlier experiments in this program have led to an understanding of relativistic heavy–ion atom collisions that, in most cases, is now more complete than for nonrelativistic collisions (see for example, publications 2&3 and references contained therein). Present activities include a high-accuracy measurement of the Lamb shift in uranium. Future experiments will explore ultra-relativistic collisions and will attempt to observe electron capture from the production of e^+ - e^- pairs by the motional Coulomb fields of relativistic nuclei passing within atomic distances of each other.

RECENT RESULTS

A test-run of our Lamb shift experiment at the Bevalac in July, 1989 produced a 0.6% measurement of the $1s^22p\ ^2P_{1/2}$ - $1s^22s\ ^2S_{1/2}$ transition in lithiumlike uranium. This yields a measurement of the one-electron Lamb shift in uranium with an uncertainty of 1.6 eV, a factor of 5 improvement over previous results[1]. An extensive accelerator run is scheduled for October.

WORK IN PROGRESS

1. Lamb Shift - We are working to prepare for a Bevalac run to measure the approximately 281 eV $1s^22p\ ^2P_{1/2}$ - $1s^22s\ ^2S_{1/2}$ splitting in

---

* Institut Curie, Paris, France

† Accelerator & Fusion Research Division, LBL

§ Berkeley High School, Berkeley CA

[1] C.T. Munger and H. Gould, "Lamb shift in Heliumlike Uranium (U^{90+})" Phys. Rev. Lett. 57, 2927, 1986. (LBL- 21996).

lithiumlike uranium to a few tenths of an eV. Comparison with theory will allow a determination of the one-electron Lamb shift in uranium to a similar accuracy.

Our experiment uses a Doppler-tuned spectrometer in which the energy of the Doppler-shifted photon from the $1s^2 2p\ ^2P_{1/2}$ - $1s^2 2s\ ^2S_{1/2}$ transition in lithiumlike uranium (traveling at about half the speed of light) is measured by determining the angle at which it Doppler shifts across the argon L edge near 248 eV. This is seen as a sharp decrease in the transmission of the photons through an argon gas cell. The photons are detected by an array of six two-dimensional position-sensitive multi-wire proportional counters located 0.75 meters from the beam. Angular definition is provided by a Soller-slit array in front of each detector. Since these low-energy photons are absorbed in air, the entire apparatus is housed inside of a 6 foot diameter vacuum chamber. Elaborate precautions have been taken to minimize background. A time-of-flight apparatus measures the beam velocity. Our experiment is probably the largest and most complex atomic physics experiment ever run at an accelerator in the U.S.

2. Screening- Antiscreening Experiments - The first measurements of charge changing cross sections for relativistic heavy ions in gas targets including hydrogen and helium will be performed to measure the contributions of the target electrons to ionization of relativistic heavy ion projectiles (screening and anti-screening effects). Accuracies of a few-percent are being sought for the ionization cross sections in H, He and heavier gasses of very heavy ions with from one- to 30- electrons. These measurements also serve the practical purpose of providing direct data for determining the survival of relativistic heavy-ion beams for heavy-ion upgrades at the Brookhaven AGS and CERN SPS. Hydrogen and CO (and possibly He) will be the dominant residual gasses in these accelerators.

RECENT PUBLICATIONS

1. N. Claytor, B. Feinberg, H. Gould, C. E. Bemis Jr., J. Gomez del Campo, C.A. Ludemann, and C.R. Vane, "Electron impact ionization of U^{88+} - U^{91+}", Phys. Rev. Lett. **61**, 2081 (1988); LBL-25534.

2. R. Anholt W.E. Meyerhof, X-X Xu, H. Gould, B. Feinberg, R.J. McDonald, H.E. Wegner and P. Thieberger, "Atomic collisions with relativistic heavy ions. VIII Charge-state studies of relativistic uranium ions." Phys. Rev. **A36**, 1586 (1987), LBL-22699.

3. W.E. Meyerhof, R. Anholt, X-X Xu, H. Gould, B. Feinberg, R.J. McDonald, H.E. Wegner and P. Thieberger, "Multiple Ionization in Relativistic Heavy-Ion Atom Collisions" Phys. Rev. (rapid communications) **A35**, 1987 (1987), LBL-22186.

This work was supported by the Director: Office of Energy Research, Office of Basic Energy Science, Chemical Sciences Division; of the U.S. Department of Energy under contract No. DE AC03 76SF00098.

PAPERS

NOT

PRESENTED

NEW INFRARED PHOTON ABSORPTION PROCESSES

James E. Bayfield
Department of Physics and Astronomy
University of Pittsburgh
Pittsburgh, Pennsylvania 15260

It is now recognized that new nonperturbative phenomena occur when atoms are exposed to very short pulses of electromagnetic radiation at field strengths sufficient for significant ionization probability. Of particular interest are pulse lengths of 1 to 1000 field oscillation periods and field strengths 5% of the atomic Coulomb field and much larger. Two aspects of this regime are under investigation both theoretically and experimentally in our laboratory. First is the role of the instantaneous field and second is the possibility of semiclassical behavior. At present, experimental studies of such questions have been and are being carried out for relatively low frequency electromagnetic fields, as visible laser pulses that are both short enough and intense enough are not yet available.

The time oscillation of the applied field is known to modulate single bound state wave functions, an effect that is particularly large and easy to understand for the case of the parabolic states of the hydrogen atom (1). This modulation is an important quantum mechanical aspect of the mechanism for microwave ionization of Rydberg atoms, both hydrogenic and nonhydrogenic (2). In addition, the present picture of infrared ionization of ground state atoms is that of quantum tunneling near the peak of the instantaneous field oscillation (3), although this needs further verification. At the fields where the instantaneous field plays a role in rapid many photon ionization, there is copious above threshold ionization (ATI) (3,4).

When applied field strengths are high enough for two-state Rabi flopping times to approach classical electron orbit times, quantum intermediate states for multiphoton absorption become bands of states. When these bands contain many states, semiclassical evolution of the atom field system becomes possible. A simple example recently considered theoretically is one photon photoionization of Rydberg atoms in the regime where boundstate to continuum Rabi flopping occurs on the time scale of the bound state electron orbit time (5). The problem becomes that of the time evolution of a band of bound states coupled to a band of continuum states. For very short pulses and a range of high field intensities, a destructive quantum wave interference is predicted to occur that reduces the ionization probability as the field intensity is increased. A second case of semiclassical evolution is the classically chaotic microwave ionization of highly excited hydrogen atoms, where the band of strongly coupled bound states extends from the initial state up close to the edge of the continuum (6). When the microwave frequency is a few times the initial electron orbit frequency, again destructive wave

interference reduces ionization probabilities, an effect recently observed experimentally in our laboratory (7).

Our recently initiated DoE experimental research program is designed to search for and investigate the above phenomena in the intermediate frequency regime of mid infrared wavelengths. Excited hydrogen atoms with low values of principal quantum number n are to be exposed to carbon dioxide laser pulses initially of 3000 period duration and much less in the future, at laser peak field strengths between 5% and 5 times the initial state mean Coulomb field. The measurements involve a fast atomic beam apparatus, a pulsed dye laser to excite selectively atoms initially prepared in the metastable state by charge exchange collisions, and an infrared pulsed laser system that will undergo a series of upgrades to shorten the pulse time and increase the pulse intensity. The apparatus will initially be capable of exposing n=8 atoms to peak instantaneous fields above the initial state Coulomb field, with pulse lengths of a few thousand periods that should be short enough to avoid experimental saturation of two photon ionization (8). In addition, measurements of two photon ionization of n=10 will involve a coupling to a band of highly excited bound states as the intermediate "state". The band can be moved from near n=40 up to n=100 by changing the laser line that the carbon dioxide laser is producing. This experimental study of multistate quantum wave interference effects in multiphoton ionization can be supported by quantum numerical calculations (9).

1. J. E. Bayfield, L. D. Gardner, Y. Z. Gulkok and S. D. Sharma, "A Spectrscopic Study of Highly Excited Hydrogen Atoms in a Strong Microwave Field", Phys. Rev. A 24, 138 (1981).

2. T. F. Gallagher, "Microwave Excitation and Ionization" in Photons and Continuum States of Atoms and Molecules, N. K. Rahman, C. Guidotti and M. Allegrini, editors, Springer-Verlag, Berlin, 1987, page 2.

3. P. B. Corkum, N. H. Burnett and F. Brunel, "Above Threshold Ionization in the Long-wavelength Limit", Phys. Rev. Lett. 62, 1259 (1989).

4. T. F. Gallagher, "Above Threshold Ionization in Low Frequency Limit", Phys. Rev. Lett. 61, 2304 (1988).

5. M. V. Federov and A. M. Movsesian, "Interference Suppression of Photoionization of Rydberg Atoms in a Strong Electromagnetic Field", J. Opt. Soc. Am. B 6, 928 (1989).

6. J. E. Bayfield and D. W. Sokol, "Excited Atoms in Strong Microwaves: Resonances and Localization in Experimental Final State Distributions", Phys. Rev. Lett. 61, 2007 (1988).

7. J. E. Bayfield, G. Casati, I. Guarneri and D. W. Sokol, "Localization of Classically Chaotic Diffusion for Hydrogen Atoms in Microwave Fields", Phys. Rev. Lett. 63, 364 (1989).

8. J. E. Bayfield and D. W. Sokol, "Resonant Infrared Two-photon Ionization of D(n=8) Atoms", Phys. Rev. A 34, 2977 (1986).

9. R. V. Jensen and S. M. Susskind, "Ionization of One-dimensional Hydrogen Atoms with Intense Microwave and Laser Pulses", in Atomic and Molecular Processes with Short Intense Laser Pulses, A. D. Bandrauk, editor, Plenum Press, 1988, page 253.

Interactions of fast atomic and molecular ions with matter[1]

A. Belkacem, E. P. Kanter, and Z. Vager,
Argonne National Laboratory, Argonne, Illinois 60439

Argonne's 5-MV Dynamitron accelerator is used to study the interactions of fast (MeV) atomic and molecular ions with matter. A unique feature of the apparatus is the exceptionally high resolution, in angle and time-of-flight, obtained in detecting particles emerging from the target. New imaging detector systems have been developed which allow detection of multiparticle events consisting of up to 12 particles. The work has as its main objective a general study of the interactions of fast charged particles with matter, but with the emphasis on those aspects that take advantage of the unique features inherent in employing molecular-ion beams (e.g., the feature that each molecular ion incident upon a solid target forms a tight cluster of atomic ions that remain correlated in space and time as they penetrate the target). In particular, these techniques have allowed the direct determination of the geometrical structures of the molecular ions entering the target, providing the first direct measure of the fully correlated nuclear densities within small molecules. Some of the highlights of the past year include:

(1) Development of a segmented-anode MWPC

Our previous experiments with molecules containing protons and 2 or more heavy ions had been severely hampered because of the finite area of the MUPPATS detector. As a result, we either sacrificed charge state information (as was the case for $C_2H_3^+$) or information about the proton geometries. This limited our most extensive studies before now to molecules of the form XH_n^+.

In an effort to alleviate these limitations, we have developed a new detector specifically optimized for heavy ion detection. The new detector is a single stage multiwire proportional counter with a unique anode structure consisting of a plated-through PC board (25 x 50 cm^2) which interweaves 3 non-intersecting "wire planes" onto a single anode board. We have obtained time resolutions below 160 psec over the entire surface of this large-area detector. With this new detector, we are now able to separate the heavily ionizing heavy ions from the more weakly ionizing protons and thus have improved the detection efficiencies for molecules containing both types of fragments. Additionally, the large area of the new detector permits sufficient electrostatic deflections to resolve heteronuclear heavy-ion fragments and this feature has enabled us to study a variety of heavy diatomic systems which are described below.

(2) The ultrashort bond length in $^3He^4He^{++}$

Although not very common in the laboratory, because of the abundance of helium in stellar atmospheres and in interstellar clouds, long-lived helium-containing molecules (e.g. HeH^+, He_2, He_2^+, He_2^{++}, etc.) are of considerable astrophysical interest. Among these, He_2^{++} is perhaps the simplest, but least known. As the isoelectronic analog of the neutral H_2 molecule, it provides an unusual example of the most basic electron pair bond. It was first studied theoretically by Pauling in 1933. Using a variational treatment, he showed that while the internuclear potential between two He^+ ions is repulsive at large separations, the exchange and electron-nuclear attraction integrals overcome the repulsion at intermediate distances. Since that time, several workers have

---

1. This work was supported by the U.S. Department of Energy, Office of Basic Energy Sciences, under Contract W-31-109-Eng-38.

improved upon that simple treatment and it now appears that with a predicted bond length of 0.70 Å, it will prove to be the smallest known diatomic molecule.

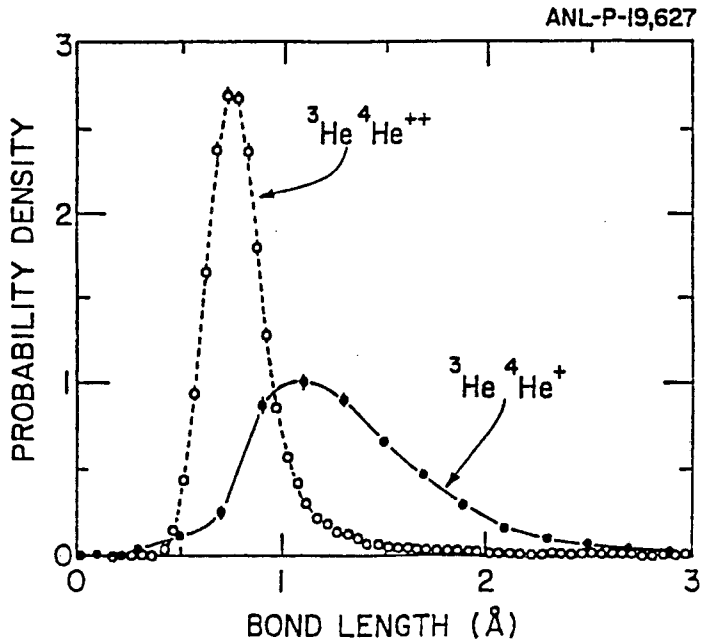

Fig. 1: Distributions of bond lengths for $^3He^4He^+$ (solid points) and $^3He^4He^{++}$ (open circles) deduced from the Coulomb explosion measurements. The curves are drawn to guide the eye.

In order to test that prediction, we have measured the bond length distribution within He_2^{++} by Coulomb explosion imaging. In the accompanying figure we show the experimental results for both the singly-charged and doubly-charged dihelium molecules. The results of our measurement for He_2^+ show a most probable bond length of 1.10 Å and the distribution, which is confined to the allowed region of the predicted potential well, shows good agreement with theory. The data on the doubly-charged molecule (prepared by gas-stripping of the singly-charged species) yield a most probable bond length of 0.75 Å. This value and the shape of the distribution are consistent with the calculations, providing the first experimental confirmation of the theory for this, the simplest doubly-charged molecule. This experiment has demonstrated that the Coulomb explosion method is suitable for the measurement of structures of doubly-ionized molecules. Further work is underway studying the repulsive region of the potential by investigating collision-induced dissociations of He_2^+ in gas.

During the past year, we have also carried out a systematic series of measurements of the bond-length distributions of other doubly-charged molecules. These studies included CN^{++}, CO^{++}, N_2^{++}, and NO^{++}. By exploiting a simple model of electronic screening in the early stages of the Coulomb explosion, we were able to account for the observed charge-state dependence of these measurements and achieve a bond-length resolution of ±.02 Å for these fast molecular-ion beams.

(3) Stereostructures of hydrocarbon cations

The chemistry of hydrocarbon ions in the gas phase is an active field of research not only because of the intrinsic interest in the properties of such

molecular ions but also because of their importance in the synthesis of interstellar molecules and combustion. For example, ions such as $C_3H_3^+$ are known to be important precursors to sooting in flames. Many of the ions are nonrigid (e.g. $C_2H_3^+$) and thus difficult candidates for spectroscopic studies.

We have conducted a study of the structures of molecular ions of the form $C_2H_n^+$ (n=1-6). Preliminary findings show an extreme range of proton motions within these molecules. For example, in experiments with $C_2H_2^+$ ions, we have observed exceedingly sharp proton distributions while for C_2H^+, the hydrogen appears to be completely delocalized. The data for $C_2H_3^+$ clearly show a bridged structure while our measurements of $C_2H_5^+$ do not. $C_2H_4^+$ exhibits a planar geometry with only small twisting vibrations. Further work is underway to repeat these measurements with the deuterated forms $C_2D_n^+$ to test what influence the breakdown of the Born-Oppenheimer approximation may play in these findings.

Future Plans

With the results of these recent investigations, it has become clear that Coulomb explosions provide a rich source of information about molecular properties. While conventional high-resolution spectroscopy yields precise, unambiguous structures for near-rigid molecules exhibiting sharp spectra, Coulomb explosions can provide data leading directly to stereochemical structures even for molecules too non-rigid or short-lived to have assignable spectra. For polyatomic molecular ions with many degrees of freedom, such structural information can provide guidance for theoretical predictions of precise optimized geometries enabling accurate spectral computations. One of the limitations in our studies to date has been the uncertainty in the vibrational distributions of the molecules formed in our ion source. Our studies of $C_2H_2^+$ however has shown us that we can form cold beams by limiting collisions in the source. To generalize upon this result, we have begun construction of a pulsed nozzle ion source to form a supersonic expansion in the Dynamitron terminal. With this new source, we will be able to study the structures of vibrationally cold molecules. Our immediate aim is to apply these techniques to molecules for which spectroscopic results are incomplete and/or quantum chemical calculations remain inconclusive. Among the systems to be studied in the near future with this new source are carbocations of the form $C_mH_n^{+q}$ (m=1-6, n=0-6, q≥1), hydronium ion hydrates, and a variety of light cluster ions (He_n^+, Li_n^+, B_n^+, and C_n^+).

Some recent publications on these subjects include:

COULOMB EXPLOSION IMAGING OF SMALL MOLECULES, Z. Vager, R. Naaman, and E. P. Kanter, *Science*, **244**, 426 (1989).

STRUCTURES OF MOLECULES AND CLUSTERS AS DETERMINED BY COULOMB EXPLOSIONS, Z. Vager, R. Naaman, and E. P. Kanter, in *"Ion and Cluster Ion Spectroscopy and Structure"*, J. P. Maier, Ed. (Elsevier, Amsterdam, 1989), pp. 1-26.

THE STRUCTURE OF SMALL MOLECULES WITH THE COULOMB EXPLOSION METHOD, Z. Vager and E. P. Kanter, Nucl. Instrum. and Meth. **B33**, 98 (1988).

GEOMETRICAL STRUCTURE OF C_3^+, A. Faibis, E. P. Kanter, L. M. Tack, E. Bakke, and B. J. Zabransky, J. Phys. Chem. **91**, 6445 (1987).

ULTRATHIN FOILS FOR COULOMB-EXPLOSION EXPERIMENTS, G. Both, E. P. Kanter, Z. Vager, B. J. Zabransky, and D. Zajfman, Rev. Sci. Instrum., **58**, 424 (1987).

Low Energy Collisions Involving Negative Ions

R. L. Champion and L. D. Doverspike
Department of Physics
College of William and Mary
Williamsburg, VA 23185

The principal focus of this project during the past year has been an investigation of the collisional dynamics for the systems H^- (D^-) and atomic hydrogen. An apparatus which employs a crossed beam configuration has been utilized in this study. We have also recently completed a study of the collisional decomposition of the molecular anion SF_6^-. Brief descriptions of these recent activities along with future plans for the project are given below.

1. H^- and D^- collisions with atomic hydrogen.

Cross sections for collisional detachment

$$X^- + H \rightarrow X + H + e, \qquad (1)$$

and charge transfer

$$X^- + H \rightarrow X + H^- \qquad (2)$$

have been measured for laboratory collision energies ranging from a few eV up to several hundred eV for $X^- \equiv H^-$ and D^-. Atomic hydrogen is produced by a radio-frequency discharge source and the effusing beam intersects the negative ion beam within a cylindrical electrostatic energy analyzer. The electric field between the curved plates of the analyzer is chosen such that the negative ion beam will pass resonantly through the device. This same electric field serves simultaneously to extract the reaction products from (1) & (2) above; ions and electrons are subsequently separated by a weak magnetic field. The dissociation fraction in the neutral H/H_2 beam (≈85%) is determined by comparing the charge transfer and detachment cross sections for H^- + H and H_2 to the total electron loss cross sections recently reported by Gealy and Van Zyl[1]. The experimental results are given in Figure 1.

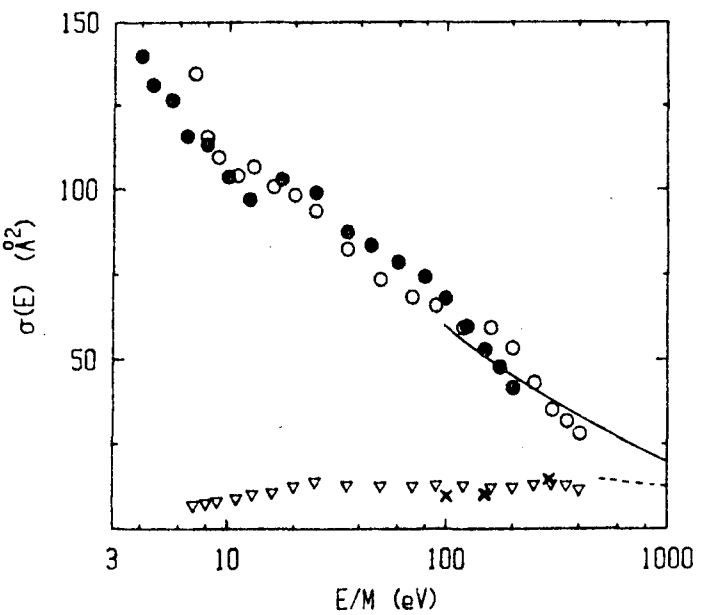

Fig. 1. - Charge transfer cross sections for H^- (0) and D^- (●) + H and detachment for H^- + H (▽) as a function of E/M. The results of Hummer et al.[2] (— & ---) and Esaulov[3] (x) are also shown.

The cross section for resonant charge transfer, $\sigma_{ct}(E)$, continues to increase as the collision energy is decreased below 400 eV. Isotopic substitution reveals that $\sigma_{ct}(E)$ for H^- and D^- are approximately equal at the same collision velocities. The detachment cross section, $\sigma_e(E)$, does not exhibit a steep rise for $E < 400$ eV, as has been suggested previously. Rather, $\sigma_e(E)$ remains approximately constant and is very close to the geometrical cross section $(1/2)\pi(R_a^2 + R_b^2)$, where R_a and R_b are the crossing points of the $^2\Sigma_u$ and $^2\Sigma_g$ states of H^- + H with the relevant H + H states.

2. Collisional decomposition of SF_6^-

Interest in SF_6 stems mainly from its use as a gas dielectric in high voltage applications. Two properties of SF_6 make it attractive for such applications: it has a large attachment cross section for thermal energy electrons and it is apparently stable against collisional electron detachment for relative collision energies which exceed the electron affinity of SF_6 (≈1 eV) by as much as a factor of eight. There is further evidence which suggests that the destruction of the negative ion is dominated by collisional dissociation of SF_6^- into various ionic fragments. However, all existing experimental data concerning decomposition of SF_6^- are model dependent, being inferred from drift-tube measurements.

In particular, very little information is available on how SF_6^- decomposes in binary collisions with gaseous targets. The purpose of this project was to measure various absolute cross sections for collisions of SF_6^-, SF_5^- and F^- with the rare gases and SF_6. Results for the SF_6 target are shown below.

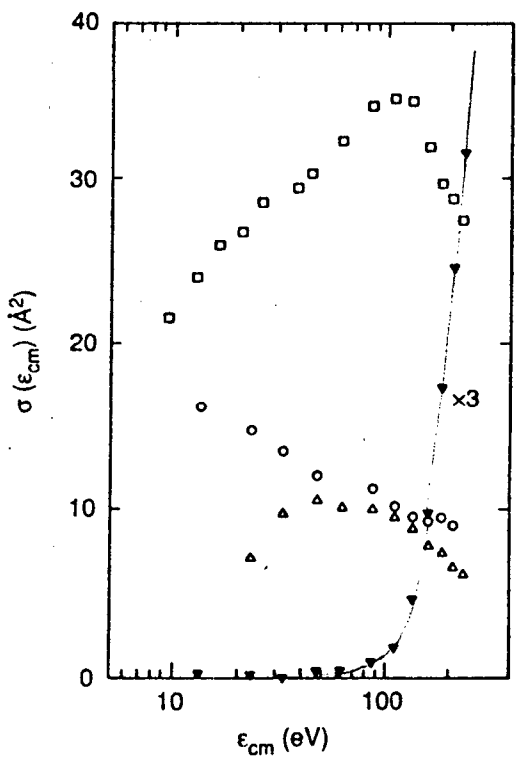

Fig. 2. - Cross sections for collisional detachment(▼), F^- production (□), SF_5^- production (0), and charge transfer (Δ) as a function of the relative collision energy. Note that the detachment data have been multiplied by a factor of three.

The cross sections for electron detachment of SF_6^- are observed to be surprisingly small for relative collision energies below several tens of electron volts. The cross sections for the collision induced dissociation into either F^- or SF_5^- dominate at low collision energies. These observations are clearly important for developing an understanding of electrical breakdown when using SF_6 as a dielectric.

3. Future studies.

Work will continue on the crossed beam apparatus with measurements of the cross sections for collisional and associative detachment and charge transfer being the immediate goal. Systems to be studied will include halogen anions, O^-, and S^- in collisions with atomic H and D. Charge transfer cross sections for low energy collisions of selected positive ions with atomic hydrogen will also be measured. We are currently investigating the possibility of expanding this apparatus to enable us to measure ionization cross sections:

$$X + H \longrightarrow X^+ + H + e \quad \text{or} \quad X + H^+ + e,$$

for energies in the near-threshold region. The primary ion beam (X) may be generated by collisionally detaching X^- after accelerating it to the desired collision energy. Very litle is known about such mechanisms in this energy range.

---

[1] M.W. Gealy and B. Van Zyl, Phys. Rev. A36, 3091 (1987)
[2] D.G. Hummer et al., Phys. Rev. 119, 668 (1960)
[3] V.A. Esaulov, J. Phys. B 13, 4039 (1980)

4. Five most recent publications.

(1) Reactive scattering and electron detachment for collisions of halogen negative ions with HCL, DCL and HBr.
R.L. Champion, L.D. Doverspike, M.S. Huq, D. Scott, and Yicheng Wang, J. Chem. Phys. 88, 5475 (1988).

(2) Electron detachment in low energy H^- (D^-)-Na collisions.
J.P. Gauyacq, Yicheng Wang, R.L. Champion, and L.D. Doverspike, Phys. Rev. A 38, 2284 (1988).

(3) Negative ion formation on alkali surfaces.
Yicheng Wang, M.A. Huels, D.R. Gallagher, R.L. Champion, and L.D. Doverspike, Phys. Rev. Let. 61, 1194 (1988).

(4) Positive ion production in halogen negative ion collisions.
F. Penent, R. L. Champion, L. D. Doverspike, V. A. Esaulov, J. P. Grouard, R. I. Hall and J. L. Montmagnon, J. Phys. B 21, 3375 (1988).

(5) Collisional electron detachment and decomposition cross sections for SF_6^-, SF_5^-, and F^- in SF_6 and rare gas targets.
Yicheng Wang, R.L. Champion, L.D. Doverspike, J.K. Olthoff, and R.J. Van Brunt, J. Chem. Phys. 91, 2254 (1989).

High-Precision Laser and RF Spectroscopy of Atomic and Molecular Beams

W. J. Childs, Y. Azuma, G. L. Goodman*, and T. C. Steimle**

Argonne National Laboratory, Argonne, IL 60439

Work has continued during the past year on structure studies of both many-electron atoms and diatomic radicals. This report will focus on the molecular work.

Considerable time was spent studying the isoelectronic molecules PrO and CeF. In PrO, laser-rf double resonance was used to measure precisely the hyperfine structure (hfs) of the electronic groundstate ($\Omega = 3.5$) for all J-values up to 60.5. The measurements reveal that the splittings are negative at the lowest J-values, and then increase almost linearly with J, becoming positive for all $J \geq 5.5$ as shown in Fig. 1. The measured J-dependence shows that

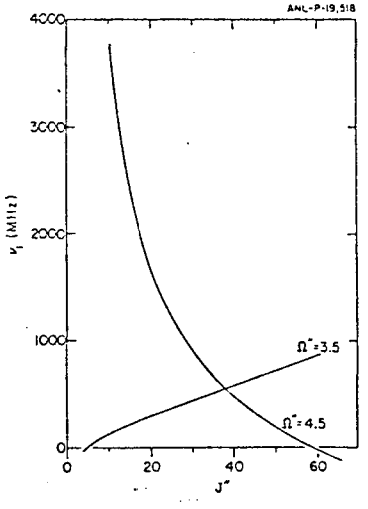

Fig. 1. Largest hfs interval in two electronic states of PrO as a function of rotational angular momentum.

previously published results inferred from optical spectra are wrong and once again demonstrates the need for direct measurement of hfs splittings. The unusual J-dependence appears to arise from off-diagonal interactions between the ground ($\Omega = 3.5$) and first excited ($\Omega = 4.5$) electronic states. The double-resonance technique was accordingly used to measure the hfs in the excited state and these results are also shown in Fig. 1. The molecular electronic states X ($\Omega = 3.5$) and A ($\Omega = 4.5$) are closely related to states of Pr^{2+} ($4f^2 6s$) coupled with the oxygen ion O^{2-} with a full 2p-shell. If we denote the electronic angular momentum of the $4f^2$ core as $\vec{J}_c$ and the spin of the 6s electron as $\vec{s}$, then as a start we must consider the operators $H_{rot} = B(\vec{J}-\vec{J}_c-\vec{s})^2$ and $H_{hfs} = b\vec{I}\cdot\vec{S}$. The total hfs in the state X or A is then composed of two parts: (1) the intrinsic hfs caused by evaluating H_{hfs} within each state, and (2) that due to the mixed interaction $\langle X|H_{hfs}|A\rangle \langle A|H_{rot}|X\rangle$ or $\langle A|H_{hfs}|X\rangle \langle X|H_{rot}|A\rangle$, i.e. the

*Chemistry Division, Argonne National Laboratory.
**Department of Chemistry, Arizona State University, Tempe, Arizona.

off-diagonal hfs between the states of different Ω. In order to calculate these matrix elements we need a specific model for the coupling of electronic angular momenta. We have adopted the coupling scheme J_c, Ω_c σ, Ω, where Ω_c gives the projection of J_c on the internuclear axis and σ gives the projection of the outer s electron spin on this axis. In this scheme the X state is 4,4,-0.5,3.5 and the A state is 4,4,0.5,4.5. The necessary Racah algebra has been worked out, and it is found that the model is in very close agreement (~1-2%) with experiment if the interaction strengths are regarded as adjustable parameters. The best-fit values determined for the off-diagonal hfs parameters are very nearly equal and opposite (as expected from the opposite signs of the energy denominators), but the parameter values for the diagonal terms are found to be very different for the two states. This result is not yet understood.

Studies of the isoelectronic molecule CeF show that the hfs is essentially zero in the electronic ground state but appreciable in the excited state. The situation in CeF is not directly comparable to PrO, however, since in the CeF the metal-centered electron is interacting with the ^{19}F spin (I=1/2) while in PrO the metal-centered electron is interacting with the ^{141}Pr spin (I=5/2). Papers will be prepared on both studies.

In 1981 we published detailed measurements of the spin-rotation and hyperfine structure of the $X^2\Sigma^+$ electronic ground state of $^{88}Sr^{19}F$ and $^{86}Sr^{19}F$. The corresponding spectral features for the 7% abundant $^{87}Sr^{19}F$ molecule (the nuclear spin of ^{87}Sr is I=9/2) were searched for at that time but, being two orders of magnitude weaker, were not seen. Since that time a number of improvements in the sensitivity of our techniques have taken place, and accordingly we tried again and we are now able to see the $^{87}Sr^{19}F$ features. Figure 2 shows, for example, the spectral region near the line $R_2(J"=70)$ in the

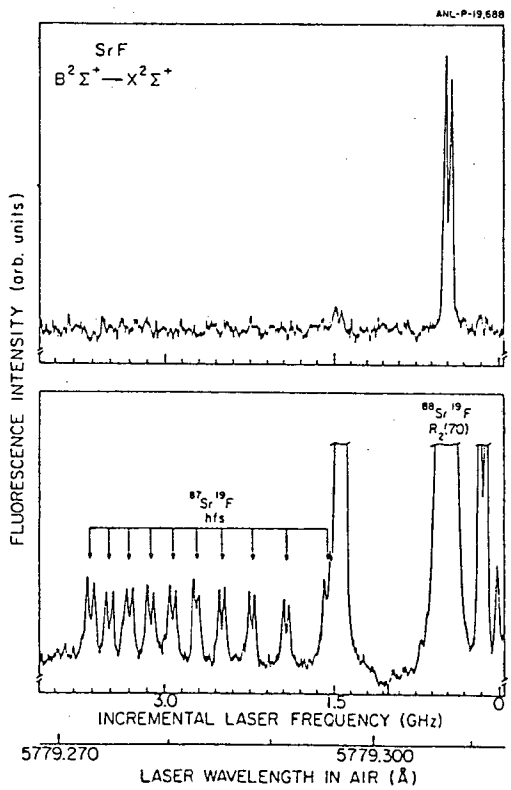

Fig. 2. $B^2\Sigma^+ \leftrightarrow X^2\Sigma^+$ spectrum of SrF in the vicinity of $R_2(70)$. Upper spectrum shows sensitivity attainable in study of $^{88}Sr^{19}F$ and $^{86}Sr^{19}F$ in 1981. Lower trace, with present much increased sensitivity, shows the 10 hfs peaks due to the 7% abundant ^{87}Sr in $^{87}Sr^{19}F$. Each is further split by the I=1/2 of ^{19}F.

$B \leftrightarrow X(0,0)$ band. The upper spectrum shows the appearance of the region with the sensitivity formerly achievable, while the lower shows a recent scan through the same region with the much greater sensitivity now achievable. The $2I+1=10$ hfs components due to $^{87}Sr^{19}F$ are clearly visible; each is further split by the $2I+1=2$ components due to the spin 1/2 of ^{19}F. The importance of this is that we can now for the first time observe the hfs interaction at the metal site (Sr nucleus) in addition to that at the fluorine ion. Laser-rf double-resonance measurements of the X-state spin-rotation and hfs splittings have now been carried out over a broad range of N-values in the $^{87}Sr^{19}F$ and the results are being analyzed.

This research was supported by the U.S. Department of Energy, Office of Basic Energy Sciences, under contract W-31-109-ENG-38.

Selected Journal Articles, 1988-1989

1. Hfs of the $(5d+6s)^3$ configuration of ^{139}La I: new measurements and *ab initio* (MCDF) calculations
   W. J. Childs and U. Nielsen
   Phys. Rev. A 37, 6 (1988)

2. Hyperfine structure of some excited states of $^{133}Cs^+$ by collinear laser-ion beam spectroscopy
   A. Sen and W. J. Childs
   Phys. Rev. A 40, 2159 (1989)

3. Hyperfine structure of the $4f^75d^26s\ ^{11}F$ term of $^{155,157}Gd$ by laser-rf double resonance
   W. J. Childs
   Phys. Rev. A 39, 4956 (1989)

4. Fine and magnetic hyperfine structure in the $A^2\Pi$ and $X^2\Sigma^+$ states of yttrium monoxide
   W. J. Childs, T. C. Steimle, and O. Poulsen
   J. Chem. Phys. 88, 598 (1988)

5. A molecular-beam optical and radiofrequency optical double-resonance study of the $A^2\Pi \leftrightarrow X^2\Sigma^+$ band systems of scandium monoxide
   W. J. Childs and T. C. Steimle
   J. Chem. Phys. 88, 6168 (1988)

Many-Body Processes in Atomic and Molecular Physics

Shih-I Chu

Department of Chemistry, University of Kansas, Lawrence, KS 66045

The theoretical atomic and molecular physics program at the University of Kansas is directed towards the development of new theoretical formalisms and practical computational methods for ab initio investigation of many-body resonances as well as atomic and molecular processes in intense laser fields. Our major recent accomplishments are summarized below.

1. *Quantum Fractal Behavior of Eigenstates in Intense Polychromatic Fields*

We have recently studied the quasi-energy eigenfunctions of N-level quantum systems perturbed by intense quasiperiodic or polychromatic fields,[1] using the many-mode Floquet theory[2] developed in our group. It is found that the eigenfunctions exhibit striking self-similar (fractal) behavior in the temporal Fourier space.[1] We have further developed a method for the calculation of the fractal (D_f) and entropy (D_s) dimensions of quasi-energy states. The fractal dimensions are found to be (laser) intensity-dependent and obey the relationship $D_f \leq D_s \leq M$, where M is the number of incommensurate field frequencies.

2. *Density Matrix Formulation of Complex Geometric Phases in Dissipative Systems*

We have developed a generalized version of the Feynman-Vernon-Hellwarth geometric representation and a biorthogonal density matrix formalism for the description of the non-Hermitian Schrodinger equation.[3] The theory is applied to the study of complex geometric quantum phases in dissipative systems. It is shown that the complex Aharonov-Anandan (AA) geometric phase is related to the complex solid angle enclosed by a complex Bloch vector trajectory $\vec{S}(t)$. General analytic formulas are presented for the complex AA phase for a driven dissipative two-level system undergoing multiphoton Rabi floppings.[3]

3. *Dynamics of Multiphoton Excitation and Quantum Diffusion in Rydberg Atoms*

We have recently presented a first detailed two-dimensional (2D) quantal study of the dynamical evolution of microwave-driven Rydberg H atoms.[4] We examine the range of validity of the conventional one-dimensional (1D) models and explore the frequency- and intensity-dependent excitation and ionization mechanisms. The main findings of this study can be summarized as follows: (i) The excitation spectra of Rydberg H atoms are strongly frequency dependent and can be roughly grouped into three characteristically different regions, each with a different excitation mechanism. In this paper, we emphasize the study of the two major excitation mechanisms: quantum diffusion and multiphoton resonant excitation, the Region dominated by quantum diffusion lies in the frequency range $\omega_c < \omega_0 < \omega_d$, where ω_0 is the rescaled field frequency ($\omega_0 = \omega n_0^3$; n_0 is the principal quantum number of the initial state); ω_c, the classical chaotic threshold; and ω_d, the quantum delocalization border. In this region, quasienergy levels are strongly perturbed and mixed

and excitation is efficient, leading to the so-called *under*threshold photoelectric ionization phenomenon. On the other hand, we found a series of frequency regions (in $\omega_0 > \omega_d$) where the ionization is mainly due to multiphoton resonant excitation through the more isolated quasienergy avoided crossing points. (ii) The excitation pathways (1D versus 2D) are strongly intensity dependent. For microwave (rescaled) field strength $\varepsilon_0(\equiv\varepsilon n_0^4)$ in the range $\varepsilon_c < \varepsilon_0 < \varepsilon_q$ (where ε_c is the onset of classical chaos and ε_q the quantum delocalization threshold), large discrepancies exist between 1D and 2D results. It is found that the 1D model seriously underestimates the ionization probabilities and, more importantly, the dominant channels for Rydberg atom excitation and ionization proceed through $n_2 > 0$ ladders rather than the $n_2 = 0$ ladder, as often assumed in the 1D model. As field strength increases above ε_q, however, the 1D model improves significantly. (iii) The quantum localization phenomenon is observed in the classically chaotic region ($\omega_c < \omega_0 < \omega_d$) when the field strength ε_0 is less than ε_q. However, quantum delocalization can appear when $\varepsilon_0 > \varepsilon_q$. (iv) The stability of quantum diffusive motion is analyzed in terms of the quantal phase-space diagram and the autocorrelation function. The results lend support to the view that quantum mechanics can impose limitations on classical chaotic motion. (v) The way of turning on the field ($\sin\omega t$ or $\cos\omega t$) does not affect significantly the dynamical evolution of the system. (vi) Finally, a computationally powerful new technique, invoking the use of artificial intelligence algorithms as well as the generalized Van Vleck perturbation theory for effectively reducing the dimensionality of the Floquet matrix, is introduced to facilitate the study of multiphoton resonant excitation of Rydberg atoms.[4]

4. *Generalized Floquet Theoretical Treatments of Intense Field Multiphoton and Nonlinear Optical Processes*

Two review articles[1,5] describing recent new developments of generalized Floquet formalisms and quasi-energy methods in our laboratory for nonperturbative treatments of various intense field multiphoton excitation, ionization and dissociation processes as well as multiple wave mixings and nonlinear optical susceptibilities have been published in this period.

5. *Future Research Plans*

In addition to continuing our ongoing theoretical developments and investigations, several new projects of current importance in atomic, molecular physics and quantum optics will also be pursued. These include: (a) Theoretical investigation of quantum dynamics and chaotic behavior of Rydberg atoms driven by quasi-periodic (multi-frequency) microwave fields. (b) Development of new nonperturbative techniques for the treatment of a.c. Stark shifts of highly excited states in intense laser fields. (c) Developments of generalized coherent-state and density-matrix formalisms for the study of geometric (Berry's and Aharonov-Anandan) phases in laser-induced atomic and molecular collisions and in quantum optics. (d) Nonlinear dynamics and quantum fractals in dissipative systems perturbed by quasi-periodic fields. (e) Nonperturbative treatments of multiple harmonic generation in intense laser fields.

Selected publications

1. K. Wang and S.I. Chu, "Fractal Character of Quasi-energy States in Intense Polychromatic Fields," Chem. Phys. Lett. 153, 87-92 (1988).

2. S.I. Chu, "Generalized Floquet Theoretical Approaches to Multiphoton and Nonlinear Optical Processes in Intense Laser Fields," Advances in Chemical Physics, (John Wiley & Sons), vol. 73, 739-799 (1989), and references therein.

3. S.I. Chu, Z.C. Wu, and E. Layton, "Density Matrix Formulation of Complex Geometric Quantum Phases in Dissipative Systems," Chem. Phys. Lett. 157, 151-158 (1989).

4. K. Wang and S.I. Chu, "Dynamics of Multiphoton Excitation and Quantum Diffusion in Rydberg Atoms," Phys. Rev. A39, 1800-1808 (1989).

5. K. Sando and S.I. Chu, "Pressure Broadening and Laser-Induced Spectral Line Shapes," Advances in Atomic and Molecular Physics, (Academic Press), vol. 25, pp. 133-162 (1988).

Collision Processes in Ionized Gas

A. Dalgarno

Multi-charged molecular ions ordinarily dissociate rapidly because of the Coulomb repulsion between the pair of charged species into which the molecule separates. The states that separate to a neutral species and a multi-charged atomic ion have potential energies that tend at large internuclear distances to an attractive polarizaton potential and they may contain several vibrational levels. They are excited electronic states of the molecule and the vibrational levels are quasi-bound because they can predissociate into the lower-lying states with potential energy curves characterized by their long range Coulomb repulsion. The predissociation often occurs because of the occurrence of avoided crossings in the adiabatic potential energy curves. The predissociation mechanism is just that which drives the charge transfer process so that the study of the predissociation by, for example, measuring the kinetic energies of the products, would provide considerable insight into the details of the potential energy curves and the couplings of the electronic states that control the charge transfer process and might allow their empirical determination. Conceivably the role of translation factors could be clarified. The quasi-bound vibrational levels can usually decay radiatively by spontaneous emission into lower-lying repulsive states and a successful observation of the emission spectrum would provide additional information. In some cases, spontaneous emission is slow and long-lived states of the multiply-charged ion exist that can participate in chemical reactions.

Several systems are under study. Fig. 1 shows the results of calculations on the $^2\Pi$ states of the cation NHe^{2+} carried out in collaboration with K. Kirby and G. Lafayatis. Because of an avoided crossing the lowest state, labelled X on the figure, has a deep inner well inside a potential barrier. The well may be deep enough that the lowest vibrational levels are stable with energies lying below the asymptotic dissociation limits but in any case the well will contain many long-lived vibrational levels. Calculations of the level structure are continuing. The excited states labelled A and B will also contain vibrational levels. To determine their location will involve a solution of the coupled equations.

We are carrying out a similar study of NH^{4+} using potential energy surfaces and radial couplings obtained by D.L. Cooper. At the same time we are calculating the cross sections for the charge transfer process

$$N^{4+} + H \rightarrow N^{3+} + H$$

using a quantum-mechanical formulation of the scattering.

Investigations of the proton impact excitation of fine-structure levels of positive ions continue. The theory has been extended to deal with states involving d-electrons and cross sections for excitation of the $3d_{3/2}$-$3d_{5/2}$ fine structure levels of singly-ionized sulfur have been determined.

We have repeated earlier calculations of the quenching of metastable 2^1S helium atoms (B. Zygelman and A. Dalgarno, Phys. Rev. A. 38, 1877, 1988) with the incorporation of an accurate transition dipole moment function between the participating $A^1\Sigma_u^+$ and $X^1\Sigma^+_g$ states. Rate coefficients have been determined for temperatures up to 3000K.

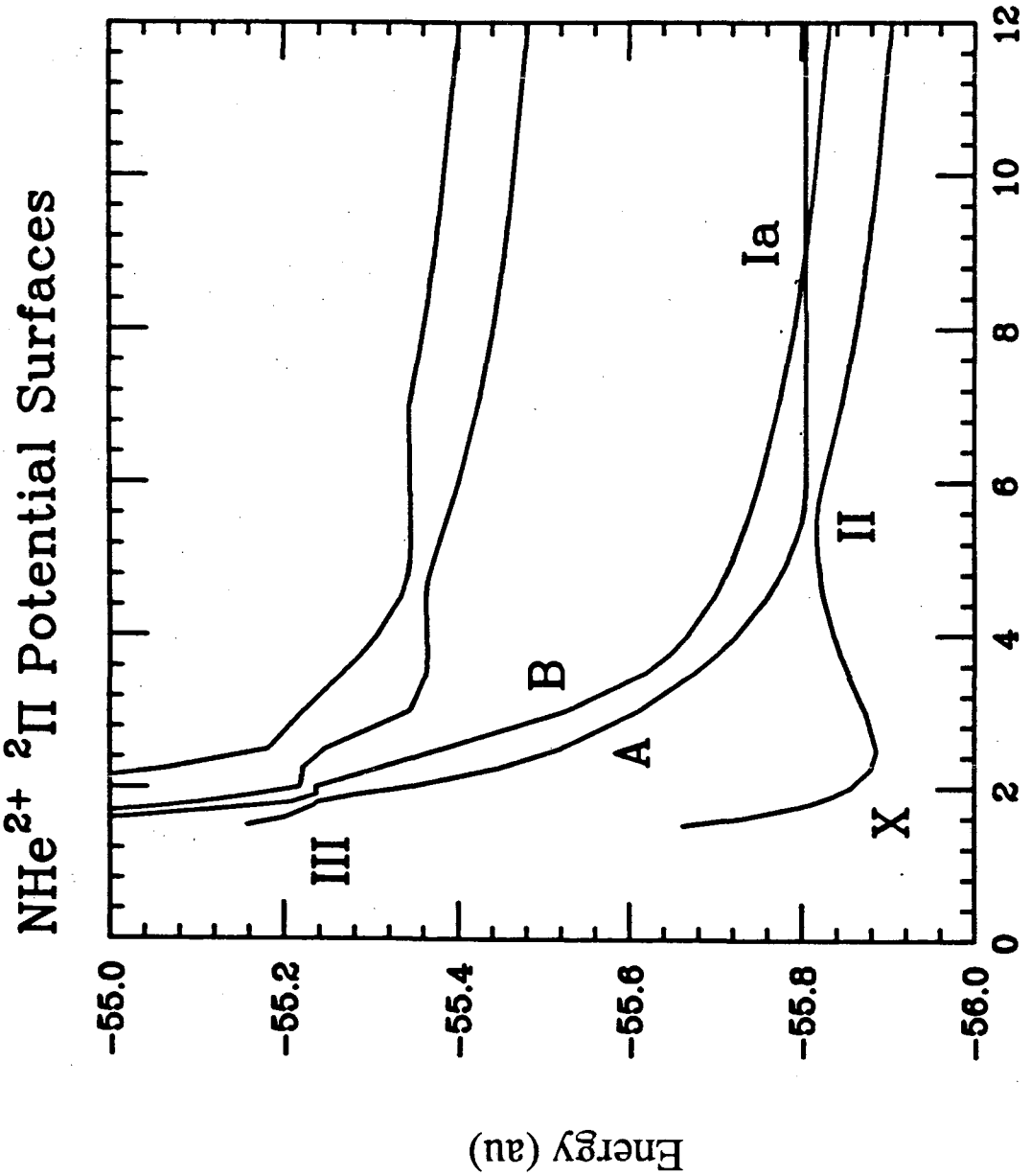
NHe2+ 2Π Potential Surfaces
Energy (au)
R (a0)
-55.0
-55.2
-55.4
-55.6
-55.8
-56.0
0
2
4
6
8
10
12
III
B
A
Ia
II
X

Figure 1

Studies of manifestations of the Berry phase in atomic collision continue. One consequence is a modification of the long range forces between an ion and an atom in a state of non-zero orbital angular momentum (B. Zygelman, Phys. Rev. Lett. submitted (1989)).

Future work involves the study of the effects of intense photon fields on collision processes and the investigation of phenomena analogous to above threshold ionization occurring in molecular dissociation.

Publications

M. L. Du, Eigenvalues for an exponentially screened Coulomb potential, Phys. Lett. A. 133, 109 (1988).

M. L. Du, Photodetachment spectra of H^- in parallel electric and magnetic fields, Phys. Rev. A.40, 130 (1989).

D. A. Neufeld and A. Dalgarno, Electron impact excitation of molecular ions, Phys. Rev. A. 40, 633 (1989).

B. Zygelman, QED Potentials in many-electron atoms, in Relativistic, quantum electrodynamic and weak interaction effects in atoms, Ed., W. Johnson, P. Mohr and J. Sucher, p. 408, (1989).

B. Zygelman, A. Dalgarno, M. Kimura and N. F. Lane, Radiative and non-radiative charge transfer in He^+ + H collisions at low energies, Phys. Rev. A. 40, 2340 (1989).

Nonlinear Interactions Involving The Real Gaussian Field

D. S. Elliott
Purdue University, West Lafayette, IN

The interaction of atomic and molecular systems with laser fields whose power is spread over a band of frequencies is the major topic of this experimental investigation. In this abstract we will describe a technique we have developed to generate a field known as the real Gaussian field, and critical tests of the intensity auto-correlation of this field. We will also describe results of related studies of calculations of intensity auto-correlations and power spectra of broadband lasers when transmitted by a Fabry-Perot interferometer. Interferometers find applications in optical filtering and gravitational wave detection, and these calculations are needed in determining signal to noise ratios. In a third project, we report results of measurements of the output of a cw diode pumped Nd:YAG laser when the pump laser intensity is not constant. In this work, we have seen excitation of the relaxation oscillation resonance and its harmonic, and effects resulting from the intensity modulation of the diode laser, including chaotic behavior.

The real Gaussian field is one model of laser field which theorists have used in calculations of laser bandwidth effects. It is characterized by very strong intensity fluctuations, and can be written in the form

$$E(t) = E_o\, \varepsilon(t)\, e^{-i\omega_o t}$$

where $\varepsilon(t)$ is a real random variable, and ω_0 is a constant optical frequency. We use a random amplitude modulation technique based on radio frequency electronic components and an acousto-optic modulator to generate this field. The random amplitude, $\varepsilon(t)$, is defined by an exponentially decaying correlation function, $\langle\varepsilon(t)\, \varepsilon(t+\tau)\rangle = \exp(-b|\tau|)$, where b is the width (HWHM) of the laser, and has an average value of zero. To achieve this the carrier of the amplitude modulated signal is suppressed to a very high degree.

An important test we have developed of the real Gaussian field involves a measurement of the intensity autocorrelation function of the light. The light is projected onto a photodiode which monitors the laser intensity. The intensity is displayed on an oscilloscope which is fitted with a CCD camera interfaced to a PC computer. When the oscilloscope is triggered at random times, the intensity waveform is digitized and recorded in the computer. Repetitive sampling of the traces of the intensity waveform allows us to compute the intensity autocorrelation function of the light, defined as $\langle I(t)I(t+\tau)\rangle/\langle I(t)\rangle^2$. This function is expected to decay exponentially from a value of three to one with a time constant of 1/2b. The strong fluctuations of the real Gaussian field manifest themselves in the initial value of three for the autocorrelation function. Measurements of this autocorrelation function for the values $b/2\pi$ = 0.80 MHz, 2.4 MHz, 4.5 MHz, 6.2 MHz and 7.0 MHz compare very well with this expected behavior, and form a basis for identifying limitations to the random modulation process. For the smaller bandwidths and the lower intensities which we generate, the correlation

function has an initial value typically of 2.7-2.8. Saturation of any of the components, excessive bandwidth or incomplete suppression of the carrier all tend to decrease the maximum value of the correlation function very quickly. In this way we have determined that the useful limits to this field generation technique are 14 MHz (FWHM) laser widths, and 3.5% conversion efficiencies. In addition the carrier must be suppressed to the level where it contains less than 10^{-6} of the total energy of the light. The low conversion efficiency will make tests of nonlinear processes challenging, but higher drive powers to the acousto-optic modulator clip the voltage peaks and modify the field statistics. Integration times will have to be increased to compensate.

Calculations we have been carrying out on the statistical properties of the light transmitted by a Fabry-Perot when the light incident upon it is broadband constitute a second project on which we have been working. These calculations were motivated by two recent programs. First, recent experimental and theoretical attention has been devoted to the effect of laser bandwidth on fluctuations in the fluorescence intensity scattered by an atomic system. (The P.I. of this project has been involved in an investigation of this effect at JILA at the University of Colorado.) It is expected that the characteristics of the intensity of light transmitted by the Fabry-Perot will be similar to those of the scattered fluorescence from a weakly illuminated atomic system. A second motivation for these calculations is derived from projects such as gravitational wave detectors which employ interferometers as a means to detect extremely small modulation in the position of one of the reflectors. Laser bandwidth can be seen to contribute to the noise of these measurements. Our calculations are carried out by considering that the field transmitted by the Fabry-Perot is made up of an infinite number of partial waves, each related to the incident field time delayed by an integer number of round trip transit times of the cavity. By incorporating the proper field correlations and phase delays, the intensity auto-correlation function can be calculated. We have carried out these calculations for the phase diffusion model, the chaotic field model and the real Gaussian field model. The latter two are in a closed analytic form, while the phase diffusion model relies on the computer to carry out a summation of a very large number of terms and to check for convergence of the sum. There are many features which come out of these results. Among these are the following. 1) For the phase diffusion field the fluctuations in the transmitted intensity are largest when the mean laser frequency is detuned from resonance. This is in agreement with atomic fluorescence observations and calculations. 2) The magnitude of the intensity fluctuations can be quite large. A phase diffusing field of width 1/8 the transmission width of the Fabry-Perot will produce intensity fluctuations one quarter the peak transmitted intensity. 3) The bandwidth of the intensity fluctuations depends sensitively on the detuning of the laser from resonance with the Fabry-Perot. The broadest spectra appear to occur with the laser is detuned from resonance by from 1 to 2 half widths of the Fabry-Perot. The bandwidth here can be as large as three or four times the width of the intensity spectra on resonance.

The bulk of these calculations are now completed. We would still like to obtain a closed form expression for the phase diffusion calculations, and we are performing similar calculations where the Fabry-Perot response is approximated by a Lorentizian response function. This latter approach allows us to use Fourier transform techniques which yield to direct integration.

The final project on which we will report involves experimental investigations of a cw diode laser pumped Nd:YAG laser. This work is being carried out in collaboration with Rajarshi Roy at George Tech. The laser is a longitudinally pumped standing wave laser which produces a lowest-order Gaussian transverse mode beam. Depending on the pump intensity, the YAG laser can be made to oscillate on from one to four longitudinal modes. Threshold oscillation occurs with 8-9 mW of pump power. With this system we have observed excitation of the relaxation oscillation resonance of the YAG laser by intensity fluctuations of the pump laser, and a second peak at twice the frequency of the first. The first resonance has a width of ~2KHz, a frequency of 0-150 KHz (varying as the square root of the output power), and represents intensity fluctuations of approximately 2.5% of the mean intensity. Outside of this frequency band the laser noise spectral density is extremely low, up to ~40dB down from the peak. This low noise density of the YAG laser is due to the high Q cavity and long fluorescence lifetime of the Nd. We have also observed the behavior of the YAG laser when the diode pump laser is modulated. When the pump intensity is modulated at a frequency below the relaxation oscillation frequency, the YAG intensity modulates in phase with the pump. Above the relaxation oscillation frequency the YAG intensity modulates 180° out of phase with the pump. When the pump is modulated at a frequency close to the relaxation oscillation frequency, or at some frequency within a ratio of small integers $\left(\frac{2}{3}, \frac{1}{2}, \frac{3}{2}, 2, \text{etc}\right)$ of the relaxation oscillation frequency, we can see the modulation of the YAG at subharmonic frequencies. This period doubling and tripling, etc, leads to chaotic behavior, characterized by a very broad spectrum of the intensity. We are carrying out further investigations of this behavior, and attempting to model the laser using theories previously developed for nonlinear systems.

These three projects are important investigations of laser bandwidth effects. Through these studies we are gaining an understanding of the effect of laser bandwidth on nonlinear optical interactions, optical filter transmission characteristics, and laser pumping dynamics.

Publications

C. Xie and D. S. Elliott, "Generation of the real Gaussian Field," in preparation.

Correlated Processes in Atomic Collisions

James M. Feagin

Department of Physics
California State University, Fullerton, California 92634

This project continues as part of a general effort to provide theoretical foundation to the wealth of laboratory and numerical data on two-electron motions in atoms and ions. Recent efforts have concentrated on developing a unified description of Wannier threshold effects in three- and four-particle systems. In the case of four-particle breakup, we predict the presence of multiple unstable normal modes in the breakup configuration and thus reveal a new feature in the Wannier formalism: the occurrence of multiple Wannier power laws. We find this prediction to be in accord with recent experimental observations of a break in the cross section near threshold for triple photoionization in atomic oxygen and neon. Ongoing efforts include the application of a *diatomic molecular description of atoms* to calculate simple cross sections for electron-pair excitations in heavy ion collisions, and quantum diffusion (Monte Carlo) computations of two-electron excited states.

• Multiple Wannier Power Laws

Application of the Wannier description[1,2] to systems more general than $2e^-$ escape was pioneered by Klar and coworkers.[3,4] Based on this work, we have developed a unified description of the Wannier formalism valid for three- and four-body systems. Our original motivation was to extract the Wannier threshold law for *four-particle* breakup of molecular hydrogen.[5] Our approach amounts to a conventional determination of normal modes, but with an unconventional emphasis on unstable motions. We thus obtain all previously deduced Wannier threshold laws.[6] In $2e^-$ escape there is only one unstable degree of freedom, which arises from displacements of the $2e^-$ CM along the interelectronic separation.[7] In $3e^-$ escape, our generalized coordinates confirm[3] that the three electrons form an equilateral triangle with the ion, charge Z, at its center. Moreover, we find the "Wannier saddle" in the potential defined by this equillibrium configuration to be characterized by *two* unstable degrees of freedom, or normal modes, corresponding to independent *longitudinal* and *transverse* motions of the $3e^-$ triangle relative to one of its axes of symmetry.

The formal similarity of the Schrödinger equation transformed to the normal coordinates with one used to describe $2e^-$ escape allows us to import with little change results from conventional Wannier theory.[7] The key point is that an unstable mode about equilibrium characterizes a Wannier index m and hence a power law for the total cross section. In $3e^-$ escape one must consider possible multiple unstable degrees of freedom. Assuming an *independent* (L=0) excitation of the ith unstable normal mode, the energy dependence of the total cross section is thus found to be $E^{n\ m_i}$, where $n = N-1$ is a phase-space factor for N outgoing particles. The index m_i depends on the reduced mass of the ith normal coordinate and its coefficient in an expansion of the Coulomb potential about the Wannier saddle.

Upon substitution of the appropriate reduced mass and potential-energy coefficient for $2e^-$ escape, we recover the familiar Wannier threshold law $E^{1.127}$ for Z=1. Likewise, for positron ionization of atoms, we confirm the $E^{2.651}$ threshold law deduced by Klar.[4] In the case of $3e^-$ escape with Z=3, substituting the parameters appropriate to the *longitudinal* normal mode, we recover the

$E^{2.162}$ threshold law deduced by Klar and Schlecht.[3] However, in addition, for the *transverse* normal mode we predict an $E^{1.821}$ power law for $Z=3$.[6] In fact, both these power laws are evident in the recently measured cross sections of Samson and Angel for the triple photoionization of atomic oxygen and neon.[8] They find that the measured yields of O^{3+} and of Ne^{3+} from threshold ($E=0$) to about 5.5eV above threshold follow an $E^{2.17\pm0.09}$ power law. They thus confirm Klar and Schlecht's prediction to better than 4%. However, above 5.5eV, they find that the yield of ions follows a secondary $E^{1.86\pm0.09}$ power law both in oxygen and in neon, consistent with excitation of the transverse normal mode. If we assume that the normal modes develop in an internal Reaction zone[1,2] as a result of a forced vibration, we can use the potential expansion coefficients to estimate their energy separation. Thus, we predict the break in the cross section to occur at 5.8eV, which is consistent with observations both in oxygen and in neon.

• Molecular-Model Atomic Form Factors

A molecular description of electron-pair excitations in atoms is being applied to the calculation of simple cross sections for heavy ion collisions. Of particular interest are observations of electron-pair states populated in excitation reactions, such as $C^{q+} + He \rightarrow He^{**}$, and even in double-capture reactions, such as $O^{8+} + He \rightarrow O^{6+} + He^{2+}$ and $Ne^{10+} + He \rightarrow Ne^{8+} + He^{2+}$.

The molecular model is based on a comparison of two-electron atoms with *diatomic* molecules.[9] In zeroth order, the model simply recognizes that the ions H^- and H_2^+ have identical electrostatic energies. The interelectronic axis in the atom is given the role of the internuclear axis in the molecule. Two-electron potential energy curves as a function of the interelectronic separation R are obtained by a direct scaling of molecular H_2^+ potential energy curves as a function of the internuclear separation. Thus, in first order, one classifies potential curves and two-electron states according to familiar molecular orbital symmetries and quantum numbers of H_2^+. For example, the molecular *gerade-ungerade* symmetry appears as an "internal" (fixed R) symmetry that remains a symmetry of the total state of the two-electron atom.

As a first step, we have analyzed the first Born approximation for direct excitation of an electron pair, in particular, the inelastic form factor $F_{fi}(\mathbf{q})$, where $\mathbf{q} = \mathbf{k}_i - \mathbf{k}_f$ is the momentum transfer to the atom.[10,11] *Of course, in an independent-electron description $F_{fi}(\mathbf{q})$ vanishes, and double excitation is not allowed in first Born approximation.* Transforming to molecular coordinates using $\mathbf{r}_{j=1,2} = \mathbf{r} \pm \frac{1}{2}\mathbf{R}$, with $\mathbf{r}$ the position vector of the electron-pair center of mass relative to the ion, the form factor separates into a familiar molecular Franck-Condon factor and a *molecular form factor*. Thus, the language of molecular spectroscopy finds full application in atomic spectroscopy. For $\Delta L=1$ transitions (e.g. $^1S^e \rightarrow {}^1P^o$), $F_{fi}(\mathbf{q})$ is just the dipole matrix element required for the study of emission and absorption of photons. With these expressions we are analyzing recent observations of double excitation. One finds for example the selection rule that the molecular form factor vanishes unless $N_\mu + L - K = even$, where N_μ is the number of nodes in the wavefunction between the two electrons and L and K are quantum numbers of the total angular momentum and its projection along the interelectronic axis. Similar though weaker rules for transitions follow when a comparison is made of the relative number of nodes in the initial and final wavefunctions.

• Quantum Diffusion

A quantum Monte Carlo algorithm based on the molecular model has been developed for two-electron atoms.[12] It is an attempt to devise a method for studying three-particle Coulomb correlation

that truly relies on simulation. The need to construct better variational or basis functions is minimized; instead, the burden of the calculation is shifted to the time development of a distribution of random walkers, which are eliminated and replicated by a diffusion process governed by the Schrödinger equation. The algorithm thus injects rudimentary "artificial intelligence" into the calculation, and its ability to compute ground-state energies is in principle unsurpassed.

We are investigating a technique recently developed by Ceperley and Bernu[13] in order to extend the method to simulate an arbitrary excited state. Their method involves the computation of an autocorrelation function of a vector of trial functions and following its development in time as a diffusion random walk. Higher states are automatically kept orthogonal to lower ones, and estimates of energy levels are determined by the eigenvalues of the matrix of correlation functions. The method has been successfully tested on a double well. Our initial goal is to compute the lowest $^1S^e$ spectrum of helium.

[1]G.H. Wannier, Phys. Rev. **90**, 817 (1953).
[2]G.H. Wannier, Phys. Rev. **100**, 1180 (1954).
[3]H. Klar and W. Schlecht, J. Phys. B**9**, 1699 (1976).
[4]H. Klar , J. Phys. B**14**, 4165 (1981).
[5]R. Stevens and J.M. Feagin, Bull. Am. Phys. Soc. Vol. 33, No. 4, 992 (1988).
[6]J.M. Feagin and Rafal D. Filipczyk, submitted for publication, September (1989).
[7]J.M. Feagin, J. Phys. B**17**, 2433 (1984).
[8]J.A.R. Samson and G.C. Angel, Phys. Rev. Lett. **61**, 1584 (1988).
[9]J.M. Feagin and J.S. Briggs, Phys. Rev. **A37**, 4599 (1988).
[10]R. Stevens and J.M. Feagin, Sixteenth International Conference on the Physics of Electronic and Atomic Collisions, New York, July, 1989, Abstracts, p. 493.
[11]J.M. Feagin and J.S. Briggs, Invited Papers to the European Study Conference on the Spectroscopy and Collisions of Few Electron Ions, Bucharest, Romania, September (1988).
[12]C.E. Beckmann and J.M. Feagin, Phys. Rev. A**36**, 4531 (1987).
[13]D. Ceperley and B. Bernu, J. Chem. Phys. **126**, 987 (1987).

• Publications since Fall 1987

a. *Molecular Model of Two-Electron Atoms*, James M. Feagin, Nuclear Instruments and Methods in Physics Research B**24/25**, 261 (1987).
b. *Molecular Description of Electron Pair Excitations*, James M. Feagin, Proceedings of the NATO Summer School on Fundamental Processes of Atomic Dynamics, Maratea, Italy, September, 1987 (Plenum, 1988).
c. *Quantum Diffusion Computation of Two-Electron Ground States*, Curt E. Beckmann and James M. Feagin, Physical Review A**36,** Rapid Communications, 4531 (1987).
d. *Collective Two-Electron Excitations*, James M. Feagin, Invited Papers to the Fifteenth International Conference on the Physics of Electronic and Atomic Collisions, Brighton, England, July, 1987 (North Holland, 1988).
e. *A Molecular Orbital Description of Two-Electron Systems*, James M. Feagin and John S. Briggs, Physical Review A**37**, 4599 (1988).
f. *Diatomic Molecular Description of Electron-Pair Orbitals in Atoms*, James M. Feagin and John S. Briggs, Invited Papers to the European Study Conference on the Spectroscopy and Collisions of Few Electron Ions, Bucharest, Romania, September (1988).
g. *Generalized Coordinates for Wannier Thresholds: Prediction of Multiple Power Laws for Triple Escape*, James M. Feagin and Rafal D. Filipczyk, submitted for publication, September (1989).
h. *Generalized Coordinates for Three and Four Particle Wannier Power Laws*, J.M. Feagin, Rafal D. Filipczyk and R. Stevens, in preparation, September (1989).

Theoretical Studies of Atomic Transitions

Charlotte Froese Fischer
Vanderbilt Univerisity
Nashville, TN 37235

The accurate prediction of energy levels and lifetimes has been the prime objective of the current research. The latter may require the calculation of many radiative transition probabilities[1] as well as autoionization rates[2] for which continuum functions are required.

Calculations have been performed using SUN workstations in conjunction with the CRAY X-MP and CRAY 2. The Davidson algorithm for the large, sparse eigenvalue problem was implemented in the MCHF Atomic Structure Package (MCHF_ASP) and the configuration interaction program multitasked for execution on a number of processors[3]. With this algorithm, it is possible to perform first-order calculations for large configuration lists (2,000 - 3,000) in order to determine the important contributors to a wave function expansion. Anticipating the arrival of FORTRAN8x, many compilers already include the pointer data type with associated dynamic memory allocation and management. An effort is well under way to unify SUN and CRAY programs, so that essentially the same programs can be compiled either with the SUN f77 or the CRAY cft77 compiler. Spline algorithms have been investigated for the calculation of continuum functions[4] and applied to the study of resonances in photoionization cross-sections. In the case of helium, good agreement is obtained with other theory and experiment, but the studies suggest that "weakly closed" channels be treated in the same manner as the continuum orbitals. In fact, the entire MCHF_ASP should be converted to spline techniques. The latter is a project for the future.

A number of atomic systems were investigated. Many-body perturbation theory (MBPT) has the advantage that, order by order, expressions can be derived for specific atomic properties. For example, third-order expressions for the binding energy[5] do not require the calculation of many terms that contribute to the total energy of the states whose energy difference defines the binding energy. At the same time, MBPT has had difficulty dealing with open shell systems where the Hartree-Fock approximation is not a good zero-order approximation. Variational procedures overcome this difficulty, but at a price. Separate calculations are performed for the two states so that the radial basis is *not* the same for both. The challenge is to perform a calculation from which a given property can be predicted accurately *without* performing a full-atom correlation study, something which is only possible for few-electron systems. At the same time, it would be desirable to have some estimate of the error. By performing a series of calculations in a systematic manner, the convergence pattern could be used as an error estimate. In the studies to be described, the orbital basis is expanded systematically. With these ideas in mind, procedures for several energy related problems were investigated.

1. Binding energies of $2s$ and $2p$ electrons in lithium

This is a standard case that has served as a test case for a number of theories. With $1s^2$ as a core, it is characterized as having i) no correlation among electrons outside the core, ii) correlation with the core, and iii) correlation in the core. Correlation with the core, namely core-polarization, can be included fairly readily. Table 1. shows that an accurate core-polarization calculation over-estimates the binding energy, that a core-valence interference can be estimated from a CI calculation. Lithium is a light atom and a mass-polarization correction (m) is needed when comparing with observation as well as a relativistic correction (r).

2. Transition energies of high-spin, core-excited states of lithium

The transition energy for the $1s2s2p\ ^4P - 1s2p^2\ ^4P$ transition in lithium is characterized as having i) outer correlation ($2s2p$ or $2p^2$), ii) correlation with the core ($1s$), but iii) no correlation in the core. Calculations that include outer correlation only converge to the wrong transition

Table 1: Convergence patterns for predicting binding energies in lithium.

Calc.	*Core-polarization*		*Full CI*	
	$2s$	$2p$	$2s$	$2p$
$n \leq 3$	.198455	.130054	.197761	.130120
$n \leq 4$	.198748	.130229	.198047	.130231
$n \leq 5$	.198816	.130337	.198102	.130246
r+m			.198113	.130250
MBPT (r)[5]			.19797	.13001
Obs.			.198159	.130245

Table 2: Results for high-spin states of lithium

Calc.	$1s2s2p\ ^4P$	$1s2p^2\ ^4P$	ΔE
Non-relativistic			
$n \leq 3$	−5.366561	−5.243707	.122860
$n \leq 4$	−5.367691	−5.245007	.122684
$n \leq 5$	−5.367917	−5.245285	.122632
Bunge et al.[6]	−5.367948	−5.245308	.122640
Chung [7]	−5.367837	−5.245262	.122575
Relativistic			
present			.122672
Chung[7]			.122624
Obs.[8]			.122643

energy. The convergence for a full correlation study, where the orbital basis always includes an extra p orbital, is shown in Table 2. Note that the excellent transition energy obtained by Bunge and Bunge[6] did not include the relativistic and mass-polarization effects.

3. Electron affinities for high-spin states

An electron affinity is the same as a binding energy of an electron in negative ion. For the high-spin states of lithium, table 3 shows that the binding energy is predicted to good accuracy by outer correlation only. But the core-excited states are special in that there is no correlation in the core. Similar calculations for the $1s^2 2s2p\ ^3P$ and $1s^2 2p^2\ ^3P$ electron affinities of beryllium will not have included the core-valence interference effects mentioned earlier. In fact, these are only important for the $1s^2 \rightarrow 2p^2$ replacements which are allowed in all but $1s^2 2p^3\ ^4S$. With this correction, we get

	EA($2p^2\ ^3P$) - EA($2s2p\ ^3P$)
present	4.9 meV
Bunge[9]	−10. meV
Obs.[10]	4.2 meV

Table 3: Electron affinities for high-spin states of lithium

Calc.	$1s2s2p\ ^4P$		$1s2p^2\ ^4P$	
	outer	full	outer	full
$n \leq 3$	.016305	.016284	.007553	.007895
$n \leq 4$	.018069	.018000	.010194	.010036
$n \leq 5$	.018322	.018308	.010419	.010459

Because there is so much more correlation in the core than among the outer electrons, present codes would not have been able to predict the difference in electron affinities to this accuracy. This was the approach taken by Bunge.

References

1. J. Carlsson, H. Lundberg, W.X. Peng, A. Perrson, C.-G. Wahlström, T. Brage, and C. Froese Fischer, Z. Phys. D **3**, 345 (1986).
2. C. Froese Fischer and M. Idrees, Phys. Scripta **39**, 70 (1989).
3. V. Umar and C. Froese Fischer, Int. J. Supercomputer Appl. (accepted).
4. C. Froese Fischer and M. Idrees, Computers in Phys. **3**, 53 (1989).
5. W.J. Johnson, J. Saperstein, and M. Idrees, Phys. Rev. A **35**, 3218 (1987).
6. C.F. Bunge and A.V. Bunge, Phys. Rev. A**17**, 816 (1978).
7. K.T. Chung, Phys. Rev. A**29**, 682 (1984).
8. M. Leavitt and P. Feldman, Phys. Rev. **180**, 48 (1969).
9. A.V. Bunge, Phys. Rev. A**33**, 82 (1986).
10. J.O. Gaardsted and T. Andersen, J. Phys. B: At. Mol. Opt. Phys. **22** L51 (1989).

Publications

1. "The $1s2s2p^2\ ^5P - 1s2p^3\ ^5S$ transition in Be I-like ions " (with T. Brage), J. Phys. B: At. Molec. Phys. **21**, 2563-2569 (1988).
2. "Non-orthogonal orbitals in the MCHF or configuration interaction wave functions " (with A. Hibbert and M.R. Godefroid), Comput. Phys. Commun. **51**, 285-293 (1988).
3. "Interpretation by orthogonal operators of Hartree-Fock analyses for Fe VI $3d^24p$ " (with J.E. Hansen and B.R. Judd), J. Opt. Soc. Am. B **5**, 2446-2451 (1988).
4. "Spline Algorithms for continuum functions " (with Muhammad Idrees), Computers in Physics **3**, 53-58 (1988).
5. "Binding energies for p electrons in negative alkaline-earth elements", Phys. Rev. A **39**, 963-970 (1989).

Radiative Diagnostics of Electron-Atom Collisions

A. Gallagher

Joint Institute for Laboratory Astrophysics

University of Colorado, Boulder, Colorado 80309-0440

Our measurements of Na 3S → 3P excitation have now been fully analyzed to yield the partial, differential cross sections in the threshold energy region. Here the cross section has been separated into its partial components with respect to spin and m_L charge of the bound electron, and the differential character with respect to the electron scattering angle has been established for each component. These uniquely detailed and low-energy results demonstrate the exceptional power of this new spectroscopic method. The only available calculation capable of the accuracy and detail this achieves is the close-coupling calculation of Moores and Norcross. Detailed comparisons to this calculation verify the exceptional quality of this longstanding guide, while also pointing to the need for improvement.

Our research is currently focussed on achieving higher electron energy resolution, without excessive loss of net current, utilizing E × H energy selection. This will be combined with high photon collection efficiency to study higher-state excitations in metal atoms.

Recent Publications:

X.L. Han, G.W. Schinn and A. Gallagher, "Spin-exchange cross section for electron excitation of Na 3S-3P determined by a novel spectroscopic technique," Phys. Rev. A 38, 535-538 (1988).

Studies of Autoionizing States Relevant to Dielectronic Recombination

T.F. Gallagher
Department of Physics
University of Virginia
Charlottesville, VA 22901

This is an experimental program to study autoionizing atomic states with particular attention to the properties relevant to the inverse process, dielectronic recombination. We focus on the alkaline earth atoms which can be studied with great precision using laser spectroscopy techniques. A particularly useful aspect of our laser excitation technique is that it is precisely the inverse of the radiative stabilization in dielectronic recombination. The intrinsic atomic properties we measure are the autoionization rates, the branching ratios for autoionization to specific ionic states, and the angular distributions of ejected electrons. To simulate the effects of the many ions present in a plasma we also investigate the effects of external fields on the autoionization rates. The data from the experiments can be compared to an existing theoretical work in some cases, such as energy levels and autoionization rates. In others, for example autoionization in strong fields, there exist no predictions and the data serve to guide the development of the theory.

During the past year we have worked primarily on two projects, the study of the Ba 6pnf states and the initiation of experiments with Mg.

The Ba 6pnf states are the only Ba 6pnℓ states which had not been examined, and this study completes the study of the Ba 6pnℓ states. The Ba 6pnd states have autoionization widths which are 15 of the n spacings, and the 6png states have autoionization widths which are 5 of the n spacings. Therefore a reasonable estimate for the 6pnf widths is 10 of the n spacing. Somewhat to our surprise the 6pnf widths are 30 of the n spacings, making them the most rapidly decaying of the 6pnℓ states. With our excitation method the observed spectrum is a product of an overlap integral and the spectral density of the autoionizing series. Normally the latter function is the more rapidly varying by a substantial amount, and it dominates the observed spectrum. Usually the spectral density is a series of high peaks above a nearly zero background. In the case of the Ba 6pnf states, however, the spectral density has only a small, 30, modulation about a constant level. As a result our spectra are dominated by the overlap integral, making the analysis more difficult.

Although the large widths of the Ba 6pnf states are initially surprising, they in fact resolve an outstanding discrepancy. In our previous measurements of autoionization rates in electric fields we found rates scaling as n^{-4}, however the magnitudes of the rates were smaller by about a factor of two than rates we had calculated based on the known 6pnℓ autoionization rates. The calculated rates in fields are only sensitive to the autoionization rates of low ℓ states. Thus the fact that the 6pnf autoionization rate is a factor of four higher than our initial estimate is enough to bring the calculated and observed autoionization rates in fields into agreement.

Our second major project during the past year has been to initiate the study of Mg. The Mg 3pnℓ autoionizing states are interesting from a practical point of view since dielectronic recombination rates have been measured in Mg. The Mg 3pnℓ states are interesting from a fundamental point of view since there are only two accessible continua for any 3pnℓ state below the 3p limits, making interference effects particularly pronounced.

The experimental study of Mg poses several technical problems which are not present in the study of the other alkaline earth atoms. First, all three transitions we use lie in the ultraviolet, necessitating higher power, oscillator amplifier dye lasers. Second, the Mg 3s3p $^1P_1$ state lies more than halfway from the ground state to the Mg^+ 3s ionization limit, and the absorption of two of the photons which drive the $3s^2 \rightarrow$ 3s3p transition produce ions. As a result we cannot saturate first

transition by supplying arbitrary amounts of laser power without photoionizing a substantial number of the Mg atoms.

At this point we have developed the techniques for exciting the Mg 3pnℓ states and have recorded the excitation spectra for the 3pnd states. We are presently analyzing the data, using quantum defect theory. Rather than fit our data to parameters, as we have done in the past, we are comparing our data to the synthetic spectra calculated from the K matrix supplied by Greene. The same K matrix can be used to calculate both vuv excitation spectra and our laser excitation spectra. Although we have not completed our analysis, preliminary indications are that our data fit the spectra calculated from Greene's K matrix fairly well.

Our plans for the future are to conduct a study of the Mg 3pns states analogous to the one currently underway for the Mg 3pnd states. Assuming that the study of the 3pns states goes smoothly, we plan to then examine the angular distributions of the electrons ejected from the Mg 3pns and 3pnd states. Such measurements will be a stringent test of the calculated K matrix and should show pronounced interseries interactions. In our previous measurements of autoionization rates in static and microwave fields, we found an n^{-4} scaling of the autoionization rates. For fields with randomly varying polarization the rate should have an n^{-5} scaling, a prediction we plan to check using a circularly polarized microwave field.

Publications

C.J. Dai, S.M. Jaffe and T.F. Gallagher, "Ba $5d_{5/2}nd_j$, J = 4 states and their interaction with the $5d_{3/2}$ $\epsilon d_{5/2}$ J = 4 continuum," J. Opt. Soc. Am B 6, 1486 (1989).

R.R. Jones and T.F. Gallagher, "Autoionization of Ba $6p_{1/2}nk$ states in static and microwave fields below the Inglis Teller limit," Phys. Rev. A 39, 4583 (1989).

T.F. Gallagher and R.R. Jones, "The Effect of Static and Dynamic Fields on Autoionization Rates" in Spectral Line Shapes, ed J. Szudy (Ossolineum, Wroclaw, 1989).

R.R. Jones and T.F. Gallagher, "Autoionization of high ℓ Ba $6p_{1/2}n\ell$ states," Phys. Rev. A 38, 2846 (1989).

ELECTRON COLLISIONS WITH POSITIVE IONS

Ronald J. W. Henry

Department of Physics
Auburn University
Auburn, Alabama 36849

The work of my theoretical atomic physics group was originally directed towards the computation of detailed and accurate cross sections for the electron impact excitation of ions using a close coupling approximation expansion, sometimes using pseudostates. This has been extended to include some ionization mechanisms. A major theme is to provide a systematic understanding of electron ion collisions, particularly in the energy region from threshold to five times excitation threshold. Thus, the average effect of resonances is being investigated, as is the effect of excitation-autoionization processes on total ionization cross sections.

Projects completed in the recent past include:

(1) Contributions of excitation-autoionization and resonant-excitation-double-autoionization (REDA) indirect ionization processes to the electron-impact ionization of Fe^{15+} have been calculated /1/ using a close-coupling approximation. The total ionization cross sections were obtained by adding the cross sections for these indirect processes to the direct ionization cross sections. Eleven autoionizing levels arising from the $2p^6 3s^2$, $2p^5 3s3p$, $2p^5 3p^2$ and $2p^5 3s3d$ configurations together with the ground $2p^6 3s$ state are included in the close-coupling expansion. The present results are in good agreement with crossed beam measurements of Gregory et al. /2/. Our calculation does not show large resonance enhancements due to REDA process, in disagreement with the predictions of Lagatutta and Hahn /3/.

(2) Coupling effects among the channels for collisional excitation of $2s^2 2p^4$, $2s2p^5$, and $2p^6$ configurations of oxygenlike krypton have been reinvestigated /4/ and found to be small. Msezane et al. /5/ reported that coupling to the $2s2p^5 3p^o$ state had a strong influence on the cross section $\sigma(2s^2 2p^4\,{}^3P \rightarrow 2p^6\,{}^1S)$. That apparent coupling is shown to be due to an inconsistency involving orthogonality and correlation functions. We solve the correct set of equations using the NIEM, IMPACT, and RMATRIX codes. We find very good agreement among the cross sections obtained from all three codes when the same target states and configurations are used.

(3) Density sensitive emission-line rations $R_1 = I(338.27\ \text{Å})/I(364.47\ \text{Å})$ and $R_2 = I(338.27\ \text{Å})/I(352.10\ \text{Å})$ for FeXII have been calculated /6/ using electron collision rates /7,8/ which are substantially larger than those previously published /9/. The ratios are calculated as a function of electron density at the temperature of formation of Fe XII. Electron densities deduced from the observed values of R_1 and R_2 for solar active regions and flares obtained by NRL SO82 A slitless spectrograph on board Skylab are in excellent agreement.

The work currently in progress includes:

(1) Very accurate measurements of ionization cross sections for electron impact of CIV has been made recently at Giessen /10/. This work has stimulated a re-examination of the inner shell excitation contributions in the energy range $200 < E < 340$ eV. Effects of REDA as well as direct inner shell excita-

tion are being included in a thirteen state close coupling calculation.

(2) Coupling effects in the carbon isoelectric sequence are being examined for low Z ions. Sensitivity for various types of transitions in the energy region beyond the resonance region is being investigated, in particular for $\Delta n = 0(2\rightarrow 2), \Delta n \neq 0(2\rightarrow 3)$, E1 allowed, E1 forbidden, spin allowed, and spin forbidden.

(3) Absolute crossed-beam emission cross section measurement /11/ for excitation of $Cd^+ 5s^2\,^2D$ and $5p^2\,P^\circ$ from the ground state $5s^2S$ have been reported with the surprising result that the cross section for the former excited state is comparable or even exceeds that of the latter. The surprise stems from the fact /12/ than for the homologus ion Zn^+, the resonance transition $4s\rightarrow 4p$ is at least an order of magnitude larger than the inner shell $4s\rightarrow 4s^2\,^2D$. We are constructing an accurate target wave function to describe various states in Cd^+. The challenge is not only to obtain the atomic data for Cd^+ but also (and more importantly) to understand the atomic physics underlying this ion.

REFERENCES

1. S. S. Tayal and R. J. W. Henry, Phys. Rev. A 39, 3890 (1989)
2. D. C. Gregory, L. J. Wang, F. W. Meyer, and K. Rinn, Phys. Rev. A 35, 3256 (1987)
3. K. J. Lagututta and Y. Hahn, Phys. Rev. A 24, 2273 (1981)
4. K. J. Reed and R. J. W. Henry, Phys. Rev. A 40, 1823 (1989)
5. A. Z. Msezane, K. J. Reed, and R. J. W. Henry, Phys. Rev. A 34, 2540 (1986)
6. S. S. Tayal, R. J. W. Henry, F. P. Keenan, S. M. McCann, and K. G. Widing, Astrophys. J. 343, 1004 (1989)
7. S. S. Tayal, R. J. W. Henry, and A. K. Pradhan, Ap. J. 319, 951 (1987)
8. S. S. Tayal and R. J. W. Henry, Ap. J. 329, 1023 (1988)
9. D. R. Flower, Astr. Astrophys. 54, 163 (1977)
10. A. Muller, G. Hofman, K. Tinschert, and E. Salzborn, Phys. Rev. Letts. 61, 1352 (1988)
11. K. Hane, T. Goto, and S. Hattori, J. Phys. B 16, 629 (1982); Phys. Rev. A 27, 124 (1983)
12. W. T. Rogers, G. H. Dunn, J. O. Olsen, M. Reading, and G. Stefani, Phys. Rev. A 25, 681 (1982)

RECENT PUBLICATIONS

Generalized Oscillator Strengths for Dipole Forbidden Transitions in CuI, ZnII, and MgII
A. Z. Msezane and R. J. W. Henry
Phys. Rev. A 37, 988-991 (1988)

Role of Indirect Processes in the Electron-Impact Ionization of Fe
S. S. Tayal and R. J. W. Henry
Phys. Rev. A 39, 3890-3894 (1989)

Electron Impact Excitation
R. J. W. Henry and A. E. Kingston
In "Advances in Atomic and Molecular Physics" 25, 267-302
Edited by D. R. Bates and B. Bederson, Academic Press (1988)

New Close-Coupling Cross Sections for Electron Impact Excitation of Kr
K. J. Reed and R. J. W. Henry
Phys. Rev. A 40, 1823-1827 (1989)

Electron Density Diagnostics for Fe XII in the Solar Plasma
S. S. Tayal, R. J. W. Henry, F. P. Keenan, S. M. McCann, and K. G. Widing
Astrophys. J. 343, 1004-1006 (1989)

Experimental Study of Interactions of Highly Charged Ions with Atoms at keV Energies**

V.O. Kostroun

Nuclear Science and Engineering Program, Ward Laboratory
Cornell University, Ithaca, NY 14853

The objective of this program is to investigate interactions of low energy, very highly charged ions with atoms at keV energies. In order to accomplish the objective, the research carried out during the past year followed two complementary paths. One, to develop an electron beam ion source or EBIS capable of producing the ions of interest, and the other, to use the source and the ions produced in atomic physics experiments.

During the past year, we have finished rebuilding our superconducting solenoid, cryogenic electron beam ion source CEBIS II. The original 6.5" diameter, warm bore, 38" long, 3 Tesla superconducting solenoid was replaced by a solenoid manufactured by Nicolet Instruments Corporation of Madison Wisconsin. The Nicolet solenoid is 31" long, has a 6" diameter warm bore, and at 3 Tesla, a field profile similar to the old one. The solenoid operates in the persistent current mode and has a LHe and LN_2 consumption of 60 and 120 liters per month respectively. Because of the smaller bore and shorter length, a number of the original components of CEBIS II had to remade. The remaking of much of the source provided us with the opportunity to simplify and improve on the original design. CEBIS II uses an external electron gun operated in the DC mode. For the time being, the Litton Industries type M-707 electron gun is run at 1.5 kV. This is far from its normal operating voltage of 10 kV, and hence the optical properties of the gun are not optimal. At present, CEBIS II can generate Ar^{16+} ions in 40 msec when argon gas is injected into a 3.5 keV, 15 mA electron beam (2 kV on the drift tubes and 1.5 kV on the gun cathode). The ion charge distribution, as measured with a time-of-flight spectrometer, is about equally divided on charge states 13^+ and 14^+, the dominant species, and extends from 11^+ to 16^+. The extracted ion beam contains very little hydrogen and only a trace of residual background nitrogen ions.

Two source related investigations are in progress. The first involves a study of ion trapping and the effects of electron beam misalignment on ion output yield and charge state distribution. This problem is closely related to the launching of the electron beam into the magnetic field. At present, only results for a 1.5 keV electron beam from the gun are available. At 1.5 kV, the electron gun optics are strongly influenced by thermal transverse velocity components and the beam launching conditions are not optimal. As we gain more experience with the source, in particular, how to align the electron beam without destroying

anything, we plan to gradually increase the cathode voltage to 10 kV, the proper operating voltage for the gun. As we increase the electron beam energy, we plan to study ion production and trapping, with the view towards trapping ions for long periods of time. Preliminary results at the low voltage are very encouraging and indicate that the source behaves as an EBIS should.

The second source related effort is tied to the production of ions of elements other than gases. The Lawrence Livermore National Laboratory electron beam ion trap EBIT [1] has demonstrated that highly charged ions of heavier elements are trapped more easily in an electron beam than ions of lighter elements. Accordingly, an external ion injection system has been designed, constructed and tested. The system consists of a commercial sputter PIG ion source and a beam transport system to inject singly charged ions from the PIG source into CEBIS II. Singly charged ions of either aluminum or lead, the two elements tested in the sputter PIG source so far, are separated from other ions by a Wien filter at the PIG extractor. The ions are then bent through 90^{o} by a quadrupole deflector into the CEBIS II beam line. (During the injection cycle, the 90^{o} quadrupole deflector deflects singly charged ions into CEBIS II, while during the extraction cycle, highly charged ions have to pass through the quadrupole undeflected.) Appropriately placed einzel lenses and horizontal and vertical deflection plates focus and deflect the beam onto the EBIS electron collector-ion extractor. Thus far, a two microampere beam of 3 keV Al^{+} or Pb^{+} ions has been obtained at the position where it would enter CEBIS II. The injection system is fully operational and we plan to install it on CEBIS II shortly.

In the atomic physics area, we are continuing with our doubly differential, (energy and angle) cross section measurements. The scattering angle scale for medium mass, highly charged projectiles colliding with helium can be obtained from the kinematics of elastic, nuclear coulomb collisions. For collision energies less than 0.5 keV/amu, charge transfer between highly charged argon ions and helium results in scattering angles of a few tens of milliradians. At low collision velocities, the electron captured by the highly charged argon projectile populates high n states, and the corresponding Q values are small compared to the projectile kinetic energy. In order to investigate collision dynamics in some detail, e.g. to distinguish simultaneous two electron capture from two consecutive single electron captures or to follow the capture to a specific state of the projectile as a function of impact parameter, requires, in the cases of interest, an angular resolution of a fraction of a milliradian and an energy resolution of an eV. This means that the angular and energy spread of both the incident ion beam and the detector have to be made as small as possible. This minimization requires precision ion optics and a thorough understanding of source properties and behavior.

The scattering apparatus used with CEBIS I to measure angular and energy distributions in single and double electron capture of Ar^{8+} on He [2] has been moved to CEBIS II. It consists of a gas cell, 2.5 cm long, a 1 m long drift region, and an

analyzer/detector. The latter is a 127^{o} cylindrical electrostatic analyzer with an adjustable entrance and exit slit. The ions are detected by a 25 mm diameter channeltron electron multiplier. The analyzer, located behind a bow tie collimator and a retarding grid, can be translated at right angles to the incident beam, and scattering angles of $\pm 2.8^{o}$ measured. (The apparatus is essentially a translational energy spectrometer with angular distribution measurement capabilities.) The entire vacuum chamber is mounted on a system of linear bearings and positioners, which, together with segmented collimators, allow one to align the incident ion beam with the axis of the apparatus. (The magnetic field due to the unshielded EBIS main solenoid has proven to be somewhat of a nuisance as far as the alignment is concerned and has required a more thorough design of the beam transport optics than anticipated originally.)

At present, the overall resolution of our apparatus is limited mostly by the spread in energy and angle of the incident ion beam. Under suitable source operating conditions, an energy spread of 3q eV at 2000q eV ion energy has been obtained. This can be reduced further by momentum selection, but at the expense of beam intensity. (For the experiments contemplated, a reduction by another factor of 30 is required.) The angular spread of the ion beam is ±2.5 mrad, still about a factor of 10 too high.

**Work supported in part under U.S. DOE grant DE-FG02-86ER13519

References

1. M.B. Schneider, M.A. Levine, C.E. Bennett, J.R. Henderson, D.A. Knapp and R.E. Marrs, Proc. Int'l. Symposium on EBIS Sources and their Appl., A. Hershcovitch Ed. AIP Conference Proceedings No. 188, 1989. p.152.

V.O. Kostroun, Program and Abstracts IX^{th} Atomic Physics Program Workshop, 1988. p.165

1988-89 Publications

1. V.O. Kostroun, "The Cornell Electron Beam Ion Source", Proc. XI National Conference on Particle Accelerators, 25-27 October, 1988 Dubna, USSR

2. V.O. Kostroun, "The Cornell Superconducting Solenoid Cryogenic EBIS", Proc. Int'l. Symposium on EBIS Sources and their Appl., A. Hershcovitch Ed. AIP Conference Proceedings No. 188, 1989. p.65.

3. E.N. Beebe, "Evidence for Ion Cooling and and Observation of IOn Heating in CEBIS I",Proc. Int'l. Symposium on EBIS Sources and their Appl., A. Hershcovitch Ed. AIP Conference Proceedings No. 188, 1989. p.166

Measurements of Scattering Processes in Negative Ion-Atom Collisions

T. J. Kvale

Department of Physics and Astronomy
The University of Toledo, Toledo, OH 43606

Experimentally-determined, state-resolved angular differential cross sections (ADCS) have provided stringent tests [1,2] of theoretical models for positive ion scattering in the intermediate energy region. The present research concentrates on providing comparable information for negative ion projectiles. Specifically, absolute ADCS measurements for the following processes are scheduled:

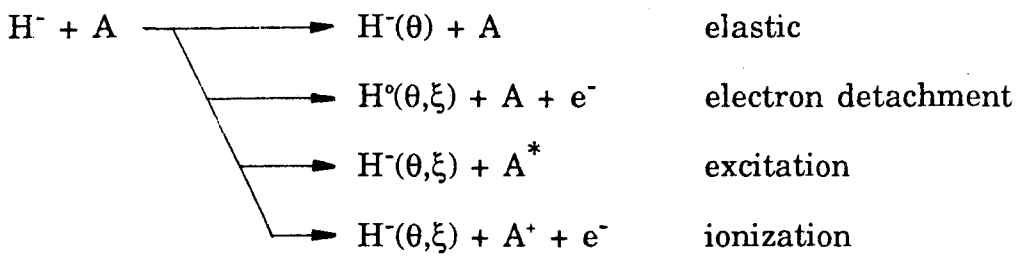

where A includes the noble gases of He, Ne, Ar, & Xe. Here, ξ and θ are the energy loss and scattering angle of the projectile, respectively. For the latter three processes, total cross sections (TCS) will also be obtained. The impact energy region is from 5 to 55 keV (lab) and the scattering angular range is from 0 to 2.5 deg (lab) on either side of the zero scattering angle. The values were chosen so that the experiments will be in the intermediate energy region and to examine the structure in the elastic ADCS discussed later in this abstract. Because the apparatus is new, the vast majority of the activity this year was directed toward construction of the apparatus needed to carry out the these measurements. Progress has been steady and it is expected that the system will be available for experiments shortly. Brief descriptions of the apparatus and the scheduled experiments for it are given below.

APPARATUS

The UT-Negative Ion Energy Loss Spectrometer (UT-NIELS) is the apparatus upon which these measurements will be conducted and is shown schematically in Figure 1. Technical aspects of this facility have been reported recently elsewhere [3,4]. The accelerator will be mounted on a frame which pivots about the center of the scattering chamber. The accelerator angle defines the scattering angle and the apparatus is designed to have an angular step size of 10 μrad. Data can be acquired on either side of the zero scattering angle, so systematic errors resulting from the actual zero scattering angle position are reduced. An H^- ion beam is produced in a duoplasmatron ion source located in the accelerator. In order to obtain the full benefit of Ion Energy-Loss Spectroscopy, a low energy spread is necessary and the design goal of UT-NIELS is an energy spread of 0.3 eV. This will be accomplished by using a Wien Filter in the ion source region as a velocity

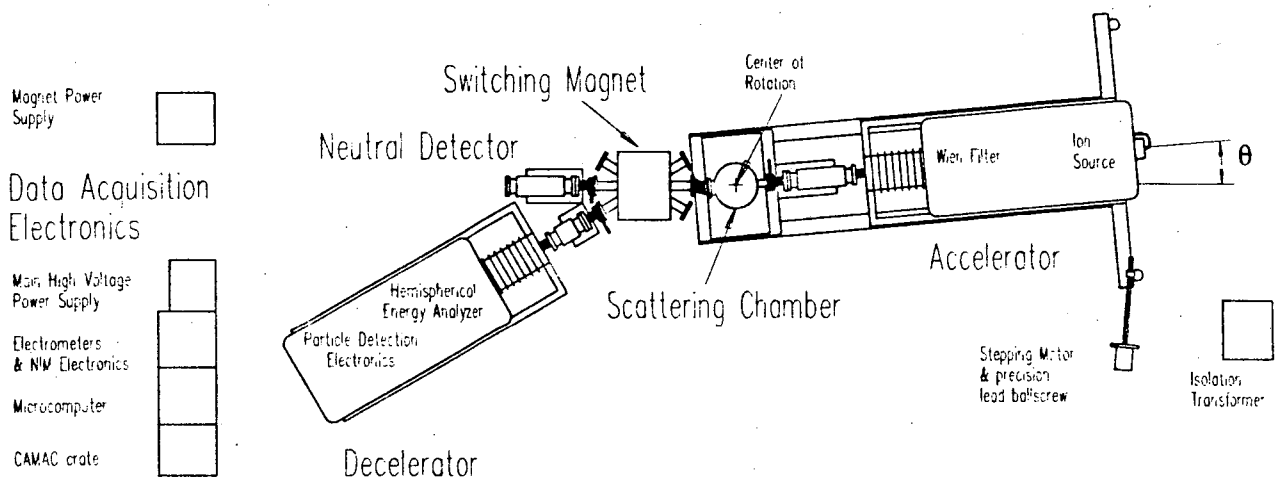

University of Toledo - Negative Ion Energy Loss Spectrometer (UT - NIELS)

Figure 1.

monochromator. The target gas in the scattering chamber is accurately controlled by a solenoid valve-capacitance manometer system. A switching magnet located after the scattering chamber is used to direct the scattered particles into different beamlines according to their charge state. This permits the simultaneous measurements of the processes named earlier. A detector on the zero-degree port is employed for detachment measurements, while the surviving H^- ions are directed into the decelerator for energy analysis. All the data and apparatus control is through a CAMAC-based data acquisition system. This allows the computer to control the electronics in the scattering chamber and electron detachment channel at ground potential and, via high speed fiber optic links, the electronics in the decelerator terminal at high potential.

Outline of Experiments for This Year

A) Energy-loss Spectra and Cross Section Measurements of H^- + Noble Gas Collisions.

The energy-loss spectra will be the primary data obtained from this apparatus and will form a basis for both the total and differential cross section measurements. In all cases, spectra will be obtained for H^- + (He, Ne, Ar, and Xe). These data will be valuable in identifying elastic scattering and target excitation/ionization processes. The apparatus is designed so that the total cross sections for target excitation can be obtained directly as well as cross sections that are differential in energy loss ($\partial\sigma/\partial\xi$) for target ionization events. A numerical integration technique will be used to also obtain the total ionization cross sections from the energy-loss differential cross sections. Results for these processes are expected shortly after initial operation of the apparatus. In addition to target related processes, total cross sections will be measured for electron detachment.

B) **Angular Differential Cross Section Measurements.**
The main goal for this apparatus is to obtain cross sections that are differential in scattering angle (ADCS). The ADCS are valuable because the approximations inherent in the various calculations are more sensitive to the angular dependence than are the integrated total cross sections. Structure was observed [5] in the angular H^- charged particle fraction for H^- + He collisions and recent calculations [6] show a minimum in the elastic ADCS for this system. The apparatus has been designed to provide measurements exploring this feature. Work has begun on the angular motion capability and the ADCS measurements are estimated to commence in the Fall of 1990.

C) **Collaborative Studies.**
My primary research efforts are devoted to this project. Collaborations with Drs. David Ellis and Constantine Theodosiou are providing theoretical support in calculations for scattering processes of interest to this project. Another collaboration is with Dr. Larry Curtis on the atomic spectroscopic studies being conducted at The University of Toledo. The emphasis of this research is on the measurement of the lifetimes and transition probabilities of multiply-excited atomic states.

REFERENCES

1. T.J. Kvale, D.G. Seeley, D.M. Blankenship, E. Redd, T.J. Gay, M. Kimura, E. Rille, J.L. Peacher, and J.T. Park, Phys. Rev. A32, 1369 (1985).

2. J.L. Peacher, T.J. Kvale, E. Redd, P.J. Martin, D.M. Blankenship, E. Rille, V.C. Sutcliffe, and J.T. Park, Phys. Rev. A26, 2476 (1982).

3. T.J. Kvale and J.C. Corcoran, Bull. Am. Phys. Soc. 34, 1260 (1989).

4. T.J. Kvale, "An Apparatus for the Study of Negative Ion-Atom Scattering in the Intermediate Energy Region," XVI International Conference on the Physics of Electronic and Atomic Collisions, New York, ed. A. Dalgarno, R.S. Freund, M.S. Lubell, and T.B. Lucatorto, 818 (1989).

5. M.P. McCaughey and J.A. Bednar, Phys. Rev. Lett. 16, 1011 (1972).

6. C.E. Theodosiou, Bull. Am. Phys. Soc. 34, 1358 (1989).

RECENT PUBLICATIONS

1. T.J. Kvale, G.D. Alton, R.N. Compton, J.S. Thompson, and D.J. Pegg, "Autodetachment Spectroscopy of Metastable Negative Ions," Nucl. Instrum. Meth. B24/25, 325 (1987).

2. R.R. Haar, T.J. Kvale, D.G. Ellis, I. Martinson, L.J. Curtis, and D.J. Beideck, "J-Dependent Lifetimes of Quintet Levels in Neutral Carbon," Phys. Lett. A, 1989 (Accepted).

Atomic Physics of Strongly Correlated Systems

C. D. Lin
Department of Physics, Cardwell Hall
Kansas State University, Manhattan, Kansas 66506

This abstract describes the programs currently underway in our study of (a) doubly excited states of atoms, (b) hyperspherical approaches to the three body problems, and (c) the calculation and understanding of two-electron transitions in ion-atom collisions.

In the field of doubly excited states of atoms and ions, we are making progress in three areas: (1) A systematic study of the energy levels of doubly excited states of atoms and ions along the isoelectronic sequence. We showed that it is possible to use either the double Rydberg formula or the traditional quantum defect formula to extract the Z-dependence of the quantum defect parameters from which the energy levels along the isolectronic sequence can be calculated. (2) Systematics of autoionization widths of doubly excited states. By designating each doubly excited state in terms of the K, T and A quantum numbers, we showed that not only the energy levels show rotor-structure for a given K, T and A, (but different L), the autoionization widths along the rotor series also show novel systematics that the widths are comparable for all the members in the rotor series, except for the second member from the last of the series which is often very narrow. We are currently seeking explanations of this behavior in hyperspherical method. (3) The energy and decay width of beryllium-like ions. We employed the model potential approach to calculate the energies and widths of doubly excited states of beryllium-like ions to help experimentalists identifying observed spectra in ion-atom collisions. It is found that the classification based on the K, T and A quantum numbers is still preferable to the independent electron designation. It was found that the spectra do not show the rotor structure but the autoionization widths still show similar novel behavior as in helium-like sequence.

In the field of Coulombic three-body systems in hyperspherical coordinates, we have calculated hyperspherical potential curves in the adiabatic approximation for a number of systems. Consider a three-body system, AAC, where two of the particles are identical. We used hyperspherical coordinates to calculate the potential curves vs $\lambda = m_A/m_C$

where m_A and m_C are the masses of particle A and particle C, respectively, for different symmetries. The range of λ is from 10^{-4} for H^- in the atomic limit to 10^3 for H_2^+ in the molecular limit. By observing the variation of the potential curves we can follow the evolution of the three-body systems from the atomic limit to the molecular limit and establish the quantum numbers describing the three-body systems in each limit as well as for systems where λ is in between, for example, systems such as $e^-e^+e^-$ and $d^+d^+\mu^-$. Such calculations allow us to identify relation between the K, T and A quantum numbers used in the designation of doubly excited states and the diatomic molecular quantum numbers. The analysis also allows the identification of states which behave like molecules and those which do not. Currently we are applying this approach to three-body systems where the interaction potential between the pair is a confined potential. Using the potentials which reproduce the spectra of quarkonium, we are examining the spectra of the bound states of three-quark systems.

In the field of ion-atom collisions, we have been looking into two-electron processes, particularly double excitation at high energies, to study the role of electron correlations and one-step vs two-step mechanisms for these two-electron transitions. At high energies, one can look at the problem from the Born-series viewpoint. Within the first-Born term, two-electron transition is possible only if one goes beyond the independent electron approximation. In other words, one needs to consider electron correlation in the initial and final state wave functions. In the first Born apprxomation, the electron interacts with the projectile only once and thus the matrix element depends linearly on Z_p. If two-step mechanism is important, where two-electron transition is due to two successive electron-projectile interactions, the transition matrix element will depend on Z_p^2. If, in a given energy region, the one-step and two-step mechanisms are of comparable importance, then the total cross section will include a Z_p^3-term, representing the interference between the one-step and two-step mechanisms. This term is responsible for the differences in the cross sections between particle and antiparticle projectiles. For double ionization of He, it has been observed that the cross section due to antiproton impact is about twice those observed from proton impact at the same velocity at energies around 1 MeV. When analyzing the relative importance of the one-step vs two-step mechanisms responsible for these differences, it is not convenient to study double ionization since

integration over many variables has to be carried out before comparison with experiment can be made. Recent experiments attempted to address this question by looking into double excitations. To unravel the mechanisms of double excitations we studied the formation of $2s^2\ ^1S^e$, $2p^2\ ^1D^e$, $2s2p\ ^1P^o$ and $2p^2\ ^1S^e$ states of He in collisions with bare projectiles with Z_p=1-9 and -1,-2 at 1.5 MeV/u and at 6 MeV/u using the two-electron close-coupling code developed earlier in this program. To this end, we carried out two coupled-channel calculations at each energy, one in which the singly excited states, $1s2s\ ^1S^e$ and $1s2p\ ^1P^o$, are included in the basis set. In another calculation, these singly excited states are not included so that the two-step mechanism is presumably removed. By comparing the results from the two calculations we can identify the importance of the two-step mechanism. Another way to identify the one-step vs two-step mechanisms is to look at the Z_p dependence of the calculated cross sections. We have found that one-step mechanism is dominant at the calculated energies for small Z_p for all the doubly excited states considered except for $2p^2\ ^1D^e$ where the two-step mechanism is still important. For higher Z_p at the same velocity, we have clear evidence that the two-step mechanism is dominant. We conclude that the critical energy where the one-step process dominates over two-step process is lower for double excitation than for double ionization.

Publications

1. W. Fritsch and C. D. Lin, " Analysis of Electron Correlation in Simultaneous Electron Transfer and Excitation in Atomic Collisions," Phys. Rev. Lett. 61, 690 (1988).
2. W. Fritsch and C. D. Lin, " A Comment on Atomic-Basis Calculations for the Collision System Li^{2+}+H," Phys. Lett. 127, 425 (1988).
3. C. D. Lin, " Systematics of Energies of Doubly Excited States of Heliumlike Ions," Phys. Rev. A.39, 4355 (1989).
4. Z. Chen and C. D. Lin, " Calculations of Energies of Doubly Excited States of Berylliumlike Ions," J. Phys. B.22, 3422 (1989)
5. C. D. Lin, R. Shingal, A. Jain and W. Fritsch, " On the Orientation and Alignment of Collisionally Excited States,", Phys. Rev. A.39, 4455 (1989).

STUDIES OF ELECTRON/PHOTON-ION/ATOM COLLISION

Alfred Z. Msezane

Department of Physics, Clark Atlanta University, Atlanta, Ga 30314

In the past year, together with graduate students, we have investigated and obtained results for the following systems:

A. Photoionization of ground state Na: 3 and 7 state R-matrix calculation

Total and partial photoionization cross sections of Na 3s leaving the residual Na^+ ions in the three($2p^6\ ^1S$, $2p^5 3s\ ^{3,1}P^o$) and the seven($2p^6\ ^1S$, $2p^5 3s\ ^{3,1}P^o$, $2p^5 3p\ ^3S$, $^{3,1}D$, ^1P) lowest LS states are calculated using the R-matrix method.[1] Correlation and polarization effects are taken into account through use of extensive CI target wave functions. The results cover the photon energy range from near the 3s $^3P^o$ threshold to about 3.8 Ry(multi-channel region).

We find that the three-state total cross section for Na 3s is characterized by resonance structure dominated by two main peaks at 2.84Ry(22Mb) due entirely to the $2p^5 3s\ ^3P^o$ state and at 3.34Ry(18Mb) and by an unexpected deep minimum at 2.39Ry($\sim 10^{-4}$Mb). In the multi-channel region, the single channel cross section is greatly enhanced by roughly two-orders-of-magnitude due mainly to contributions from 3s $^{3,1}P^o$ states. The seven-state calculation[2] reproduces the main features of the 3-state result, but somewhat modifies some of the positions and magnitudes. We conclude, from comparison of the three- and seven-state results, that coupling effects are important in the multi-channel region.

B. Photoionization of K 4s: Giant Resonance

A five-state R-matrix method has been used to calculate the total and partial photoionization cross sections of K 4s leaving the residual K^+ ions in their five lowest LS states $3p^6\ ^1S$, $3p^5 4s\ ^{3,1}P^o$, $3p^5 3d\ ^3P^o$ and $^3F^o$.[3] The results cover the photon energy range from near the 4s $^3P^o$ threshold to about 3.5Ry. The main contributors to the new giant resonance in the total photoionization cross section for K 4s are the 4s $^{3,1}P^o$ and 3d $^3P^o$ terms. The details of the calculations and construction of the CI target functions are given in Mensah et. al.[3] Comparison of the partial photoionization cross sections for Na 3s and K 4s in the multi-channel energy region demonstrates the vast difference in them even though the two atoms are structurally the same. Total photoionization cross section will be presented showing the giant resonance in K 4s photoionization.

C. Collisional Excitation of Some Core-Excited NaI Quartet States

Electron-impact cross sections for core-excited quartet levels of NaI, which are metastable against autoionization, are required for the understanding of atomic spectroscopy[4] and the construction of xuv lasers. Holmgren et. al.[4] have identified a number of core-excited quartet levels in NaI and also have observed population transfer between the quasimetastable level $3s3d\ ^4S_{3/2}$ and the laser level $3s3p\ ^4D_{3/2}$. Froese Fischer[5] has studied the core-excited quartet energy levels using relativistic MCHF. We[6] have used

extensive CI target wave functions in a twelve-state R-matrix calculation to obtain excitation cross sections from ground 3s ^2S and excited 3s3p ^4S states to the lowest core-excited quartet states of NaI arising from the configurations 3s3p, 3s3d and 3s4s. The calculation cover the energy range from threshold to 6Ry. The quartet states 3s3p ^4S, ^4D, ^4P; 3s4s $^4P^o$ and 3s3d $^4P^o$, $^4F^o$ and $^4D^o$ were LS coupled with the 3s ^2S and the lowest inner-shell excited doublet states $2p^5 3s^2\ ^2P^o$, $2p^5 3s3p\ ^2D$, ^2P and ^2S. Resonance structure characterizes the cross sections near threshold with those from the 3s3p ^4S dominating the corresponding ones from the ground state by at least two-orders-of-magnitude on the average. Significantly, the cross sections from the inner-shell 3s3p ^4S state are on the average comparable to or even greater than those from the ground state to the 3d ^2D, 4s ^2S, 4p $^2P^o$ or 4d ^2D previously calculated[7]. Thus the results may have the same interesting implications for the NaI xuv laser as the quartet states in the copper vapor laser.[8]

D. Electron Excitation of Neonlike Na and Argonlike K

Electron-impact excitation of neonlike and argonlike ions is important inter alia in understanding energy balance in astrophysical objects, fusion plasmas and feasibility of new lasers. We[9] have used extensive CI target wave functions in a 9-state R-matrix calculation and program NIEM[10] to obtain electron collision cross sections from ground state to the eight lowest $2p^5 3l$(l= 0 and 1) LS excited states of neonlike Na. The results cover the energy range from near threshold to 6Ry. Additional calculation was also performed coupling only the lowest three states $2p^6\ ^1S$ and $2p^5 3s\ ^{3,1}P^o$ to assess the importance of coupling on them. For argonlike K the R-matrix method and Program NIEM were employed to compute collision strengths from ground state to the four excited states 4s $^{3,1}P^o$, 3d $^3P^o$ and 3d $^3F^o$ for impact energy from near threshold to 6Ry. We find that the results for all the inelastic except the dipole-allowed transitions are characterized by maxima near threshold and that the excitation cross section for K^+ are approximately an order-of-magnitude larger than the corresponding ones for Na^+. Furthermore, for Na^+ near threshold the 3s $^{3,1}P^o$ cross sections are significantly overestimated by the three state calculation in comparison with the nine state results. This clearly demonstrates the importance of coupling for these transitions. At higher energies, the three state is a resonable approximation to the nine state calculation.

E*. Inner-Shell Excitation of Cr^{5+} by Electron-Impact

Calculations of electron-impact excitation cross sections are sensitive to the representation of the target wave functions and strength of the couplings among the various channels. Electron collision cross sections for Cr^{5+} from ground state to 4s ^2S, 4p $^2P^o$, 4d ^2D, $3p^5 3d^2(^1D, ^1S)\ ^2P^o$, $3p^5 3d^2(^1D)\ ^2D^o$, and $3p^5 3d^2(^1G, ^1D)\ ^2F^o$ excited states are obtained in a nine state R-matrix and Program NIEM calculations. The results cover the energy range from near threshold to about five times threshold. Extensive CI target wave functions are employed. We[11] find that some of the inner-shell cross sections such as for $3p^5 3d^2(^1D, ^1G)\ ^2F^o$ are comparable to the outer-shell ones. Results are presented and compared with available theoretical data for the outer-shells.[12]

Spectral lines of boronlike ions may be useful for purposes of plasma diagnostics. Multi-state close coupling approximation using extensive CI target wave functions and Distorted Wave (DW) approximation have been used to study electron collisional excitation of boronlike nitrogen[13] from ground state to various excited levels for impact energies ranging from near threshold to 50eV. The states $2s^22p\ ^2P^o$, $2s2p^2\ ^4P$, $2s2p^2\ ^2D$, $2s2p^2\ ^1S$, $2s2p^2\ ^2P$, $2p^3\ ^2D^o$, $2s^23s\ ^2S$, $2p^3\ ^2P^o$, $2s^23p\ ^2P^o$ and $2s^23d\ ^2D$ were LS coupled in a ten state R-matrix calculation.

Large discrepaancy between DW and R-matrix results near threshold is noted for most of the transitions particularly the $2s^22p\ ^2P^o$ - $2s2p^2\ ^2D$ and $2s^22p\ ^2P^o$ - $2s2p^3\ ^2D^o$ ones. Coupling among the various states is very important for boronlike N.

* Project E was suggested by Dr. R. Phaneuf and originally supported by DOE, Division of Fusion Energy through ONRL. We have used support from this project to complete the Cr^{5+} calculation.

REFERENCES

1. K. A. Berrington et. al., Comput. Phys. Commun 14, 367 (1978)
2. A. Z. Msezane, W. Armstrong-Mensah and J. Niles, Phys. Rev. A (sumitted) (1989)
3. W. Armstrong-Mensah, J. Niles and A. Z. Msezane, Phys. Rev. A. (submitted) (1989)
4. D. E. Holmgren, D. J. Walker, D. A. King and S. E. Harris, Phys. Rev. A 31, 677 (1985)
5. C. Froese Fischer, Phys. Rev. A34, 1667(1986)
6. A. Z. Msezane and P. Awuah, J. Phys. B.(submitted) (1989)
7. A. Z. Msezane, Phys. Rev. A 37, 1787 (1988)
8. K. F. Scheibner and A. U. Hazi, Abstracts XVI ICPEAC, p37, eds. A. Dalgano et. al. (1989)
9. A. Z. Msezane and F. Nyandeh, Phys. Rev.A (submitted) (1989)
10. R. J. W. Henry, S. P. Rountree and E. R. Smith, Comput. Phys. Commun. 23, 233 (1981)
11. A. Z. Msezane, W. Richards and R. J. W. Henry, Phys. Rev. A(to be submitted) (1989)
12. M. S. Pindzola, D. C. Griffin and C. Bottcher, Phys. Rev. A 39, 2385 (1989)
13. A. Z. Msezane, R. E. H. Clark and K. J. Reed, Abstracts XVI ICPEAC p361, eds. A. Dalgano et. al. (1989).

ATOMIC AND MOLECULAR COLLISION PROCESSES

David W. Norcross
Joint Institute for Laboratory Astrophysics
National Bureau of Standards and University of Colorado
Boulder, Colorado 80309-0440

This program is concerned with developing and testing techniques for calculations of atom and ion excitation by electron impact in high temperature plasmas. The credibility of calculations, likely to be the only source of essential data for most highly-ionized heavy species, depends on successful comparisons with available ion data. Detailed calculations are being carried out for excitation of some of those very few ions for which experimental data are, or are likely to become, available, and for selected neutral atoms. By their nature neutral atoms generally present a much more demanding test of theory than do ions. In addition, much more elaborate measurements are possible for neutral atoms than for ions, such as projectile and target spin before and after the collision, and transitions between excited states, as well as between ground and excited states.

Electron-ion Collisions

Recent scattering calculations have been devoted to studies for lithium-like Be^+ and sodium-like Al^{2+}. The cross section for the transition 2s-2p in Be^+ and for the polarization of the fluorescence radiation were calculated in a variety of models, including 9-state close-coupling, at low incident electron energies.[1] The object was to resolve serious discrepancies between several previous calculations and some of the most precise measurements ever made for ion excitation. The cross section remains about 18% higher than the measured results independent of energy, and well outside the experimental uncertainties (at the 98% confidence level). The discrepancy for the polarization of the resonance fluorescence was resolved.

The calculations for excitation of Al^{2+} employed both the unitarized Coulomb-Born approximation and the close-coupling approach.[2] The inclusion of the core-polarization potentials resulted in cross sections for the resonance excitation that are about 10% smaller. In this case experimental data for comparison is almost nonexistent, but what data there is suggests an even larger (about 25%) discrepancy near threshold than for Be^+. As an additional check on these calculations, binding energies of Al^+ bound states and oscillator strengths for Al^{2+} transitions were also computed and compared with the results of measurements and other calculations.

In more formal studies of electron-ion interactions, we found that several previous calculations of the resonance fluorescence polarization, including one of our own, were based on a formulation that erroneously omitted the Coulomb phase.[3] It was also shown that the neglect of the Coulomb phase

can have a small but measurable effect on differential cross sections for electron-ion collisions at all angles, and on the generalized oscillator strength (GOS) at intermediate energies, clearly invalidating Lassettre's hypothesis in this situation. Further investigation[4] of the behavior of small-angle differential cross sections for inelastic electron-ion collisions showed that forward-angle differential cross sections for ions will be generally much smaller than for neutral atoms. One consequence of this has already been mentioned, i.e., that the limiting value of the GOS for a dipole-allowed transition at zero momentum transfer is not the optical oscillator strength. Another is a precipitous reduction in the forward angle differential cross section for intermediate energies, as illustrated for the Be^+ 2s-2p transition, that should be observable experimentally.

Spin-dependent Electron Impact Excitation of Sodium

The use of laser light to prepare atoms in pure states, in conjunction with the use of spin polarized electron beams, opens up the possibility of a "complete" measurement of the scattering amplitudes that characterize the collision. While there have been no "complete" experiments performed to date, there have been a number of experiments that have made partial measurements of the set of all possible observables. One of the most recent, by Gallagher and his group, produced angle-integrated partial cross section for exciting the 3p state of sodium as a function of the change in both the spin (M_s) and orbital angular momentum (M_l) projections of the target electron. Four quantities are obtained, Q_0^0, Q_1^0, Q_0^1, and Q_1^1. The last was found to be from ten to fifteen times smaller than the other three, and thus particularly interesting as a test of both the measurement technique and of theory.

In most respects the results of this experiment are very consistent with those of an earlier four-state close coupling calculation by the author and D. L. Moores (hereafter MN). In the case of the partial cross section Q_1^1, however, the calculations predicted a result lower than that measured by factors of two to four. This particular cross section is ten to fifteen times smaller than the others. To address this discrepancy, we carried out new close-coupling calculations using both a Lippman-Schwinger integral equations method and the Belfast R-matrix method. Unlike the MN calculation, the present model employed an **ab initio**, rather than semiempirical, treatment of the static-exchange interaction with the core electrons, and a representation of two- as well as one-body core polarization effects. A systematic series of four-, five-, and six-state calculations were performed at energies just above threshold for excitation of the 3p state.[5]

In addition to the total cross section, results were obtained for excitation of the 3p state as a function of the change in the spin and orbital angular momentum projection quantum numbers of the target electron. The calculations are in good agreement with each other and with the earlier MN calculation. Agreement with the measurements of Gallagher **et al.** is also excellent below 3 eV or so, where additional excitation channels open up. The major source of the discrepancy between the MN calculation and the measurements for the Q_1^1 cross section was traced to a very substantial

contribution from cascade to the 3p state following excitation of the 4s and 3d states. A discrepancy in the Q_1^1 cross section of a factor of two remains at energies below the cascade threshold.

Plans and Prospects

The calculations for sodium were preliminary exploratory calculations in anticipation of a more extensive study in the near future, in which more energy points will be treated (to fully resolve and average resonance structure), more states will be included in the close-coupling expansion (to ensure convergence in results for transitions between excited states), and a detailed analysis of cascade effects will be carried out. The calculations are also being extended to treat almost any possible elastic or excitation event involving electron collisions with the lowest few states of sodium, including the measurements of spin-dependent superelastic and elastic scattering of spin-polarized electrons carried out by the Celotta group at the NIST, and excited-excited state measurements underway in the Gallagher group.

Work on fully relativistic calculations for heavier systems such as cesium is planned for the longer range. As a starting point, we have available (developed with other support) a fully relativistic model potential for cesium based on solutions of the Dirac equation, extensively tested against energy levels, oscillator strengths, and scalar and tensor polarizabilities of both the ground and several excited states. Fully relativistic scattering calculations, as opposed to the more common implementation of the Breit-Pauli approximation, are now quite feasible for a multi-channel, open-shell system such as cesium that possesses but one active valence electron.

Recent Publications

1. "Electron-impact excitation of the resonance transition in Be^+," J. Mitroy and D. W. Norcross, Phys. Rev. A 37, 3755 (1988).

2. "Electron impact excitation of Al^{2+}," J. Mitroy and D. W. Norcross, Phys. Rev. A 39, 537 (1989).

3. "Coulomb-phase effects in electron-ion scattering," J. Mitroy, Phys. Rev. A 37 (rapid), 649 (1988).

4. "Coulomb phase interferences for small-angle inelastic scattering from ions," J. Mitroy, J. Phys. B: At. Mol. Opt. Phys. 21, L25 (1988).

5. "Spin dependent electron impact excitation of sodium," H. L Zhou, J. Mitroy, B. L. Whitten, G. Snitchler, and D. W. Norcross, Phys. Rev. A (in press).

CROSS SECTIONS FOR THE PHOTODETACHMENT OF He^-

David J. Pegg
Department of Physics
University of Tennessee, Knoxville, TN 37996-1200

Energy- and angle-resolved photoelectron spectroscopy has been used to determine partial cross sections (differential and integral in angle) for photodetaching an electron from the metastable He^- ion (formed in the spin-aligned $(1s2s2p)^4P$ state). When the He^- ion interacts with visible radiation, two competing photodetachment channels to the continuum are open: $h\nu + He^-(2^4P) \rightarrow He(2^3S) + e^-$ and $h\nu + He^-(2^4P) \rightarrow He(2^3P) + e^-$. In the present work the partial cross sections, $\sigma(^3S)$ and $\sigma(^3P)$, for each of these processes have been measured relative to the known cross section, $\sigma(^2S)$, for photodetaching the $D^-(1^1S)$ ion via the process: $h\nu + D^-(1^1S) \rightarrow D(1^2S) + e^-$. The cross sections are determined from measurements of the yields and angular distributions of photoelectrons ejected from the ions at the intersection of crossed laser and negative ion beams. Details of the apparatus have been given by Pegg et al.[1] Following photodetachment events, electrons ejected in the direction of motion of the ion beam (forward-directed electrons) are collected, energy analyzed and detected using a spherical-sector electron spectrometer. The angular distributions of these detached electrons have been determined by measuring their yields as a function of the angle between the linear polarization vector of the laser beam and the collection direction. This is accomplished in the present apparatus by keeping the collection fixed in the forward direction and rotating the laser polarization vector using a $\lambda/2$ phase retarder.

In the present measurements relative cross sections are obtained by comparing, under the same geometrical conditions, the yields of electrons produced in the photodetachment of the He^- ions and reference D^- ions. The yield ratio is multiplied by measured factors that take account of the different frame-transformed solid angles, photon fluxes, ion densities and asymmetry parameters associated with photodetaching electrons from the two beams. All geometric factors, being equal, cancel out. In the present work it has been arranged, by appropriate choice of ion beam energies, that the photoelectron peaks in each spectra are kinematically shifted to the same energy in the laboratory frame. This is illustrated in Figure 1. Under this condition, the efficiency factors for collecting and detecting photoelectrons at the same energy from the He^- and D^- ions are equal and hence cancel. The ion beam velocities, which are needed to determine the ion beam densities and solid-angle transformation factors, can be measured ~0.1% from an in-situ analysis of the photoelectron spectra. The technique, which involves either kinematic shifting or doubling of the spectral lines, is described in a paper by Pegg et al.[2]

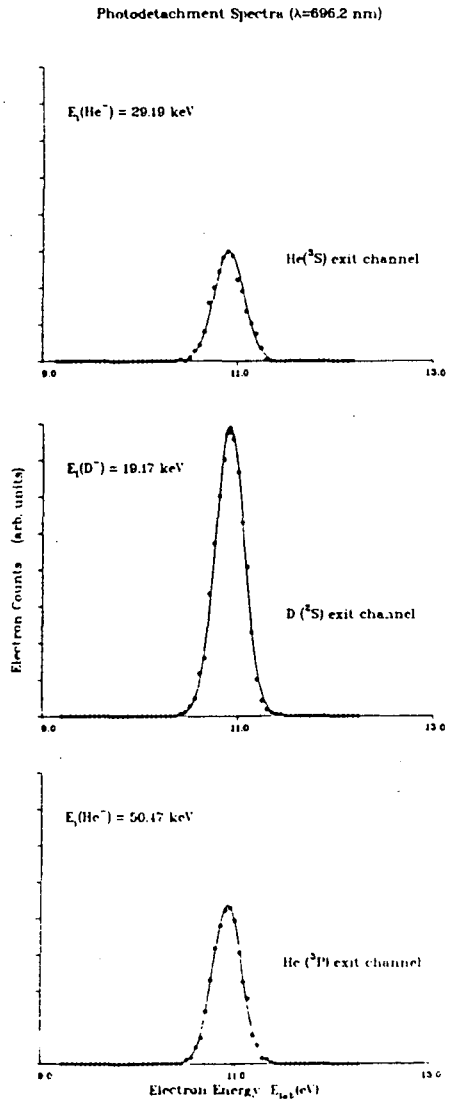

Fig. 1. Three spectral peaks kinematically shifted to the same laboratory-frame energy by an appropriate choice of ion beam energy.

The partial cross sections for photodetaching He^- relative to D^- have been measured at photon energies of 1.781 eV,

1.946 eV and 2.091 eV. The results are: $\sigma(^3S)/\sigma(^2S)$ = 0.60 ± 0.02 (1.781 eV), 0.57 ± 0.04 (1.946 eV), 0.49 ± 0.04 (2.091 eV); $\sigma(^3P)/\sigma(^2S)$ = 0.28 ± 0.02 (1.781 eV), 0.18 ± 0.02 (1.946 eV) and 0.12 ± 0.01 (2.091 eV). The uncertainties quoted on these values are at the level of two standard deviations of the weighted mean of several data sets. Systematic errors are estimated to be within the quoted limits. An absolute scale for the He^- partial cross sections has been established by assuming theoretical values[3] for the D^- photodetachment cross section (these are estimated to be accurate to better than 3%). The absolute partial (angular integral) cross sections (in Mb)) for photodetaching the He^- ion at the three different photon energies are: $\sigma(^3S)$ = 22.9 ± 1.0 (1.781 eV), 20.5 ± 1.5 (1.946 eV) and 16.6 ± 1.8 (2.091 eV); $\sigma(^3P)$ = 10.01 ± 0.6 (1.781 eV), 6.7 ± 0.6 (1.946 eV) and 4.1 ± .04 (2.091 eV). The sum of the partial cross sections can be compared with the total cross sections calculated by Hazi and Reed.[4] Figure 2 shows that there is excellent agreement between the measured and calculated total cross sections. At present there are no calculations of the partial cross sections. The measured angular integral cross sections and the asymmetry parameters can be combined to yield the angular differential cross sections. Figure 3 shows the results for a photon energy of 1.781 eV. The measured cross sections for photodetaching He^- can be used to indirectly determine, using detailed balance arguments, the cross sections, σ_a, for the far more improbable process of radiative attachment. The results are (in barns): $\sigma_a(^3S)$ = 166 ± 7 (1.781 eV), 162 ± 12 (1.946 eV), 120 ± 13 (2.091 eV); $\sigma_a(^3P)$ = 74 ± 5 (1.781 eV), 45 ± 4 (1.946 eV) and 30 ± 3 (2.091 eV).

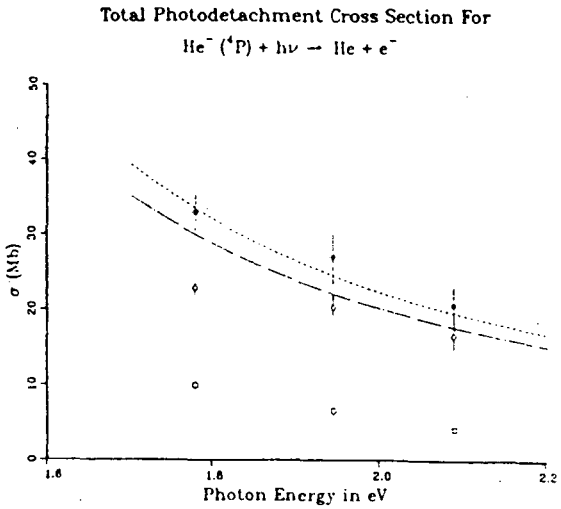

Fig. 2. Cross sections for the photodetachment of He^-. The open squares and open circles represent the partial cross sections for photodetaching He^- via the $He(^3P)$ and He (^3S) exit channels, respectively. The solid circles represent the total cross section for photodetaching He^-. The continuous curves represent the calculated total cross sections of Ref. 4. (upper curve is the length form and lower curve is the velocity form).

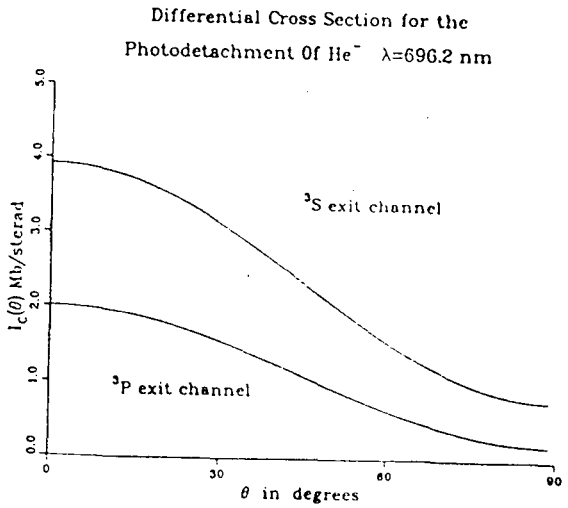

Fig. 3. Differential cross sections for photodetaching an electron from the He^- ion via the $He(^3S)$ and $He(^3P)$ exit channels.

The rather high precision (~5% in favorable cases) of the present relative cross section measurements reflects our ability to exploit, in a novel way, certain kinematic effects associated with a fast moving source of ions and the simultaneous collection of electrons in the forward direction. These features of the present apparatus have not been used in previous photodetachment studies. An absolute scale for the relative cross section measurements has been established by the use of accurate theoretical values for the cross sections for the photodetachment of the reference ion, D^-. As a result, we have been able to determine, absolutely, partial cross sections for the photodetachment of He^- to ≤10%.

We plan to continue measuring photodetachment cross sections. Emphasis during the coming year will probably be

on the stable B^- and Li^- ions. Some electron affinity measurements may also be attempted.

References

1. D. J. Pegg, J. S. Thompson, R. N. Compton and G. D. Alton, Phys. Rev. Lett. 59, 2267 (1987).

2. D. J. Pegg, J. S. Thompson, R. N. Compton and G. D. Alton, Nucl. Instr. and Methods B40/41, 221 (1989).

3. A. L. Stewart, J. Phys. B11, 3851 (1978).

4. A. U. Hazi and K. Reed, Phys. Rev. A24, 2269 (1981).

Recent publications

1. "Evidence for a Stable Negative Ion of Ca^-," D. J. Pegg, J. S. Thompson, R. N. Compton and G. D. Alton, Phys. Rev. Letters, 59, 2267 (1987).

2. "The Structure of Negative Ions Using Crossed-Beams Photoelectron Detachment Spectroscopy," D. J. Pegg, J. S. Thompson, R. N. Compton and G. D. Alton, Resonance Ionization Spectroscopy, 1988, (T. B. Lucatorto and J. E. Parks, eds. Institute of Physics Press, Bristol 1989) p. 13.

3. "Energy- and Angle-Resolved Photoelectron Spectroscopy of Negative Ions," D. J. Pegg, J. S. Thompson, R. N. Compton and G. D. Alton, Nucl. Instr. and Methods B40/41, 221 (1989).

4. "Angular Distributions of Electrons from the Photodetachment of metastable He^-," J. S. Thompson, D. J. Pegg, R. N. Compton and G. D. Alton, J. Phys. B. (submitted).

5. "Photodetachment Collisions," D. J. Pegg, Physics of Electronic and Atomic Collisions (proceedings of the XVI ICPEAC Conference, New York, 1989), (to be published).

6. "Partial Cross Sections for the Photodetachment of He^-," D. J. Pegg, J. S. Thompson, R. N. Compton, G. D. Alton, Phys. Rev. Lett. (submitted).

Research with Low Energy, Highly Charged Ions

M.H. Prior

Materials and Chemical Sciences Division
U.C. Lawrence Berkeley Laboratory

During the period since the last DOE/BES atomic physics contractors workshop, research at the LBL ECR ion source has concentrated upon studies of multiply excited energy levels populated by electron capture from atomic targets. The technique of zero degree electron spectroscopy has been used to measure projectile Auger electron energies following these collisions. The work provides new values for multiply excited energy levels and insight into the collision mechanism via the particular states populated. In addition some ion surface studies were carried out in search of charge dependent effects on sputtering yields using highly charged ions on metals and insulators. The program to measure forbidden line wavelengths from metastable beam ions has been maintained, but has not been emphasized during the last year. Much of this work is collaborative with groups from outside LBL and utilizes the low energy beam lines which are a joint LBL-LLNL maintained facility.

I. Na-Sequence Auger Spectra from Double Capture on He Atoms by the F-like Ions: Si^{5+}, Ar^{9+}, Ti^{13+} , Fe^{17+}, and Cu^{20+}.

A systematic study has been made of the energy spectra of Auger electrons emitted from Na-like products into the forward (zero degree) direction following electron capture from helium target atoms by low energy (q x 10 keV) projectile ions. The ions were produced by the LBL Electron Cyclotron Resonance (ECR) ion source. In this work care was taken to distinguish those features in each spectrum produced by single collision double capture events from those produced by two sequential single captures via an intermediate, metastable Neon-like state. The later process was prominent in the lower charged members of the sequence. Strong production of highly non-equivalent two electron states in double capture collisions was observed [see e.g. publication 1]. A striking result of these studies was the observation and energy measurement of the the metastable $2p^5 3s3p\ ^4D_{7/2}$ level, which decays predominently by the normally negligible relativistic Breit interaction. The figure shows the effect of nuclear spin, (via hyperfine mixing) on long lived components of $2p^5 3s3p$ in $^{48,47}Ti^{11+}$. This work is a collaborative effort with D. Schneider, S. Chantrenne, R. Hutton, and M.H. Chen of LLNL.

II. Double Capture to Bound and Continuum States in O^{6+}, He Collision.

Zero degree electron spectra produced by O^{6+} ions colliding with He atoms at 60 keV have been collected in coincidence with charge analyzed O^{5+} and O^{6+} projectile final states. Emphasis to date has been on the "cusp" electrons, created at near zero energy in the frame of the projectile. We observed few (consistent with zero) of these continuum electrons in coincidence with O^{6+} (no charge change) projectile products, but a clear cusp spectrum in coincidence with the O^{5+} (one electron transferred) final projectile state. These observations strongly suggest that double "capture" to one bound and one continuum state is a prominent, and perhaps dominant two electron process. It appears to be a continuation across the series limit, of the so called "correlated" double capture process observed in the same collision system by Stolterfoht et al via the low energy Coster-Kronig Auger lines produced when O^{4+} 2pnl ($n>5$) states decay. Our observations indicate that "capture" to the projectile continuum is nearly always accompanied by capture to a bound state, at the low collision energy of this work. This study is a collaboration with J.A. Tanis (U. Western Michigan), D. Schneider, S. Chantrenne, and R. Hutton (LLNL), R. Herrmann (U. Frankfurt), and G. Schiwietz (Hahn-Meitner Institute, Berlin).

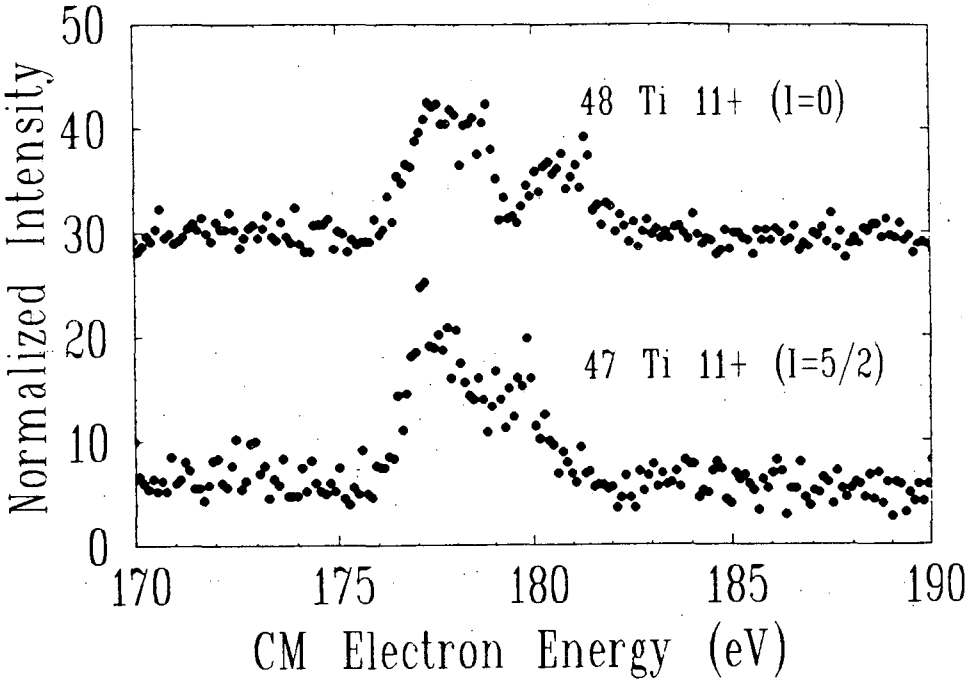

Figure

Comparison of spectra from the Auger decay of long lived components of the $2p^5 3s3p$ configuration in $^{47}Ti^{11+}$ (nuclear spin 5/2), and $^{48}Ti^{11+}$ (nuclear spin zero). Hyperfine mixing can alter the lifetimes of, e.g., the ^4D_J states of this configuration, thus producing an isotopic variation in the partially resolved line shapes seen in delayed spectra such as these.

III. Forbidden Emission Line Spectra from Highly Charged, Metastable Ion Beams.

A normal incidence vacuum spectrometer has been mounted to view forbidden emission lines from metastable ions produced by the LBL ECR ion source. This instrument will complement and extend earlier measurements [publication 5] made in the visible wavelength region. Initial tests and calibrations have been completed. The first measurement carried out with this instrument was of the transition $2p^3$ $^2D_{3/2}$-$^2P_{3/2}$ in N-like Ar^{11+}. The measured value for this line is 168.67(10) nm which agrees with, and improves upon, the indirectly determined value 168.63(18) [W.A. Deutschman, and L.L. House, Astrophys. J **149**, 451 (1967)].

IV. K-Vacancy Transfer in Slow Ion-Atom Collisions.

Oscillatory interference effects were observed due to K-vacancy transfer in Ne^{9+} + Ne collisions at 90 keV impact energy. The vacancy transfer collisions can produce structure in the charge analyzed projectile scattering angle distributions because of interference between amplitudes for transfer at avoided level crossings on the ingoing and outgoing portions of the trajectory, much as in the case of quasi-molecular X-ray interference. Observation of these interference effects is much easier in the case of vacancy transfer because one is detecting, with high efficiency, the deflection of final particle charge states rather than the weak X-ray photon spectra from the transient quasi-molecule. Data were collected for projectile product charges 4-9+ scattered through angles up to about 35 milliradians in coincidence with all tar-

get recoil-ion states. Clear interference structure appears only for certain final charge state combinations. This is a collaborative effort with a group from U. Frankfurt (H. Schmidt-Boecking, R. Doerner, R. Herrmann, and H. Berg).

V. Highly Charged Ion Sputtering of Metal and Insulator Surfaces.

Studies were made of the charge dependence of the yield and angular distribution of the sputtered atoms and ions from metal (Au) and insulators (CsI, $LiNbO_3$) using beams of 48 keV $Ar^{4,8+}$ and 60 keV Ar^{11+} ions [publication 3]. There is interest in highly charged ion surface interactions in the regime where the potential energy carried to the surface by the ion approaches (or even exceeds) the kinetic energy. This work approaches that regime but, although the potential energy varied by about a factor of 12 from Ar^{4+} to Ar^{11+}, the kinetic energy remained dominant. Our observations show a slight charge dependence of the sputtering yield (about a 10% variation) for the insulators and no variation for the Au target. It was expected that insulators would show an effect because of their much slower neutralization time. The data was taken using a collector technique: sputtered material was captured onto foils surrounding the target, the foils were analyzed after collection by heavy ion Rutherford backscattering spectroscopy to determine the angular dependence of heavy components of the target material. In a separate series of experiments, a real time technique was developed to monitor Na atoms via their optical emission spectra following ejection from a NaCl single crystal target. This work is a collaboration with R. Stokstad (LBL), D. Weathers, T. Tombrello (Cal. Inst. Tech.), and R. Tribble (Texas A&M U.).

VI. Future Prospects

The new advanced ECR ion source (14 Ghz) is nearly completed at the LBL 88-inch cyclotron. It is expected to operate for initial tests in October 1989. The new source has the potential to impact upon the atomic physics program in two ways; i) by making more time available for research with slow highly charged ions (since the cyclotron will take a beam from one of the two sources), and ii) by making increased currrents and more highly charged ion beams available. To realize this potential, planning is underway for necessary transport facilities needed to bring beams to experimental areas.

VII. Recent Publications.

[1] R. Hutton, M.H. Prior, S. Chantrenne, M.H. Chen and D. Schneider
Double and Single Electron Capture in Slow Collisions of $Ar^{9+,8+}$ Ions with He Atoms.
Phys. Rev. **A39**, 4902 (1989) [Rapid Communication].

[2] Auger Electron Emission from Na-like Fe Ions Excited in Collisions of 170-keV Fe^{17+} on He and Ne.
D. Schneider, S. Chantrenne, M.H. Chen, R. Hutton and M.H. Prior
Phys. Rev **A40**, [in press to appear October 1989]

[3] Sputtering of Au, CsI and $LiNbO_3$ by Multiply Charged Ar Ions.
D.L. Weathers, T.A. Tombrello, M.H. Prior, R.G. Stokstad, and R.E. Tribble
Nuc. Inst. and Methods in Phys. Res. **B42**, 307 (1989).

[4] H. Schmidt-Boecking, M.H. Prior, R. Dorner, H. Berg, J.O.K. Pedersen, C.L. Cocke, M. Stockli, and A.S. Schlachter
Angular Dependence of Multiple-Electron Capture in 90-keV Ne^{7+} - Ne collisions
Phys. Rev. A **37**, 4640 (1988).

[5] M.H. Prior
Forbidden Lines from Highly Charged, Metastable Ion Beams.
J. Opt. Soc. Am. B **4**, 144, (1987).

NEAR RESONANT ABSORPTION BY ATOMS IN INTENSE FLUCTUATING FIELDS

S.J. Smith, M.H. Anderson and R.D. Jones
JILA, University of Colorado and NIST, Boulder, CO

We have completed an experimental investigation of the fluctuations of the fluorescence from two-level atoms driven by a phase diffusing laser. A highly stabilized ring dye laser was extra-cavity modulated with statistically well-characterized RF noise and scanned 200 MHz across the 10 MHz natural width $3S_{1/2}(F=2,\ m_F=2) \rightarrow 3P_{3/2}(F=3,\ m_F=3)$ transition of a sodium atomic beam. Fluorescence was detected by a photomultiplier and analyzed for both its DC and AC components. The DC component is the average fluorescence intensity and is proportional to the average upper state population $\langle\rho_{11}\rangle$, while the AC component is proportional to the variance of the upper state population, $\langle\rho_{11},\rho_{11}\rangle \equiv \langle\rho_{11}^2\rangle - \langle\rho_{11}\rangle^2$. The variance of the fluorescence was found to be on the order of the average fluorescence and, due to efficient fluorescence collection, more than 10 times the shot noise. Our results for different laser powers and linewidths are in qualitative agreement with the recent theoretical predictions of Haslwanter, Ritsch, Cooper and Zoller [Phys. Rev. A38, 5652 (1988)] and a presentation of them will be submitted to Physical Review Letters.

The frequency dependences (power spectra) of these fluctuations at fixed detunings have been measured and show interesting structure. The above theory has been extended to predict these power spectra and, again, our experimental results are in qualitative agreement. Both the variance and its power spectrum have proven to be extremely sensitive indicators of the laser field statistics.

While the theory of Haslwanter et al. did consider the effect of finite detector response time, better agreement between our data and theory is obtained if the theory is adapted to also account for a non-uniform laser intensity profile and residual Doppler broadening of the atomic transition. In collaboration with Cooper and Zoller, we have augmented the original theory and written computer programs to explicitly treat these phenomena. The spatial effects introduce a considerable complication in the problem due to correlations between the emission from different positions in the atomic beam. If $\rho_{11}(\vec{x},\vec{v})$ is the population of the emitting level at position $\vec{x}$ for an atom moving with velocity $\vec{v}$, it is necessary to calculate the average of the two-position variance, $\langle\rho_{11}(\vec{x},\vec{v}),\rho_{11}(\vec{x}',\vec{v}')\rangle$, over the laser fluctuations. For a two-level atom the resulting equations lead to a 9x9 matrix in contrast to the 6x6 for a uniform field. After solving these equations, four-fold integration over $\vec{x}$, $\vec{x}'$, $\vec{v}$ and $\vec{v}'$ is required. The programs have been useful not only in understanding our data, but have assessed the feasibility of doing similar measurements in a cell of atomic vapor.

Some of our experimental results are shown on the following page. The three figures are: a) the fluorescence intensity (upper curve) and its variance (lower curve) vs. detuning and b) the power spectra of the variance at the specified detunings. In Figures 1 and 2, the Rabi frequency is below saturation and the laser linewidth is narrower and broader, respectively, than the natural linewidth of the atomic transition. The double humped variance is a characteristic of the phase diffusing field. In Figure 3 the laser linewidth is narrow but the Rabi frequency is above saturation. The power spectra of the variance, particularly at larger detunings, show local maxima at the generalized Rabi frequency.

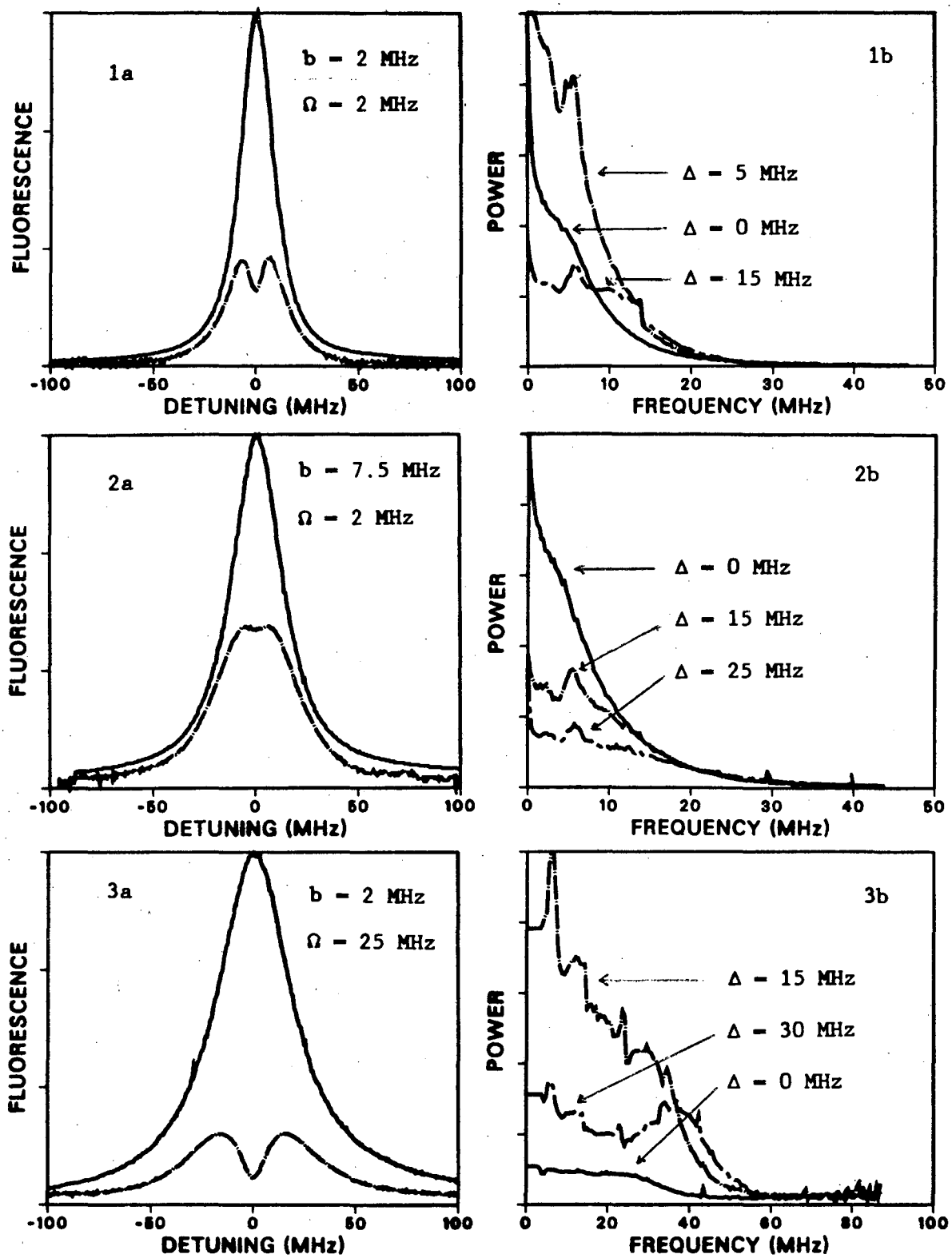

The fluorescence intensity and its variance vs. detuning and power spectra of the variance at fixed detunings, Δ, were measured at different laser linewidths, b (HWHM), and intensities, Ω (Rabi frequency).

This experimental study of variance of the resonance fluorescence signal as a function of laser coherence and intensity, and the corresponding theoretical analysis, has comprised much of the effort during the current grant year. The study and comparison of experimental and theoretical results is complete and a publication of them is in preparation.

The theoretical analysis for our earlier experimental studies of the role of phase fluctuations on the formation of Hanle resonances in the $^1S_0 \rightarrow {}^3P_1$ transition in atomic ytterbium has been completed in collaboration with R. Ryan and T. Bergeman of SUNY-Stony Brook. The comparison demonstrates that the theory of Dixit, Zoller and Lambropoulos [Phys. Rev. A21, 12 (1982)] correctly accounts for the complex behavior of Hanle resonances driven by partially coherent laser fields. A detailed manuscript describing this work has been submitted to the Physical Review.

Our immediate plans are to extend our investigations of laser noise on two-level systems by studying the effects of correlated amplitude and phase fluctuations. Preliminary results have shown interesting differences from phase fluctuations only, evidenced by drastic assymetry in the variance vs. detuning. We also plan to study the role of phase fluctuations in four-wave mixing, a topic which has been the subject of a number of theoretical studies, but for which any sort of experimental confirmation is lacking. Various configurations have been suggested [G.S. Agarwal, private communications 1987, 1989]. One possibility is forward four-wave mixing with a linearly polarized pump laser. The probe laser is noise modulated and the transfer of fluctuations to the corresponding signal beam is studied.

We have recently completed the construction of a second frequency-stabilized ring dye laser which will enable us to perform high resolution two-color experiments. A proposed collaborative effort with S. Stenholm (University of Helsinki, Finland) and co-workers involves certain zero-field level crossing configurations in a phase diffusing laser field to show the analogy between atomic collisional effects and the phase fluctuations of the laser.

DYNAMICS OF COLLISIONS PROCESSES

Anthony F. Starace
Department of Physics and Astronomy
The University of Nebraska
Lincoln, Nebraska 68588-0111

I. INTRODUCTION

This project is concerned with collision processes which are governed by the dynamics of three interacting charged particles. The systems of three interacting charged particles are described by hyperspherical coordinate wave functions. Among the collision processes currently being investigated are high energy detachment collisions of negative hydrogen ions with various target atoms, single and multiphoton detachment of H^-, and capture collisions of low energy negative muons by atomic hydrogen.

II. FAST H^- DETACHMENT COLLISIONS

We have obtained detailed theoretical results [1,2] for the electron detachment cross section, doubly differential in both the electron momentum and angle, for the process 0.5 MeV $H^- + He \rightarrow H(n=2) + e^- + He^*$. These results show that laboratory frame doubly differential cross sections (DDCS's) for electron detachment in the forward direction depend sensitively on the low-energy states of the $H(n=2) - e^-$ three-body system. In particular, the angular dependence of characteristic cusp and shape resonance features has been obtained. We find the projectile frame DDCS for detached electron energies in the vicinity of the shape resonance peak is nearly isotropic. This is due in part to the ^1P symmetry of the resonance feature, which limits the angular distribution to constant and $\cos^2\theta$ terms, and in part to cancellation in the integral over momentum transfer on which the coefficient of the $\cos^2\theta$ term depends. We find also that the rapid variation of these cusp and shape resonance features with angle in the laboratory frame requires that experimental angular and energy resolutions be accounted for in order to obtain good agreement with the measured results of M.G. Menendez and M.M. Duncan[3] on the energy spectrum of detached electrons coincident with formation of H(2p) [cf. Fig. 1]. The DDCS's for 0.5 MeV $H^- + He \rightarrow H(1s) + e^- + He^*$ have also been obtained.[2] When these latter results are added to those for producing H(n=2), the sum gives good agreement with the experimental data of M.G. Menendez and M.M. Duncan[4] which include all final states of the H atom, thereby confirming the important contribution the H(n=2) states make to the total detachment cross section [cf. Fig. 2]. Finally, we have pinpointed the origin of our predicted Gailitis-Damburg oscillations in the DDCS near threshold as stemming from a rapid decrease of an analytically known phase appropriate for long-range dipole fields.[2]

These calculations for 0.5 MeV H^- on He have most recently been extended to 0.5 MeV, 1.0 MeV, and 1.5 MeV H^- detachment collisions on all of the rare gases. Unlike the case of 0.5 MeV H^- detachment collisions on He leading to excitation of H(n=2), whose DDCS is isotropic in the projectile frame, the DDCS for other incident energies and other target atoms is in general anisotropic. Furthermore, whereas the DDCS leading to H(n=1) states is only

weakly dependent on the incident projectile energy, the DDCS leading to H(n=2) states decreases rapidly with increasing projectile energy. Lastly, as expected,[5] we find a strong dependence of the double-peaked structure in the DDCS on the average binding energy of the target atom. These voluminous results are currently being analyzed in preparation for their publication. Upon completion of this work, we shall begin work on fast negative alkali detachment collisions.

III. H_2^+ FORM FACTORS

The scattering form factors for excitation of H_2^+ in fast collisions have been calculated[6] in a sequence of approximations revealing their dependence on details of the initial and final state wave functions. Each approximate calculation is compared directly to the "exact" results obtained with separable, fixed-nuclei wave functions. Even for inter-proton separations larger than those for which the united atom limit applies, the quasi-atomic character of the final state orbital dominates transition amplitudes to low-lying dissociative states.

IV. TWO- AND THREE-PHOTON DETACHMENT OF H^-

Two-photon detachment cross sections of H^- have been obtained using a new variational procedure[7] within an adiabatic hyperspherical coordinate representation.[8] Results for both linearly and circularly polarized light have been obtained for photon energies below the one-photon ionization threshold. The two-photon cross sections compare well with other theoretical results[9,10] and the three-photon cross sections are presently being calculated.

V. SLOW MUON CAPTURE BY ATOMIC HYDROGEN

Capture of slow muons by H is being studied as a novel application of the hyperspherical coordinate representation of three-body systems. M. Cavagnero has obtained radial potential curves in two simple approximations: (a) monopole scattering; (b) linear trajectory scattering. Each approximation gives insight into the capture process. We are currently calculating capture probabilities into alternative Rydberg states using Landau-Zener-type procedures.

REFERENCES

1. C.R. Liu and A.F. Starace, Phys. Rev. Lett. **62**, 407 (1989).
2. C.R. Liu and A.F. Starace, Phys. Rev. A **40** (November 1989).
3. M.G. Menendez and M.M. Duncan, Phys. Rev. A **36**, 1653 (1987).
4. M.G. Menendez and M.M. Duncan, Phys. Rev. **20**, 2327 (1979).
5. J.H. Macek, M.G. Menendez, and M.M. Duncan, Phys. Rev. A **29**, 516 (1984).
6. M. Cavagnero, Phys. Rev. A (in press).
7. B. Gao and A.F. Starace, Phys. Rev. Lett. **61**, 39 (1988); Phys. Rev. A **39**, 4550 (1989).
8. B. Gao, C. Pan, C.R. Liu, and A.F. Starace, J. Opt. Soc. Am. B (in press).
9. M. Crance and M. Aymar, J. Phys. B **18**, 3529 (1985).
10. M.G.J. Fink and P. Zoller, J. Phys. B. **18**, L373 (1985).

BIBLIOGRAPHY

1. A.F. Starace, HYPERSPHERICAL DESCRIPTION OF TWO-ELECTRON SYSTEMS, in Fundamental Processes of Atomic Dynamics, Edited by J.S. briggs, H. Kleinpoppen, and H.O. Lutz, (Plenum, New York, 1988), pp 235-258.
2. C.R. Liu and A.F. Starace, LOW-ENERGY FEATURES OF THE e^- - H(n=2) SYSTEM EXHIBITED IN FAST H^- DETACHMENT COLLISIONS, Phys. Rev. Lett. 62, 407 (1989).
3. C.R. Liu and A.F. Starace, DOUBLY DIFFERENTIAL DETACHMENT CROSS SECTIONS FOR 0.5 MeV H^- ON He INCLUDING PROJECTILE EXCITATION TO H(n=2), Phys. Rev. A 40 (November 1989).
4. M. Cavagnero, QUASSI-ATOMIC CONTRIBUTIONS TO MOLECULAR SCATTERING FORM FACTORS, Phys. Rev. A (in press).
5. B. Gao, C. Pan, C.R. Liu, and A.F. Starace, VARIATIONAL METHODS FOR HIGH-ORDER MULTIPHOTON PROCESSES, J. Opt. Soc. B (in press).

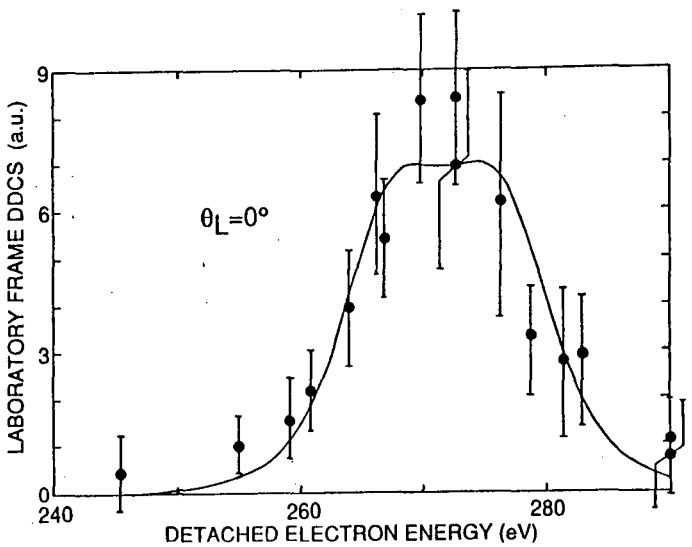

Figure 1. Comparison of experimental (Ref. 3) and theoretical (Ref. 2) results for the DDCS for 0.5 MeV H^- + He → H(2p) + He^* at $\theta_L = 0°$.

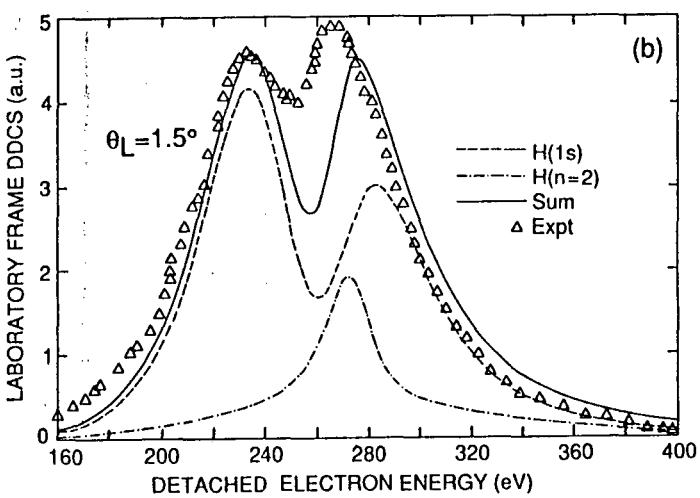

Figure 2. Comparison of experimental (Ref. 4) results for the DDCS for 0.5 MeV H^- + He → H^* + He^* at $\theta_L = 1.5°$ with theoretical results (Ref. 2) for the particular H atom final states H(1s) and H(n=2).

EXCITATION OF ATOMS AND MOLECULES IN COLLISIONS WITH FAST, HIGHLY CHARGED IONS*

R. L. Watson

Cyclotron Institute and Department of Chemistry
Texas A&M University, College Station, TX 77843

A. Relative Probabilities for Double and Single Ionization of He in Collisions with 10-30 MeV/u N^{7+} Ions

High energy beams of fully stripped nitrogen ions from the new Texas A&M K500 superconducting cyclotron have been used to explore the Z-dependence of the double-to-single ionization probability (R) in helium. The relative cross sections for production of He^{+} and He^{2+} by 10, 15, 20, and 30 MeV/u N^{7+}, and 20 MeV/u He^{2+} have been measured by time-of-flight spectroscopy. The present results are compared with experimental data and theoretical predictions of other investigators in Fig. 1. Previous measurements of R employing electrons, protons, and antiprotons (1) have established that R decreases rapidly with increasing projectile velocity and becomes constant above 5 to 10 MeV/u. The data for nitrogen, however, appear to level off at an R value of 0.01, which is over 4 times the high velocity limit set by the proton and helium-ion data. The constancy of R at high velocity is presumed to reflect the dominance of the shakeoff mechanism, and the limiting value is supposed to be independent of projectile Z, as is predicted by the theoretical curve of Ford and Reading (4) and the semiempirical curve of Knudsen et al. (3) for N^{7+} ions.

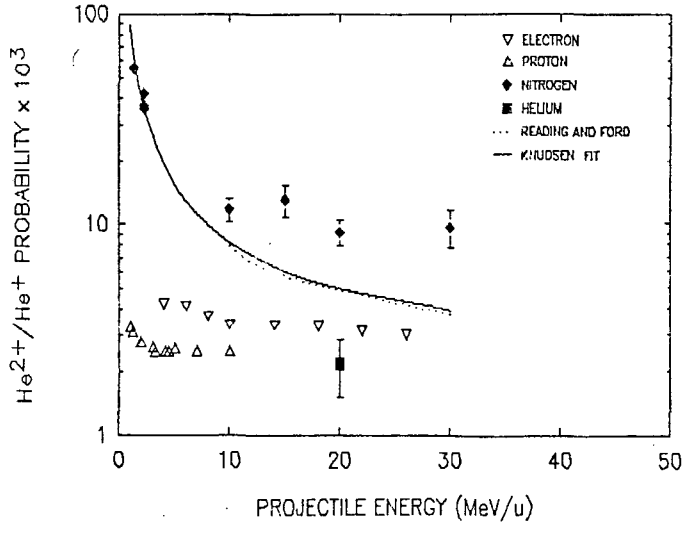

Fig. 1. Comparison of the present He double-to-single ionization ratios (data points with error bars) with other data for protons, electrons, and antiprotons (1), and nitrogen ions (2, 3). The curves show the predictions of calculations by Ford and Reading (4), and semiempirical calculations by Knudsen et al. (3) for N^{7+}.

B. Charge Distributions of Ar Recoil-Ions Produced in One- and Two-Electron Capture Collisions with 16 MeV O^{q+} Ions

The yields of Ar recoil-ions produced in collisions with 16 MeV O^{q+} (q = 3 to 8) have been measured in coincidence with one- and two-electron capture by the projectile. Time-of-flight analysis identified the charges of the Ar recoil-ions and enabled the determination of charge state distributions. The Independent Electron Approximation was employed along with a simple exponential parameterization of the ionization and capture probabilities to calculate the cross sections for multiple ionization accompanied by one- and two-electron capture. By accounting for direct L-shell ionization and Auger multiplication of L-shell vacancies, good agreement between calculated and measured charge state distributions was attained.

C. Time-of-Flight Difference Spectra for Ion-Pairs produced in the Dissociation of Multi-Charged O_2 Molecular Ions

Experiments were performed last year on multiply-charged O_2 molecular ions produced in collisions with 40 MeV Ar^{13+} ions. Oxygen ion-pairs resulting from the subsequent dissociation of a molecular ion were accelerated out of the gas cell into a time-of-flight (TOF) spectrometer and their flight time differences were recorded event-by-event. This year, considerable effort has been expended in developing a Monte Carlo procedure for simulating the ion trajectories in order to accurately translate the measured Δt distributions into kinetic energies. The initial positions of ion pairs in the gas cell are randomly generated, and their trajectories through the gas cell and TOF spectrometer are calculated with the aid of an electrostatic lens program called SIMION (5). Each set of accepted trajectories (i.e. trajectories for which both ions make it out of the gas cell and through the spectrometer) contributes a Δt event to the calculated time distribution. By running simulations for different values of the total kinetic energy release (KER), the KER's and energy widths of the measured Δt distributions may be estimated. In addition, the simulation program provides the detection efficiency for the various ion charge combinations so that fragmentation yields may be determined.

The Δt distributions for O^+/O^+ and O^{2+}/O^{2+} ion pairs produced in the dissociation of O_2^{2+} and O_2^{4+} molecular ions, respectively, are particularly intriguing in that they display several partially resolved peaks. The simulations for these cases suggest that the dissociation events proceed from well defined metastable states of the molecular ions. A preliminary analysis of the Δt distribution for O^+/O^+ gives KER's that are in reasonable agreement with those estimated from theoretical potential energy curves (6) for two sets of closely spaced excited states in O_2^{2+}.

* Collaborators: B. B. Bandong, O. Heber, B. Hill, T. Lotze, E. Moler, and G. Sampoll

References

(1) L. H. Andersen, P. Hvelplund, H. Knudsen, S. P. Moller, A. H. Sorensen, K. Elsener, K.-G. Rensfelt, and E. Uggerhoj, Phys. Rev. A**36**, 3612 (1987).

(2) A. Muller, B. Schuch, W. Groh, and E. Salzborn, Z. Phys. D**7**, 252 (1987).

(3) H. Knudsen, L. H. Andersen, P. Hvelplund, G. Astner, H. Cederquist, H. Danared, L. Liljeby, and K.-G. Rensfeld, J. Phys. B**17**, 3545 (1984).

(4) A. L. Ford and J. F. Reading (private communication).

(5) D. A. Dahl and J. E. Delmore, Idaho National Engineering Laboratory report EGG-CS-7233 Rev. 1 (1987).

(6) A. C. Hurley, J. Molec. Spectr. **9**, 18 (1962).

FIVE RECENT PUBLICATIONS

B. B. Bandong, R. L. Watson, J. Pálinkás and C. Can, "K X-ray Spectra of Highly Charged Recoil Ions Produced by Heavy-Ion Impact on Oxygen", J. Phys. B: At. Mol. Opt. Phys. **21** 1325-1351 (1988).

J. A. Demarest and R. L. Watson, "Beam-Foil Study of Neon in the EUV with Foils of Carbon, Silver and Gold", Physica Scripta **38**, 670-676 (1988).

G.-J. Yu, R. L. Watson, B. B. Bandong, C. Can, G. Sampoll, E. Moler and R. J. Maurer, "Collisional Quenching of 2^3P and 2^4P States in 33 MeV Two- and Three-Electron Mg Ions", Phys. Rev. A**39**, 1041-1048 (1989)

B. B. Bandong and R. L. Watson, "Resonant Multi-Electron Transfer in Solid Oxides Following Double K-Shell Ionization by Heavy-Ion Impact", Phys. Rev. A**39**, 1714-1724, (1989).

O. Heber, G. Sampoll, B. B. Bandong, R. J. Maurer, E. Moler, R. L. Watson, I. Ben-Itzhak, J. L. Shinpaugh, J. M. Sanders, L. Hefner and P. Richard, "Charge Multipication Via Auger Decay of L-Vacancies in the Production of Highly Charged Ar Ions by Collisions with 1 MeV/amu O^{q+} and F^{q+}", Rapid Communication in Phys. Rev. A**39**, 4898-4901 (1989).

ELECTRON TRANSFER, IONIZATION, AND EXCITATION IN ATOMIC COLLISIONS

Thomas G. Winter and Steven G. Alston
Department of Physics, Pennsylvania State University
Wilkes-Barre Campus, Lehman, PA 18627

The theoretical research being carried out at Penn State by Alston and Winter concerns basic atomic-collision processes at intermediate and high energies. In the high velocity regime, electron capture is considered using a very high order multiple-scattering approach. Separately, the effect on the capture amplitude of altering the inner part of the internuclear potential is explored. In the intermediate velocity regime, earlier work on collisions between protons and hydrogenic-ion targets is being extended to the two-electron helium target.

For high energies, a Faddeev approach[1,2] through second order has been applied to electron capture. The amplitude is simply related to the full second Born (B2) approximation containing the internuclear potential by noting that each two-body potential in the latter is replaced by a two-body transition operator, except for the two terms involving the internuclear potential alone which are replaced by the internuclear transition matrix. Guided by the B2's insight into double scatterings[3] (Thomas mechanisms[4]), the conceptual framework is retained while a much more accurate treatment of each of the scatterings is included by the use of the transition matrices.

For capture at angles less than 1 mrad, four separate regions can be identified in which different scattering effects play major roles: first, the extreme forward region (less than 0.2 mrad) where the first Born term dominates; secondly, an interference region (between 0.2 and 0.4 mrad) where large cancellations of the various terms in the amplitude occur; thirdly, the Thomas peak region (between 0.4 and 0.6 mrad) where double-scattering dominates; and finally, the region beyond (greater than 0.6 mrad) in which nuclear scattering takes over. The Faddeev theory is seen to reproduce the experimental data well for protons on hydrogen[5] and extremely well for protons on helium[6]. It has also been shown[7] analytically for symmetric collisions (each nucleus having charge Z), that the magnitude of the double-scattering contribution is increased over the B2 result by a factor of $\exp(2\pi Z/v)$ in accord with the inclusion of a better treatment[8] of each Coulomb scattering.

While the approximation of each potential of modified Coulomb form by a scaled Coulomb potential for high velocities and momentum transfers is well justified in our approach, comparision with data shows that the treatment of off-energy-shell effects is more sensitive and one must use a near-shell approximation for the more correct modified potential case,[9] as is done here.

Further, over the full range of near-forward scattering angles, it has been recognized for some time[10] that the sum of the first- and second-order terms containing the internuclear potential in the B2 approximation interfere destructively to the order of the square of the projectile or target nuclear charges over the impact velocities, which is small for large

velocities. That is, within the accuracy of the approximate evaluation no internuclear contribution to the amplitude is found, contrary to the behavior found for the eikonally transformed amplitude[11] (Bessel transform of the amplitude with a $b^{2i\nu}$ factor included, where b is the impact parameter and ν the internuclear Sommerfeld parameter). It is shown that the Faddeev treatment gives a non-zero contribution that agrees very well not only with the experimental data[5] for protons on helium but also with the eikonal results of the continuum distorted-wave approximation.[12]

Using a simple closed-form expression for the electronic part of the Faddeev amplitude, the velocity dependence of the total cross section has been studied to ascertain the modification of the B2 cross section when the double-scatterings are treated more accurately. Although the leading order v^{-11} velocity dependence is unchanged, the coefficient of the next order term is changed, because a Coulomb treatment is introduced for both the electron-projectile and electron-target nucleus collisions, as opposed to the use of this approximation in the strong-potential Born (SPB) approximation[13] for the latter collision only.

In a separate study,[14] a better representation of the short-range part of the internuclear potential in the boundary-corrected first Born (B1B) approximation[15] has been investigated. The effect of the short-range part on the amplitude is seen to vary according to how much the large momentum-transfer components contribute to the amplitude. For energies above 400 keV, good agreement with proton-helium total cross sections[16] is found using a simple model in which the non-active electrons screen the target nucleus by means of a frozen Hartree-Fock density. Comparison with the B1B amplitude[17] obtained using a bare target nucleus shows that results do not differ greatly from those of the present screened theory. This result is very puzzling in view of the greatly differing amplitudes.

A large calculation of cross sections for electron transfer, ionization, and excitation in collisions between protons and helium atoms is now underway. The higher intermediate proton energies (from 50 to 300 keV) are being considered. In this energy range, a coupled-state approach is called for rather than a perturbative approach. A basis of more than 100 Sturmian functions is being used for this two-electron system, extending earlier work on one-electron systems.[18] Both ionization channels and correlation are being accounted for. The two-electron scattering program is largely written. Direct matrix elements have been calculated,[19] and a calculation of the velocity-dependent charge-exchange matrix elements is underway. To execute the computer programs on Pennsylvania State University's IBM 3090/600S computer in a reasonable amount of time, these programs are being vectorized as fully as possible. At energies of up to 100 keV, results for electron capture into n = 3 levels will be compared with the detailed experimental results of Ashburn, Cline, van der Burgt, and Risley[20] and the coupled-state results of Shingal and Lin.[21]

Finally, in collaboration with Stodden, Monkhorst, and Szalewicz, very accurate stripping cross sections for proton-He^+ collisions have been determined at center-of-mass energies from 14 to 600 keV.[22] These calculations hve been used to determine reactivation coefficients in muon-catalyzed d-t fusion.

REFERENCES

1. L. D. Faddeev, Sov. Phys. JETP 12, 1014 (1961); K. Taulbjerg and J. S. Briggs, J. Phys. B 16, 3811 (1983).
2. S. Alston, Nucl. Instrum. Methods B 43, 19 (1989) and S. Alston, "Unified Faddeev Treatment of High-Energy Electron Capture," Phys. Rev. A (submitted).
3. R. M. Drisko, Ph.D. thesis, Carnegie Institute of Technology (1955); S. Alston, Phys. Rev. A 38, 6092 (1988) and references therein.
4. L. H. Thomas, Proc. R. Soc. London, Ser. A 114, 561 (1927).
5. H. Vogt, R. Schuch, E. Justiniano, M. Schulz, W. Schwab, Phys. Rev. Lett. 57, 2256 (1986).
6. E. Horsdal-Pedersen, C. L. Cocke, and M. Stockli, Phys. Rev. Lett. 50, 1910 (1983).
7. S. Alston, "Closed-Form Expression for 1s-1s Electron Capture Amplitude in a Second-Order Faddeev Approximation," Phys. Rev. A 40, xxxx (November, 1989).
8. See the discussion surrounding Eq. (6.45) of C. J. Joachain, Quantum Collision Theory (North-Holland, Amsterdam, 1975).
9. S. Alston, Phys. Rev. A 38, 636 (1988); H. Marxer, S. Alston, and J. Briggs, Z. Phys. D 5, 35 (1987).
10. K. Dettmann and G. Leibfried, Z. Phys. 218, 1 (1969).
11. R. McCarroll and A. Salin, J. Phys. B 1, 163 (1968).
12. R. D. Rivarola, A. Salin, and M. Stockli, J. Phys. Lett. 45, L259 (1984).
13. J. Macek and S. Alston, Phys. Rev. A 26, 250 (1982).
14. S. Alston, "Nuclear-Charge Screening in Electron Capture," Phys. Rev. A (submitted).
15. F. Decker and J. Eichler, Phys. Rev. A 39, 1530 (1989).
16. See the experimental work cited in Ref. 14.
17. N. Toshima, T. Ishihara, and J. Eichler, Phys. Rev. A 36, 2659 (1987).
18. T. G. Winter, "Electron Transfer and Ionization in Collisions between Protons and the Ions He^+, Li^{2+}, Be^{3+}, B^{4+}, and C^{5+} Studied with the Use of a Sturmian Basis, " Phys. Rev. A 35, 3799 (1987).
19. T. G. Winter, "Electron Transfer and Excitation in p-He Collisions," Abstr. XVI ICPEAC (New York, 1989), p. 538.
20. J. R. Ashburn, R. A. Cline, P. J. M. van der Burgt, W. B. Westerveld, and J. S. Risley, Abstr. XVI ICPEAC (New York, 1989); and R. A. Cline (private communication).
21. R. Shingal and C. D. Lin (calculation in progress).
22. C. D. Stodden, H. J. Monkhorst, K. Szalewicz, and T. G. Winter, "Muon Reactivation in Muon Catalyzed d-t Fusion from Accurate p-He^+ Stripping and Excitation Cross Sections," Phys. Rev. A (submitted).

LAWRENCE BERKELEY LABORATORY
TECHNICAL INFORMATION DEPARTMENT
1 CYCLOTRON ROAD
BERKELEY, CALIFORNIA 94720